NAVAL POSTGRADUATE SCHOOL
Monterey, California

THESIS

DTIC
ELECTE
S JAN 3 1 1992
D

COMPLIANCE
OF
A ROBOTIC FINGER JOINT

by

Yavuz Turkgenci

June 1991

Thesis Advisor   Morris R. Driels

Approved for public release; distribution is unlimited.

92 1 40 089

92-02436

REPORT DOCUMENTATION PAGE

1a Report Security Classification Unclassified			1b Restrictive Markings		
2a Security Classification Authority			3 Distribution Availability of Report		
2b Declassification Downgrading Schedule			Approved for public release: distribution is unlimited.		
4 Performing Organization Report Number(s)			5 Monitoring Organization Report Number(s)		
6a Name of Performing Organization Naval Postgraduate School		6b Office Symbol (if applicable) ME	7a Name of Monitoring Organization Naval Postgraduate School		
6c Address (city, state, and ZIP code) Monterey, CA 93943-5000			7b Address (city, state, and ZIP code) Monterey, CA 93943-5000		
8a Name of Funding Sponsoring Organization		8b Office Symbol (if applicable)	9 Procurement Instrument Identification Number		
8c Address (city, state, and ZIP code)			10 Source of Funding Numbers		
			Program Element No	Project No	Task No	Work Unit Accession No

11 Title (include security classification) COMPLIANCE OF A ROBOTIC FINGER JOINT

12 Personal Author(s) Yavuz Turkgenci

13a Type of Report Master's Thesis	13b Time Covered From To	14 Date of Report (year, month, day) June 1991	15 Page Count 105

16 Supplementary Notation The views expressed in this thesis are those of the author and do not reflect the official policy or position of the Department of Defense or the U.S. Government.

17 Cosati Codes			18 Subject Terms (continue on reverse if necessary and identify by block number)
Field	Group	Subgroup	Compliance

19 Abstract (continue on reverse if necessary and identify by block number)

Adaptive compliance control of a robotic single joint was studied to control the amount of torque applied on an object by an end effector, which is actuated by an electric motor through a gearbox.

For this reason, an adaptive control system was designed. Variation in stiffness and compliance was observed by simulating the system with MATRIX, package program. After observing theoretical variation of the stiffness and the compliance, experiments were done to observe and prove the stiffness control theory.

The proved theory was then applied to a prototype robotic finger joint actuated by a small DC motor.

20 Distribution Availability of Abstract ☒ unclassified unlimited ☐ same as report ☐ DTIC users	21 Abstract Security Classification Unclassified	
22a Name of Responsible Individual Morris R. Driels	22b Telephone (include Area code) (408) 646-3383	22c Office Symbol ME

DD FORM 1473,84 MAR

83 APR edition may be used until exhausted
All other editions are obsolete

Approved for public release; distribution is unlimited.

Compliance
of
a Robotic Finger Joint

by

Yavuz Turkgenci
1 st LT, TURKISH ARMY
B.S., Turkish Army Academy, Ankara, 1984

Submitted in partial fulfillment of the
requirements for the degree of

MASTER OF SCIENCE IN MECHANICAL ENGINEERING
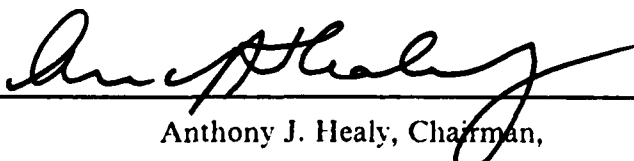
from the

NAVAL POSTGRADUATE SCHOOL
June 1991

Author: _____
Yavuz Turkgenci

Approved by: _____
Morris R. Driels, Thesis Advisor

_____
Anthony J. Healy, Chairman,
Department of Mechanical Engineering

ABSTRACT

Adaptive compliance control of a single robotic joint was studied to control the amount of torque applied on an object by an end effector, which is actuated by an electric motor through a gearbox.

For this reason, an adaptive control system was designed. Variation in stiffness and compliance was observed by simulating the system with $MATRIX_x$ package program. After observing theoretical variation of the stiffness and the compliance, experiments were done to observe and prove the stiffness control theory.

The proved theory was then applied to a robotic finger joint actuated by a small DC motor.

iii

TABLE OF CONTENTS

LIST OF TABLES

LIST OF FIGURES

ACKNOWLEDGEMENT

I. INTRODUCTION

One of the most important problems in robotics is the design of a dextrous end effector. A dextrous end effector is a kind of gripper or a tool that enables a robot to hold or handle different kinds of objects easily and skillfully, like a human being. Different techniques can be used to give that kind of ability to the end effector. Two of those techniques are direct drive and indirect drive. In indirect drive, the fingers of the dextrous end effector will be driven by tendon cords which are actuated by electric motors installed into the arm. In direct drive, the fingers are actuated by electric motors installed directly into the finger itself. Unfortunately, many actuators are best suited to relatively high speed and low torque, therefore they require a speed reduction system which is usually a gearbox.

In today's automated machinery, reliability is an important factor. Since reliability decreases with increasing complexity, it is better to try to keep the end effector simple in both its design and function. The main source of complexity in dextrous hand design comes from the finger joints. In Figure 1, tendon cord controlled dextrous end effector is shown. As can be seen from the figure, pulleys and the tendon cords used to actuate the fingers presents a considerable amount of complexity.

In a tendon cord design, the designer must consider the tension of each tendon, since any slack will cause a problem. After gripping an object, the power on the tendon cords must be kept to maintain a grasp on the object. Another problem will be the weight of the hand. Since the weight of the hand and the arm is increased by a tendon cord and pulley system, this will cause problem in arm joint (elbow) and shoulder joint designs.

By using a direct drive method in the finger joints, the difficulties listed above can be overcome to some extent. By installing DC servo motors directly to the finger joints

1
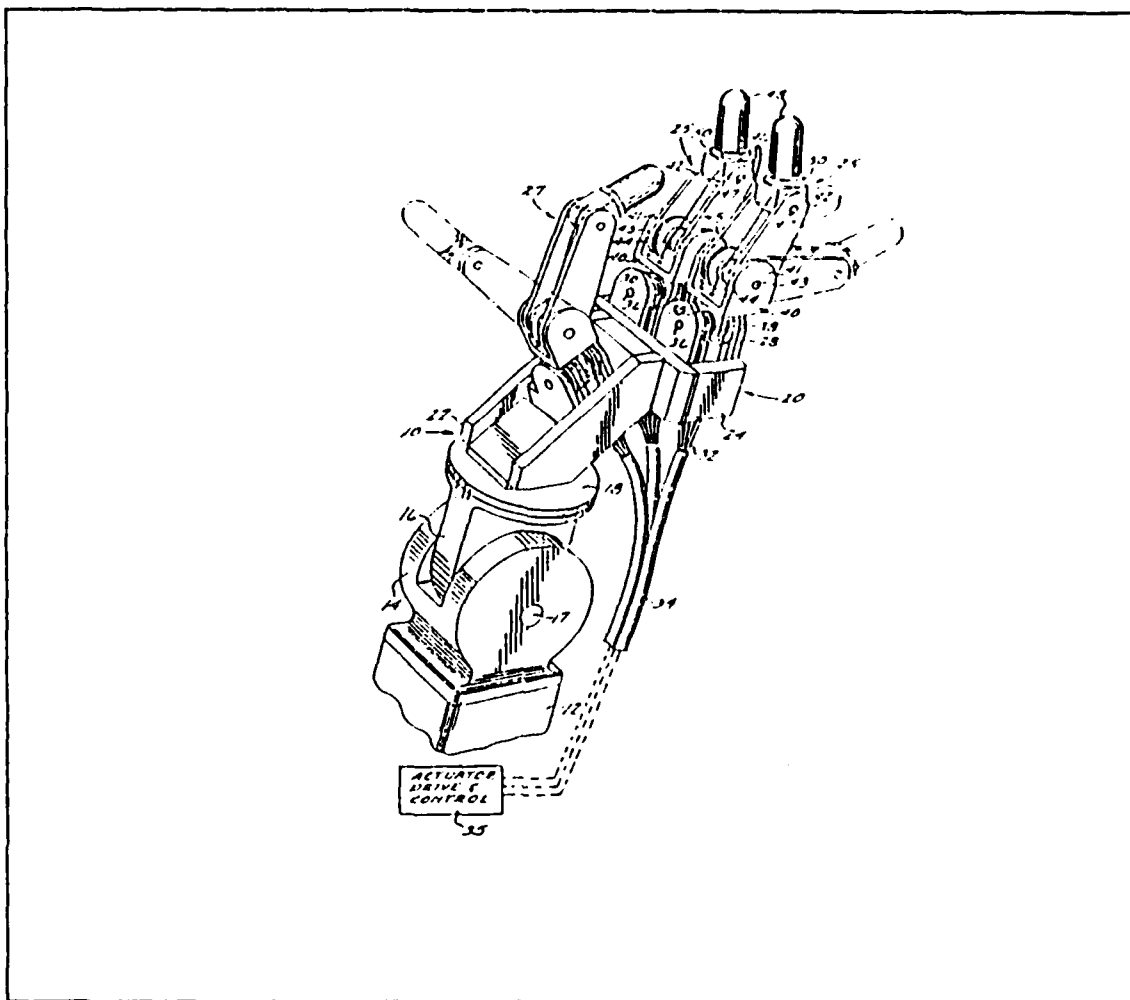
Figure 1.   Tendon Cord Controlled End Effector.

as shown in Figure 2, the finger links can be moved without tendons. The weight and

keeping the power on after the grip will not be a problem. If the motor drives the joint

through a high ratio gearbox, power may be removed from the motor, and the small

amount of armature friction will prevent the motor from being backdriven. This means

that a grasp is maintained with power removed. Since the complexity of the joint will

be less, the reliability of the system will be higher. By using a gearbox to transmit the

motor torque and installing the actuators directly into the finger, this system provides

2

torque multiplication and increased position resolution which are very critical properties in the successful design of robot joints.

Although having a joint nonbackdriveable is an advantage, there are disadvantages, for example in handling delicate objects where a relatively large compliance in the finger joint is desirable.

In a finger joint a direct drive element must therefore carry out two tasks. 1. It should be able to bring the joint to the desired position, and 2. after contact with an object it must provide enough grip to hold or to manipulate the object without breaking it.

Therefore our system must have two characteristics. It must provide position control and necessary torque without breaking the object. While position control is enough to provide a desired trajectory, when contact is made between the end effector and the object, position control may not be sufficient.

Contact force applied on an object will be the major problem with the direct drive end effector. The contact force applied by a direct drive end effector on an object will be decided by the stiffness of the servomechanism used to actuate the joint. Usually servomechanisms have high natural stiffness due to the high gear ratio. This may cause some problems when manipulating fragile objects. This problem may be overcome by changing the stiffness of the system for certain tasks. Stiffness of the servo system will be defined as

$$\frac{\tau_d}{\theta_o}. \tag{1.1}$$

Where τ_d = the disturbance torque applied to the output shaft and θ_o = the angular displacement of the output shaft. By changing the stiffness of the system, torque applied on the object can be controlled. The inverse of stiffness, namely
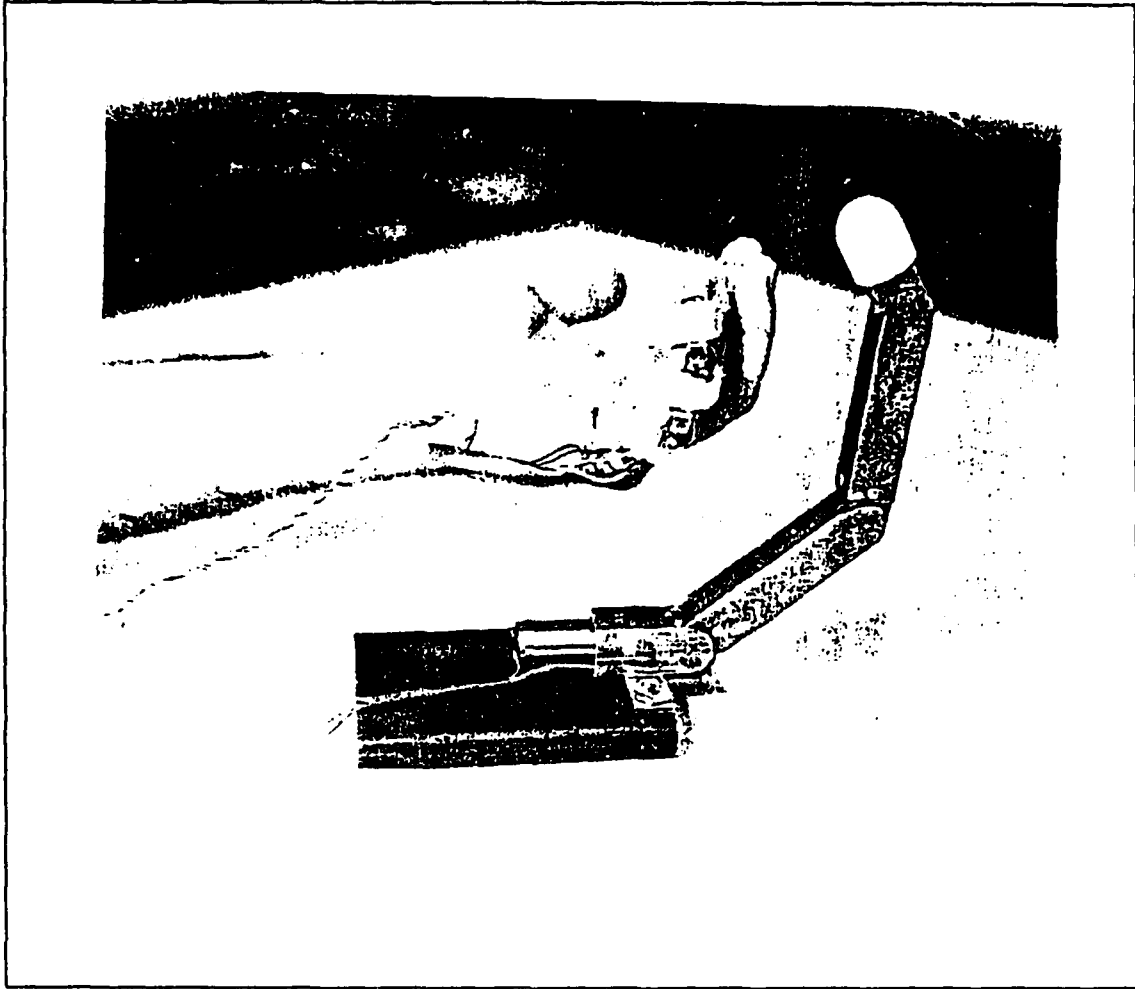
Figure 2. Direct Drive End Effector

$$\frac{\theta_o}{\tau_d} \tag{1.2}$$

will be defined as compliance of the system.

The purpose of this research is to design a simple system that will provide both position control and torque control, and by changing the stiffness of the servo system to be able to control the applied torque on the grasped object.

The thesis consists of eight chapters. Following the introduction, chapter 2 presents the theory of stiffness and compliance control. The third chapter is devoted to system parameter identification of the experimental system. Simulation results of system response are presented in chapter four. The fifth chapter is devoted to experimental stiffness control of the system while chapter six discusses the adaptation of stiffness control to a prototype finger configuration. Following the discussion chapter, conclusions are presented.

II. THEORY OF STIFFNESS AND COMPLIANCE CONTROL

Interaction between objects and the end effector presents a much more complicated problem than position control. When an end effector is moving in a free space, there isn't any constraint, namely it does not touch any object that's going to constrain its motion. When it has contact with an object, a new variable defined as a disturbance must be added to the system.

A. POSITION CONTROL SYSTEM AND STIFFNESS OF A SYSTEM

1. Standard Position Control system:

The object in a position control system is to control the angular position of the output shaft. The desired position of the output shaft is achieved by a voltage that has been generated by means of a potentiometer, as shown in the block diagram in Figure 3. The angular position (θ_i) of the potentiometer generates a proportional bipolar voltage according to the potentiometer's transfer function (k_{pot} ,volts/radian). This voltage is compared to the achieved position of the load or output shaft of the motor as measured by another identical potentiometer. An error voltage is generated by summing these two voltages. Usually after passing through an amplifier, this voltage drives the motor. This amplifier's gain is usually called the forward path gain of the system (k_a). The angular velocity of the motor shaft is obtained after the applied voltage is passed through the motor. Following the motor, there is usually a gear box. Dividing motor shaft's angular velocity by the gear ratio, the angular velocity of the motor's output shaft velocity is obtained. Since differentiation of the position gives the velocity, by integrating the angular velocity, angular displacement of the output shaft can be obtained. This angular displacement of the output shaft is fed back to the system to achieve desired position.
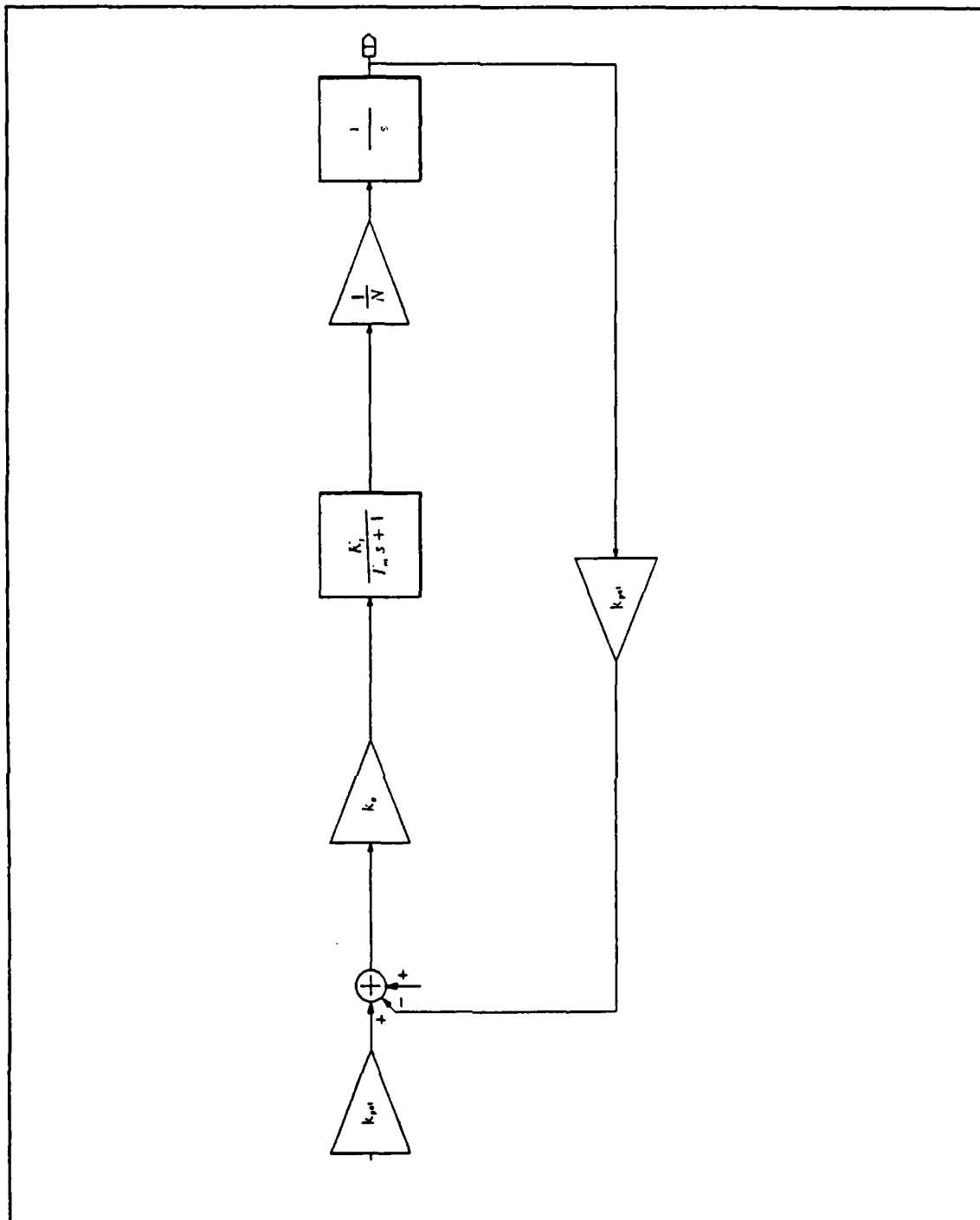
Figure 3. Standard Position Control System.

In the block diagram following constants are used.

K_t = Motor constant (rad/sec/volt)

k_{pot} = Potentiometer constant (volt/rad)

T_m = Mechanical time constant (sec)

k_a = Forward path gain

N = Gear ratio

In position control systems, different kinds of electrical motors can be used, although a DC motor has been used in this research. The DC motor is a power actuator device that delivers energy to a load. DC motors rotate due to the interaction of two magnetic fields, one in the stator, one in the rotor. The rotational speed may be varied by controlling the strength of one of these fields. The input voltage can be applied to either the field or the armature terminals. The air-gap flux of the field current is proportional to the field current. So that

$$\phi = K_f i_f \tag{2.1}$$

K_f = Field constant

i_f = Field current

The torque developed by the motor is assumed to be related linearly to ϕ and the armature current as follows

$$T_m = K_1 \phi i_a(t) = K_1 K_f i_f(t) i_a(t) \tag{2.2}$$

τ_m = Motor torque

i_a = Armature current

8

In order to have a linear element one current must be maintained constant while the other current becomes the input current. Two kinds of motor can be defined based on this principle, field controlled motor and armature controlled dc motor, as shown in Figure 4. By taking Laplace, transform of equation (2.2) the following equation is obtained.

$$T_m(s) = (K_1 K_f I_a) I_f(s) = K_T I_f(s) \tag{2.3}$$

Where K_T = Motor constant (Nm/amp)

The field current is related to the field voltage as

$$V_f(s) = (R_f + L_f s) I_f(s). \tag{2.4}$$

V_f = Field voltage

L_f = Field inductance

The motor torque is equal to the torque delivered to the load. This relation may be expressed as

$$T_m(s) = T_L(s) + T_d(s), \tag{2.5}$$

T_L = Load torque.

T_d = Disturbance torque.

The load torque for rotating the inertia shown in Figure 4 is written as

$$T_L(s) = Js^2\theta(s) + fs\theta(s). \tag{2.6}$$

9
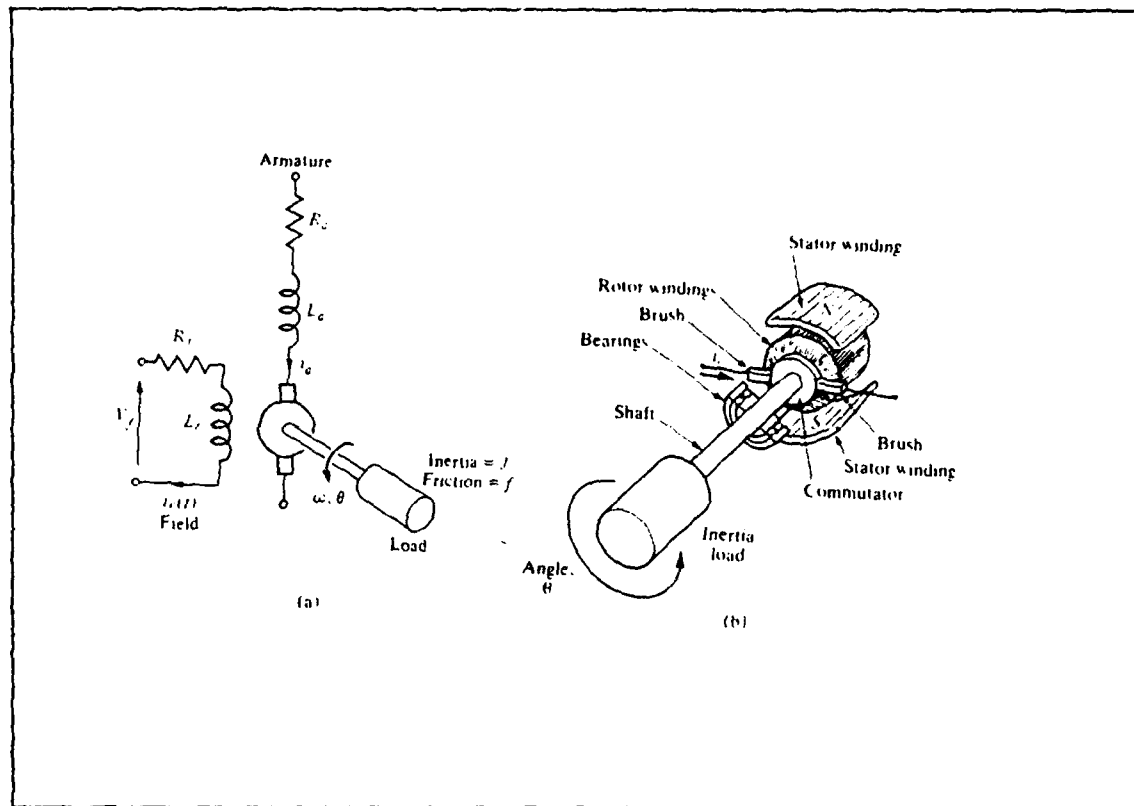
Figure 4. A DC Motor a) Wiring Diagram b) Sketch.

Rearranging equations (2.3), (2.4) and (2.5), the following equations may be obtained,

$$T_L(s) = T_m(s) - T_d(s),\tag{2.7}$$

$$T_m(s) = K_T I_f(s),\tag{2.8}$$

$$I_f(s) = \frac{V_f(s)}{R_f + L_f s}\tag{2.9}$$

Therefore, the transfer function of the motor-load combination will be as follows

$$\frac{\Theta(s)}{V_f(s)} = \frac{\dfrac{K_T}{JL_f}}{s(s + \dfrac{f}{J})(s + \dfrac{R_f}{L_f})} \tag{2.10}$$

The block diagram of the field controlled dc motor is shown in Figure 5.

Alternatively, the transfer function may be written in terms of the time constants of the motor as

$$\frac{\Theta(s)}{V_f(s)} = \frac{\dfrac{K_T}{fR_f}}{s(\tau_f s + 1)(\tau_L s + 1)} \tag{2.11}$$

where $\tau_f = \dfrac{L_f}{R_f}$ and $\tau_L = \dfrac{J}{f}$

Since usually $\tau_L > \tau_f$, the field time constant may be neglected.

The armature controlled dc motor utilizes a constant field current, therefore the motor torque may be written as by

$$T_m(s) = (K_1 K_f I_f) I_a(s) = K_T I_a(s). \tag{2.12}$$

The armature current is related to the input voltage applied to the armature by

$$V_a(s) = (R_a + L_a s) I_a(s) + V_b(s), \tag{2.13}$$

where $V_b(s)$ is the back electromotive-force voltage proportional to the motor speed.

$$V_b(s) = K_b \omega(s), \tag{2.14}$$

hence
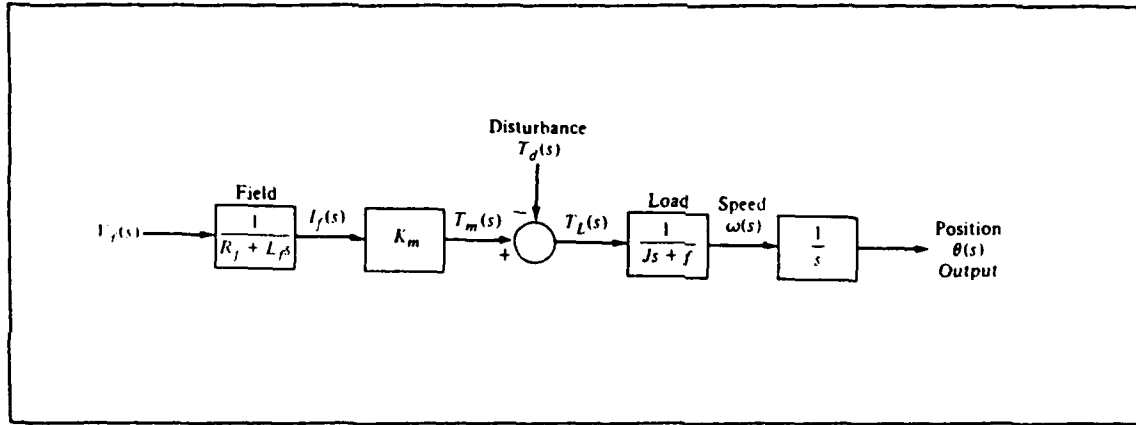
Figure 5. Block Diagram of Field Controlled DC Motor.

$$I_a(s) = \frac{V_a(s) - K_b \omega(s)}{(R_a + L_a s)} \qquad (2.15)$$

The same load torque equations, (2.6), (2.7) will be valid for armature control also. The relations for the armature controlled dc motor are shown in the Figure 6.

The transfer function of armature controlled dc motor will be as follows

$$\frac{\Theta(s)}{V_a(s)} = \frac{K_T}{s[(R_a + L_a s)(Js + f) + K_b K_T]} . \qquad (2.16)$$

For many dc motors, the time constant of the armature, $\tau_a = \dfrac{L_a}{R_a}$, is negligible. The resultant transfer function will be as follows

$$\frac{\Theta(s)}{V_a(s)} = \frac{\left[\dfrac{K_T}{(R_a f + K_b K_T)} \right]}{s(\tau_1 s + 1)} , \qquad (2.17)$$

where the time constant $\tau_1 = \dfrac{R_a J}{(R_a f + K_b K_m)}$.
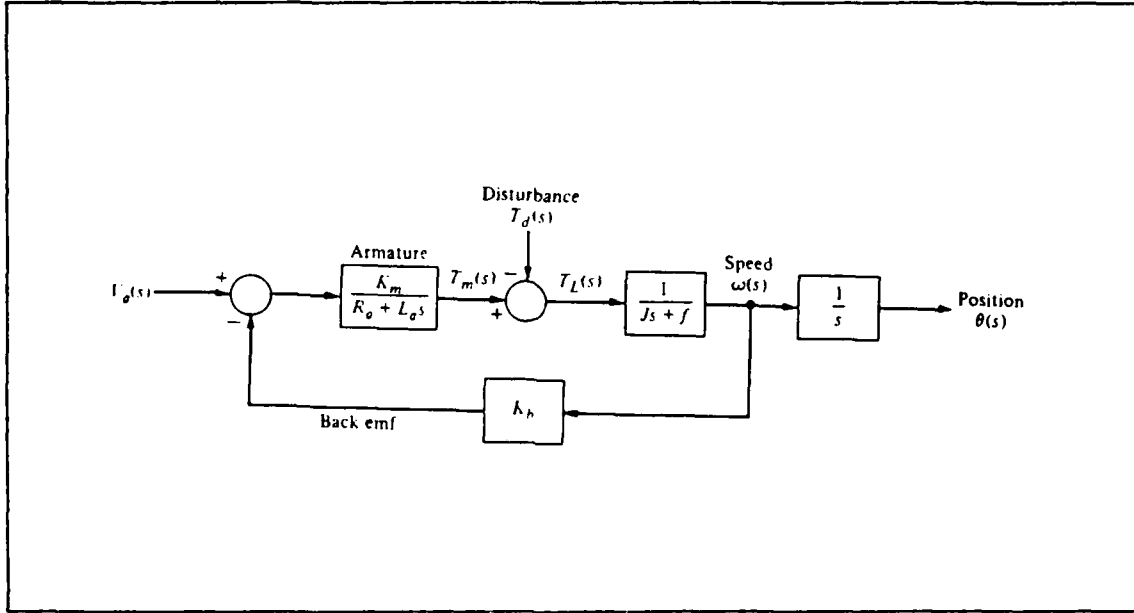
Figure 6. **Block Diagram of Armature Controlled DC Motor.**

2. Effect of load inertia:

A study of the free body diagram of the motor, gearbox and the load will be helpful to write the equation motion of the mechanical part of the dc motor in Figure 7.

Since the armature inertia and the viscose friction have to be overcome, all of the torque generated (τ_m) is not available at the gearbox input shaft. The general equation of motion of a torque generating system may be written as

$$\sum_{i=1} \tau_i = J\ddot{\theta}. \tag{2.18}$$

Considering the gearbox ratio $N > 1$ the equation of the motion can be written as follows

For the motor shaft
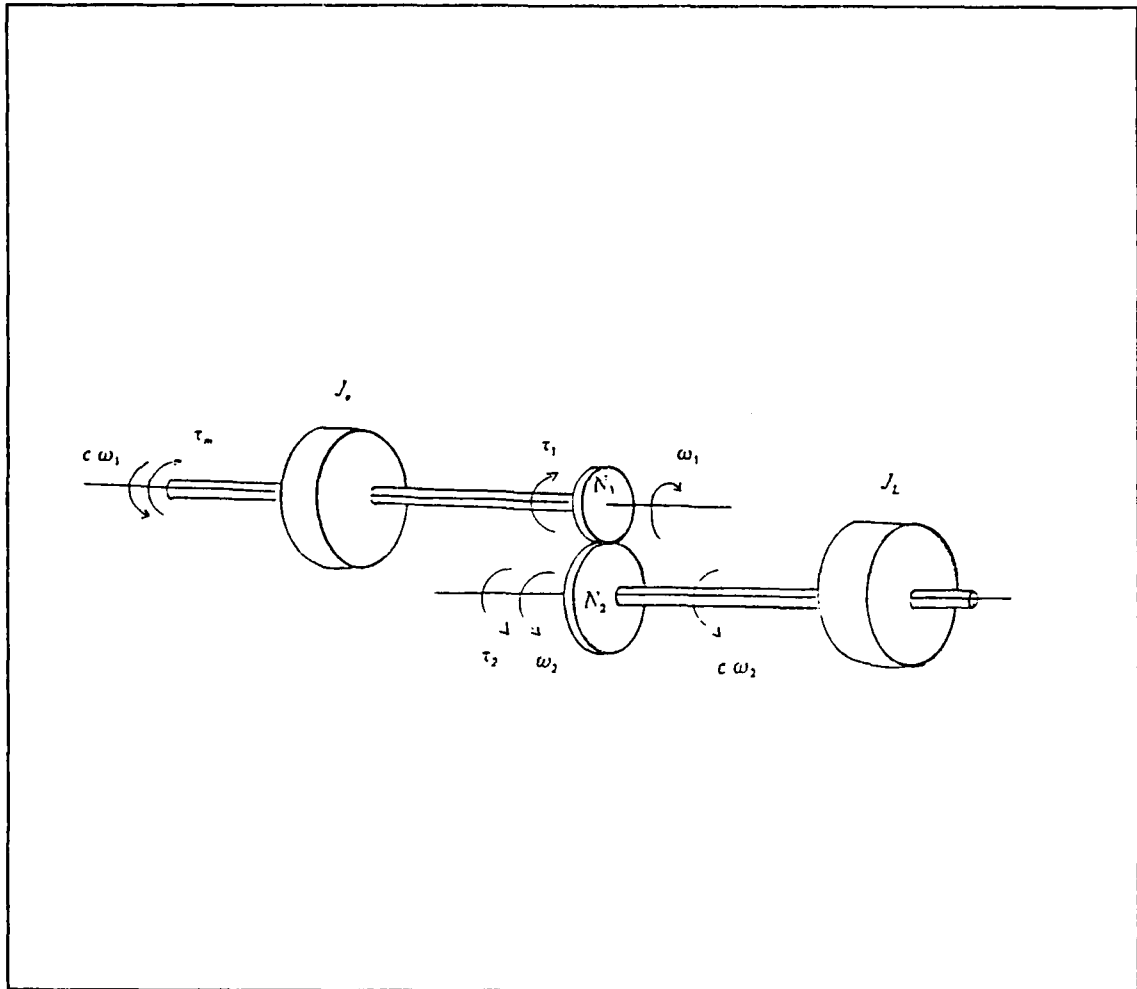
Figure 7.   Free Body Diagram of DC Motor.

$$\tau_m - \tau_1 - c_1\omega_1 = J_a\dot{\omega}_1 \tag{2.19a}$$

For the load shaft

$$\tau_2 - c_L\omega_2 = J_L\dot{\omega}_2 \tag{2.19b}$$

For the gearbox

14

$$\omega_2 = \frac{\omega_1}{N} \qquad \tau_2 = N\tau_1 \qquad (2.19c)$$

τ_m = Motor torque

J_a = Armature inertia

J_L = Load inertia

$\dot{\omega}_1$ = Motor shaft angular acceleration

ω_1 = Motor shaft angular velocity

$\dot{\omega}_2$ = Output shaft angular acceleration

ω_2 = Output shaft angular velocity

c_1 = Motor shaft damping

c_L = Output shaft damping

Referring all variables to the motor shaft gives:

$$\tau_m - c_1\omega_1 - \frac{\tau_2}{N} = J_a\dot{\omega}_1 \qquad (2.20)$$

$$\tau_m - \frac{J_L\omega_2}{N} - c_1\omega_1 - \frac{c_2\omega_2}{N} = J_a\dot{\omega}_1 \qquad (2.21)$$

$$\tau_m - \frac{J_L\omega_1}{N^2} - c_1\omega_1 - \frac{c_2\omega_1}{N_2} = J_a\dot{\omega}_1 \qquad (2.22)$$

Resulting in the final equation

$$\tau_m = (J_a + \frac{J_L}{N^2})\dot{\omega}_1 + (c_1 + \frac{c_2}{N^2})\omega_1 \qquad (2.23)$$

In the equation of motion there is an important property that has to be noticed. The effect of the gearbox reduces the load inertia and load shaft damping factor by N^2.

15

This means that, by using a gearbox we may apply less torque to the motor shaft to accelerate the load on the output shaft. Another interesting effect of the equation can be seen, when the torque is applied to the output shaft to turn input shaft. Then following equation will apply:

$$\tau_m = (J_a N^2 + J_L)\dot{\omega}_1 + (c_1 N^2 + c_L)\omega_1 \tag{2.24}$$

In this equation, the effect of input shaft's inertia will increase by N^2. As a result of this effect, it will be easier to turn the system in the figure by applying torque on input shaft rather than on output shaft. This is one of the important properties used in control systems design to reject disturbances.

3. Analysis of the servo system:

Torque generated by the armature is linearly related to the current applied. Torque generated by the armature is given by

$$\tau_m = K_T I_a. \tag{2.25}$$

Here K_T is the motor torque constant with units Nm amp. This generated torque accelerates the motor armature itself and an external load. It also overcomes viscous damping torque and any external load torque.

As demonstrated, in the preceding section of the chapter, the load inertia rather than motor inertia may be neglected, if $N >> 1$. The transfer function from motor torque τ_m to output angular velocity ω_1 is obtained by taking the Laplace transform of equation (2.24) and re-arranging in the form.

$$\frac{\omega}{\tau} = \frac{1}{Js + c} \tag{2.26}$$

16

Where J is the total inertia referred to the motor shaft and c is the total damping referred to the motor shaft. Both the mechanical and electrical part of the motor gearbox combination can be seen in Figure 8. The complete position control system block diagram, is now shown in Figure 9.

The close loop transfer function of the system becomes

$$\frac{\theta_o}{\theta_i} = \frac{1}{Ns(Js + c)} \left[\frac{K_T}{R_a} \left\{ -k_b \omega_m + k_a(\theta_i k_{pot} - \theta_o k_{pot}) \right\} \right] \qquad (2.27)$$

Using $\omega_m = Ns\theta_o$, the transfer function of the system can be written as:

$$\frac{\theta_o}{\theta_i} = \frac{K}{JNs^2 + (cN + \frac{K_T}{R} k_b NR)s + K} \qquad (2.28)$$

where $K = k_a \dfrac{K_T k_{pot}}{R}$

4. Disturbance effect on the position control system:

The main variable in stiffness and compliance control of a servo mechanism is the torque applied on the object. This torque must be adjusted according to the disturbance torque sensed from the object. When an end effector applies a torque on the object, the object will apply a reaction torque on the end effector. This will cause a disturbance effect on the system. In Figure 10 a sketch of an end effector applying torque on an object and the object's reaction torque are shown. This disturbance torque will have a braking effect on the output shaft. The analysis of the system may proceed in the same manner identical to before, except that the equation of the load shaft will be modified due to the disturbing torque τ_d.

Considering the disturbance torque and gear box effects as shown in Figure 11, the equation of motion of the system may be written as follows

17
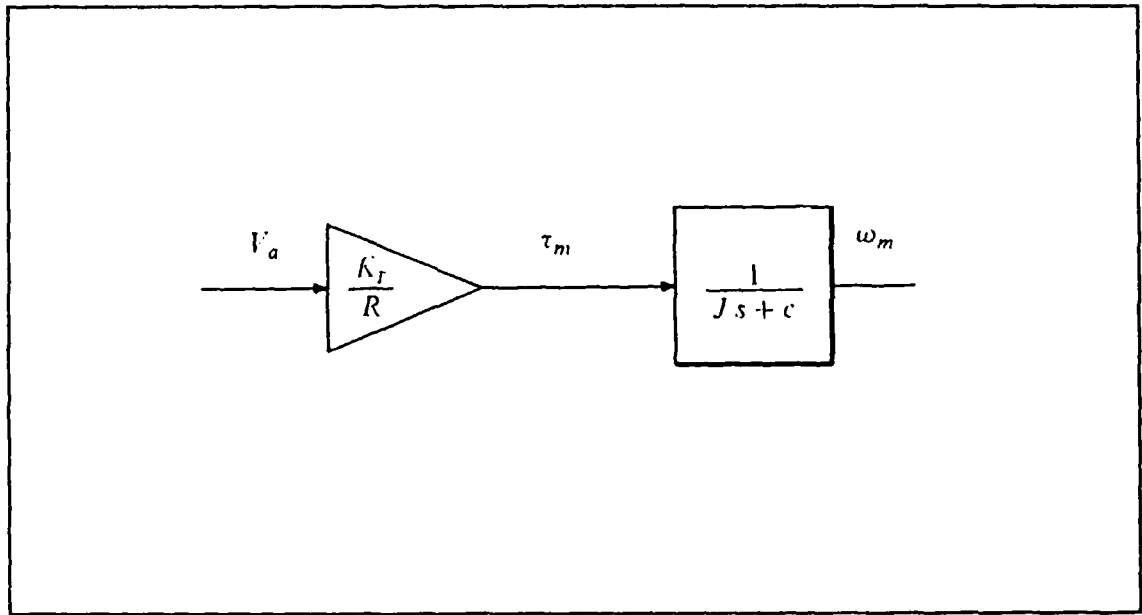
Figure 8.   Electrical and Mechanical Part of the System.

$$\sum_{i=1}^{} \tau_i = J\ddot{\theta}. \tag{2.29}$$

$$\tau_m - \frac{\tau_d}{N} = (J_a + \frac{J_L}{N^2})\dot{\omega}_m + (c_1 + \frac{c_L}{N^2})\omega_m \tag{2.30}$$

An equation may be written considering total inertia and damping of the system.

$$\tau_m - \frac{\tau_d}{N} = J\dot{\omega}_m + c\,\omega_m \tag{2.31}$$

τ_d = Disturbance torque

ω_m = Motor shaft's angular acceleration

18
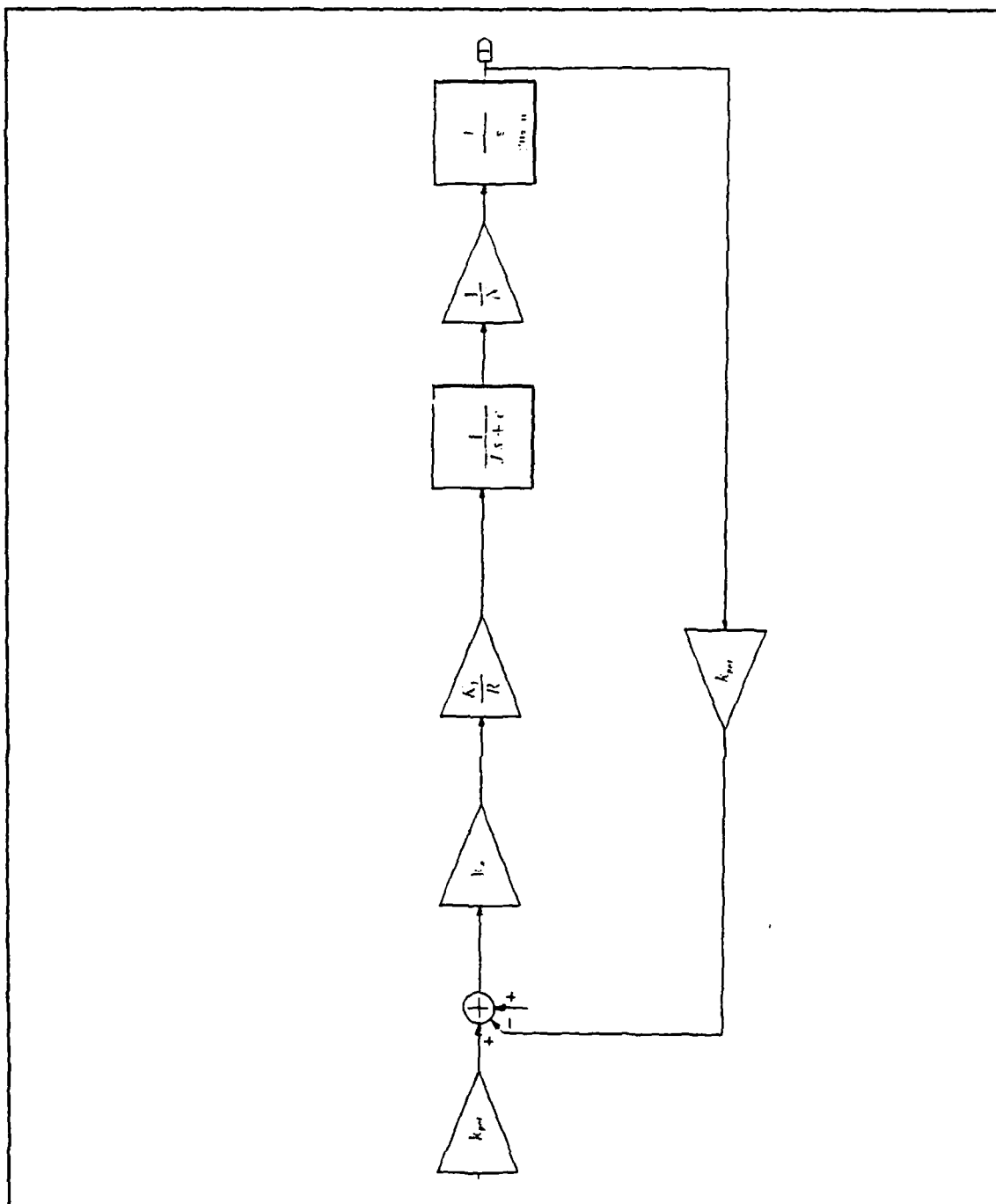
Figure 9. Position Control System.

ω_m = Motor shaft's angular velocity
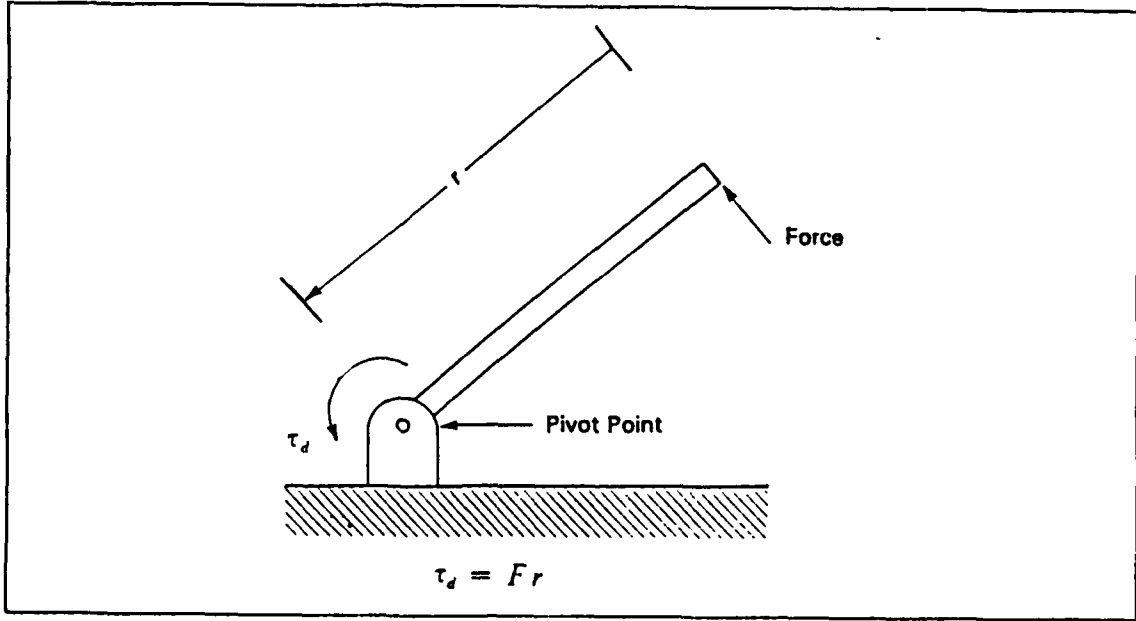
Figure 10. Free Body Diagram of a Torque Applying End Effector.

The equation of motion of the system may written as

$$\theta_o = \frac{1}{Ns(Js + c)} \left[-\tau_d + \frac{K_T}{R_a} \left\{ - k_b \omega_m + k_a (\theta_i k_{pot} - \theta_o k_{pot}) \right\} \right]$$ (2.32)

and represented in block diagram form as shown in Figure 12.

The transfer function of the system including a disturbance torque and keeping θ_i constant can be written as follows

$$\frac{\theta_o}{\tau_d} = -\frac{1}{NJs^2 + (cN + \frac{K_T}{R} k_b N)s + k_a \frac{K_T k_{pot}}{R}}$$ (2.33)

Again using $\omega_m = Ns\theta_o$, the steady state response of the system to a disturbance torque is:

20
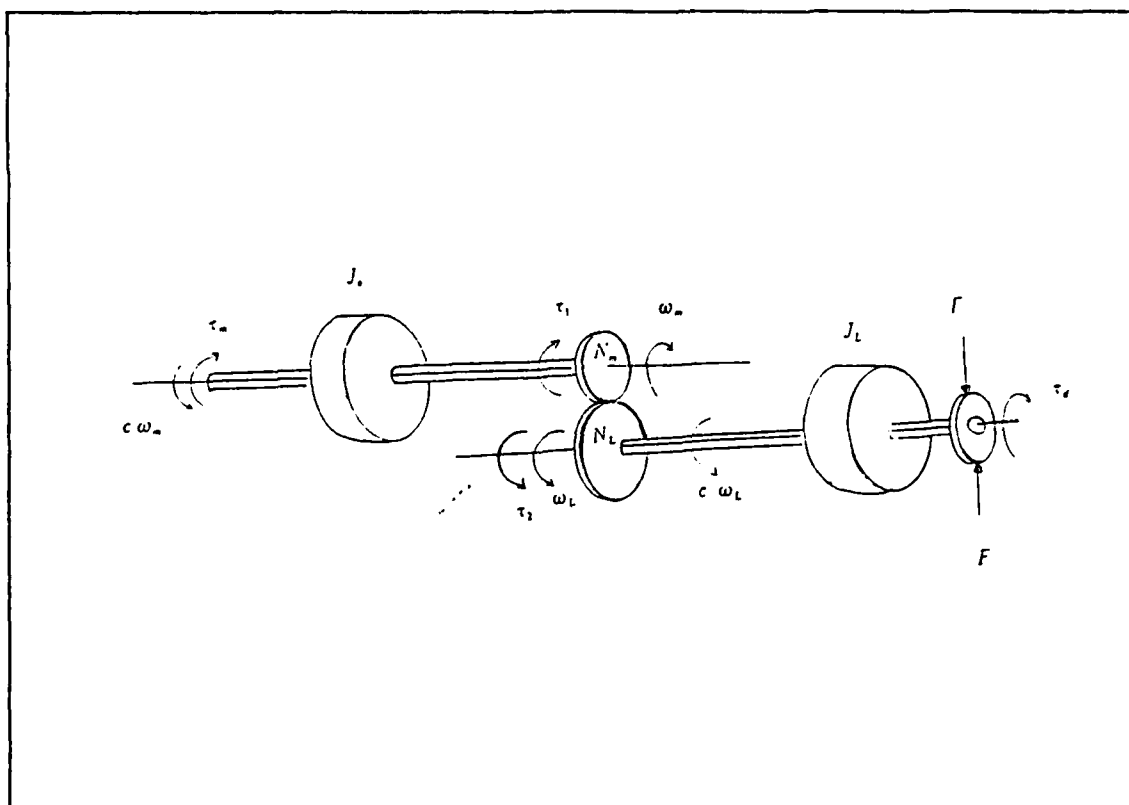
Figure 11. Free Body Diagram of Motor Shaft With Gear Box and Disturbance.

$$\frac{\theta_o}{\tau_d} = -\frac{R}{k_a k_{pot} K_T} \qquad (2.34)$$

An indication of the system stiffness can be seen when one tries to turn the output shaft of the system by hand. The system will show a resistance to the hand, opposite to the desired rotation. The resistance is caused by the voltage generated by the output shaft's potentiometer. As stated above, this voltage will be fed back to the system as a negative signal, meaning that, the motor will generate a torque opposite to the torque applied to the output shaft by the hand. The ratio of rotation to torque, given in equation (2.35) is the stiffness of the servo.

21
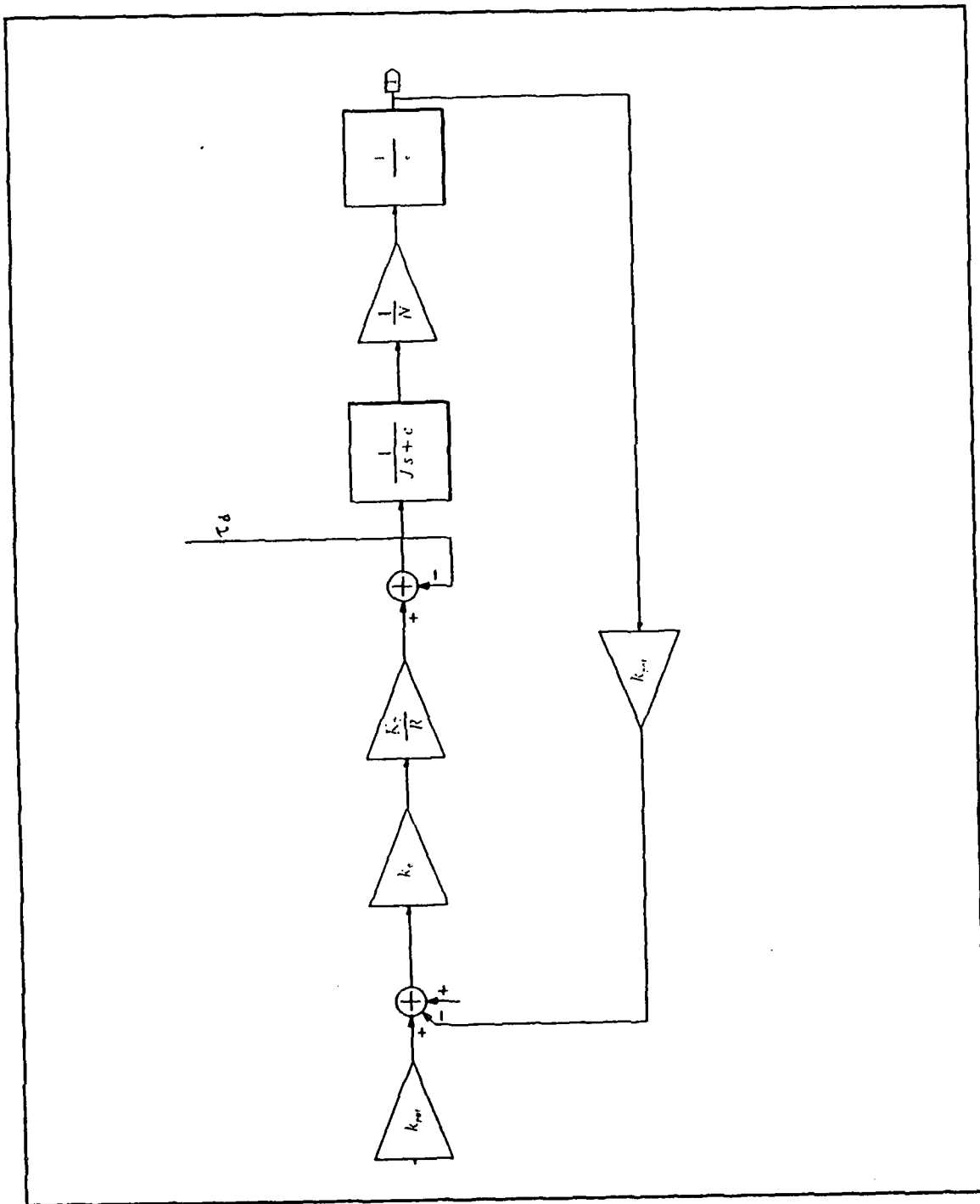
Figure 12. Position control system with disturbance.

$$\frac{\tau_d}{\theta_o} = -\frac{k_a k_{pot} K_T}{R} \qquad (2.35)$$

There are four values which may help to change the system's stiffness. These can be seen in equation (2.35). In this equation only k_a can be changed. As k_a increases stiffness of the system will be increasing. K_T & R can not normally be changed, because they are particular values which are fixed by the motor. Changing the value of k_a can be considered, but it is not going to be a very good option, since this gain easily may make the system unstable. For this reason, another way of changing the stiffness must be considered.

B. COMPLIANCE CONTROL STRATEGY

1. Description of how stiffness may be changed:

Suppose that 1 Nm. disturbance is applied to a servo system and 1 rad. rotation of the output shaft is observed. This means that the stiffness of the system is 1 Nm rad. If a higher rotation is desired by applying the same torque, the stiffness of the system will be lower. Namely, instead of 1 rad. of rotation, for example, 5 rad. of rotation is observed. Therefore, the stiffness of the system will be 0.2 Nm rad.

To be able to control the amount of torque applied on the object after contact, rotation of the output shaft must be controlled.

Since the voltage applied to the motor causes the rotation of the output shaft, by increasing the amount of voltage going to the summing junction before the motor, rotation of the output shaft can be increased. This will cause additional rotation of the output shaft for the same torque. Therefore the stiffness will be decreased. The new block diagram of a system which has variable stiffness ability is presented in Figure 13.
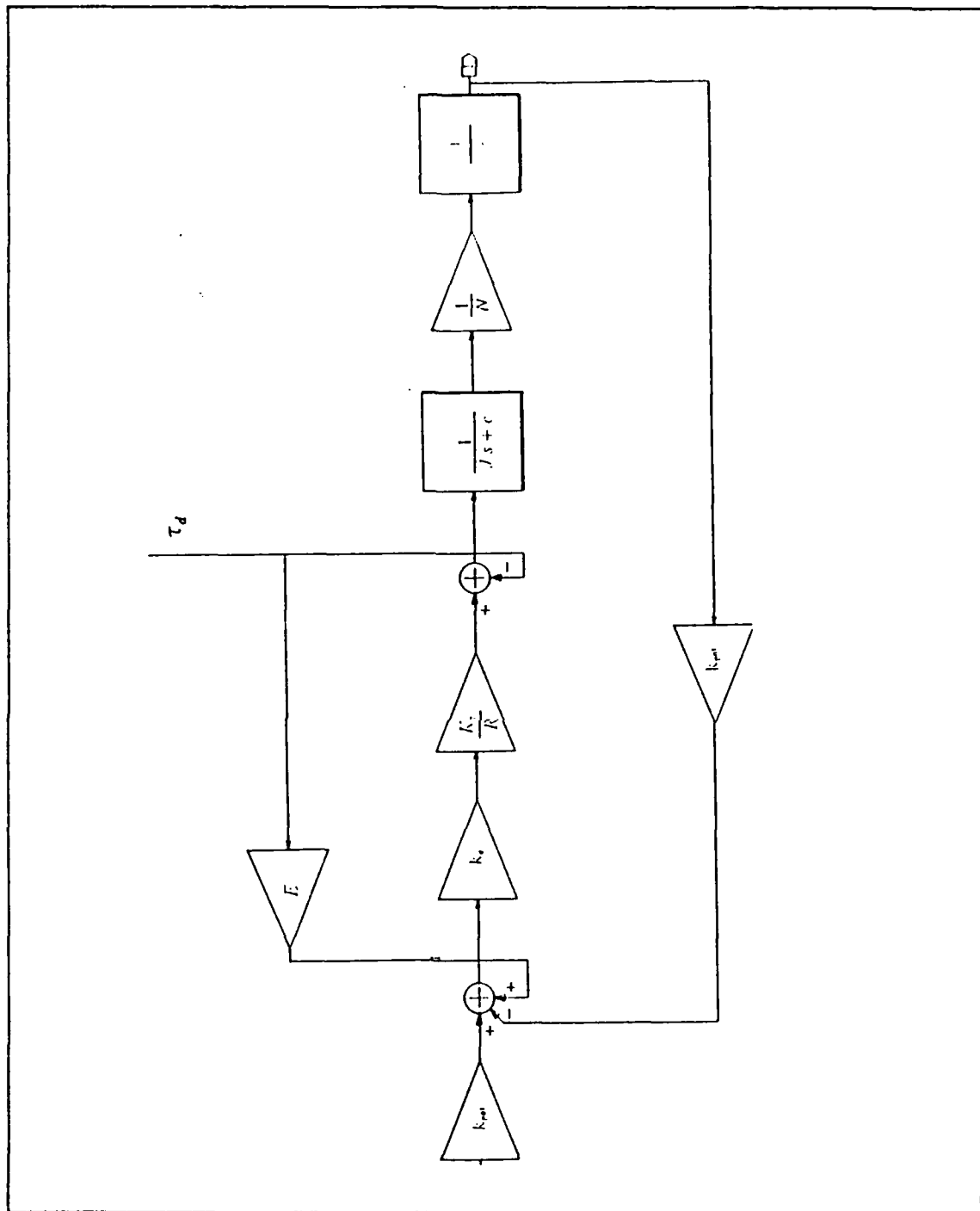
Figure 13. Position Control System With Disturbance Feedback.

The measured disturbance torque is fed back to the summing junction before the motor. By passing the measured torque through a variable gain E, we will be able to control the amount of additional rotation of output shaft.

The new equation of motion of the system will be as follows

$$\theta_o = \frac{1}{Ns(Js+c)} \left[-\tau_d + \frac{K_T}{R_a} \{ -k_b\omega_m + k_a(\theta_i k_{pot} - \theta_o k_{pot} - \tau_d E) \} \right] \qquad (2.36)$$

Keeping θ_i constant, the following transfer function of the system can be obtained.

$$\frac{\theta_o}{\tau_d} = - \frac{(E\frac{K_T}{R} + 1)}{NJs^2 + (cN + \frac{K_T}{R} k_b N)s + k_a \frac{K_T k_{pot}}{R}} \qquad (2.37)$$

Steady state output of the system, assuming $k_a = 1$ will be

$$\frac{\theta_o}{\tau_d} = - \frac{E\frac{K_T}{R} + 1}{k_{pot}\frac{K_T}{R}} \qquad (2.38)$$

where E is in volts/Nm.

2. **Stiffness as a function of gain E.**

To demonstrate the variable stiffness and compliance in a servo system , E and τ_d are assumed to be positive in equations (2.36), (2.37), (2.38). Thus the following equations were obtained as a transfer function of the system.

$$\frac{\theta_o}{\tau_d} = \frac{(E\frac{K_T}{R} + 1)}{NJs^2 + (cN + \frac{K_T}{R} k_b N)s + k_a \frac{K_T k_{pot}}{R}} \qquad (2.39)$$

$$\frac{\theta_o}{\tau_d} = \frac{(E\frac{K_T}{R} + 1)}{\frac{K_T k_{pot}}{R}} \tag{2.40}$$

This is defined as the compliance of the system. The stiffness is the inverse of compliance as shown in the following equation.

$$\frac{\tau_d}{\theta_o} = \frac{k_{pot}\frac{K_T}{R}}{E\frac{K_T}{R} + 1} \tag{2.41}$$

As can be seen in equations above, the only variable is E. Therefore by changing E, the stiffness of the system may be changed.

By giving k_{pot} and $\frac{K_T}{R}$ arbitrary values, the stiffness and the compliance curves were plotted, as shown in Figure 14 and Figure 15. The compliance of the system will be directly proportional to E. Since the stiffness of the system is the inverse of the compliance, the stiffness of the system will be inversely proportional to E. At the same time rotation of the output shaft will be directly proportional to E. The potentiometer constant will determine the slope of the curve. As k_{pot} increases, the slope of the compliance curve will be decreasing. When E is zero, the stiffness of the system will be equal to it's natural stiffness or original stiffness.

C. EFFECT OF EFFICIENCY OF A GEAR TRAIN:

Another problem which has to be discussed, concerns the disturbance torque. According to the gear theory, as presented in equation (2.19c), the disturbance applied to output shaft has to be divided by the gear ratio N to refer it to the motor shaft.

Efficiency of the gear train is another important effect which has to be addressed. It is defined as the ratio of the output power to the input power, or the ratio of the work
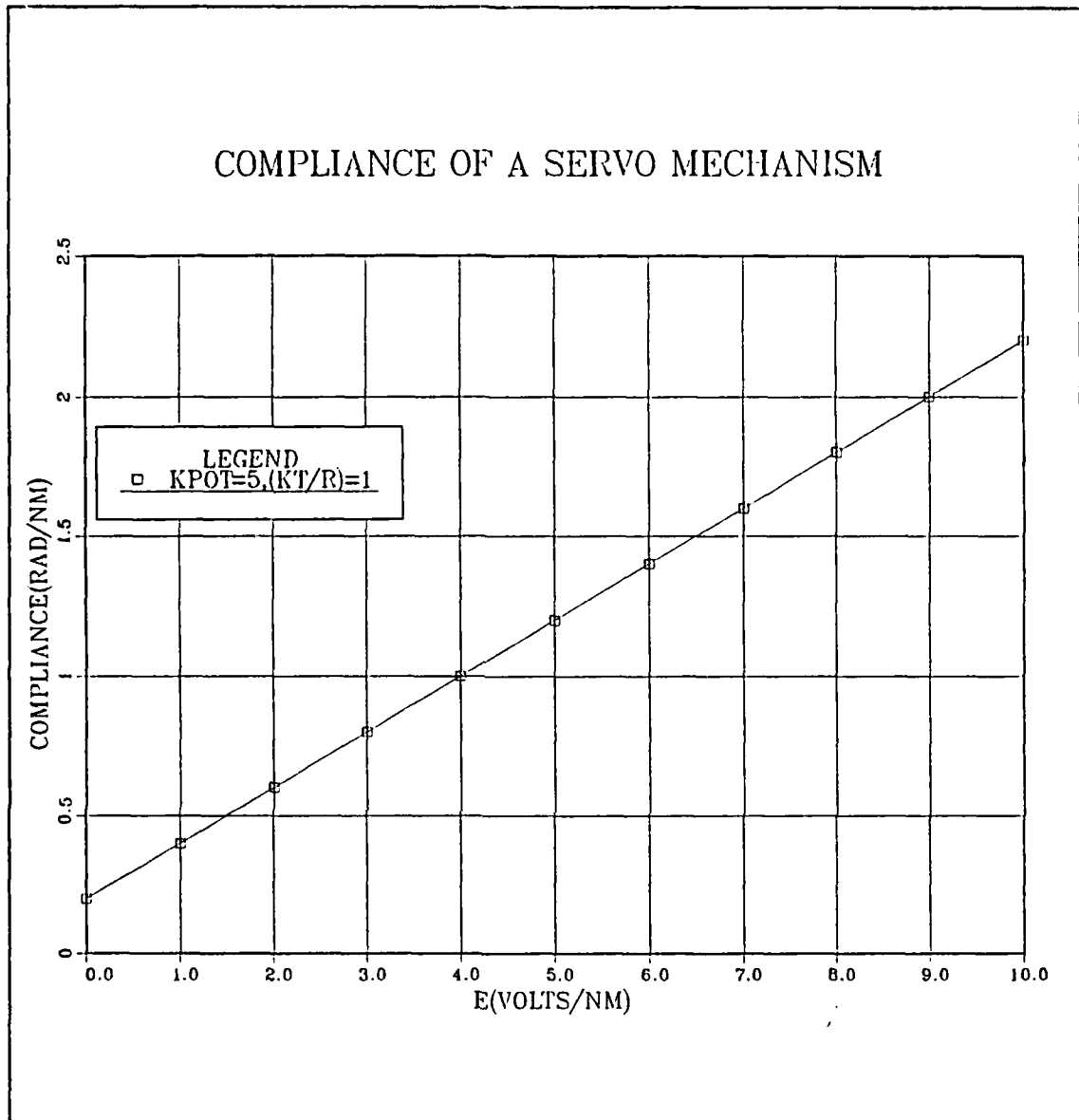
Figure 14.   Compliance Variation of a Servo System.

output to the work input over the same period of time. For an ideal mechanism, it will be 100 % or 1. In reality, a normal gear train will dissipate some of the power which has to be transmitted. Efficiency can be written as:

27

STIFFNESS OF A SERVO MECHANISM
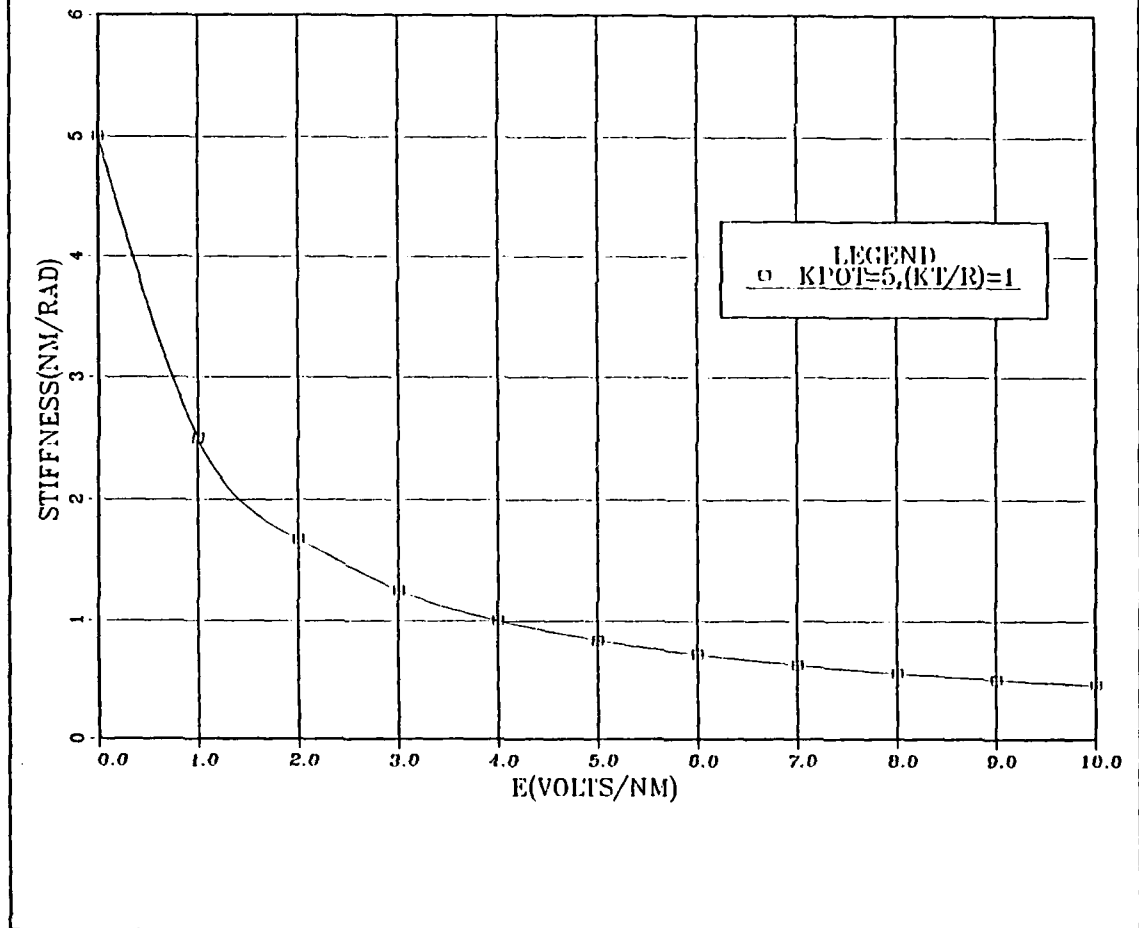
Figure 15.   Stiffness Variation of a Servo System.

$$\eta = \frac{power\ out}{power\ in} \qquad\qquad (2.42)$$

In the case of the gear train, it has to be restated, because there is a gear train ratio.
The new equation will be as following

$$\eta = \frac{actual\ output\ torque}{input\ torque} \quad \frac{1}{N} \qquad (2.43)$$

The efficiency of transmission can be determined by measuring the resulting torque on the output for static torques applied to the input shaft.

The efficiency of any mechanical device will become significant with robot end effectors actuated by motors driving through high ratio gearboxes. It is no longer safe to assume that the output loads are reflected to the input shaft by a function of the gear ratio, since any efficiency less than 1 will increase the torque required to accelerate a given inertial load or overcome an external torque. It is also important to notice that the efficiency of the gear train does not affect the actual transfer ratio of the gears in terms of displacement, velocity or acceleration, but greatly affects any torque related property. Efficiency is dependent on such factors as the coupling ratio, the material's coefficients of friction, and the angle used to define the gear teeth or the depth of cut and type of threads for screws.

Another interesting effect of efficiency is on the gear train's backdrivablity. Backdrivablity is the ability of a gear train to transmit the torque or the disturbance that has been applied on the output shaft side of the gear system, to the motor or to the torque source as shown in Figure 16.

In general as the efficiency goes higher, the backdrivablity will be higher, i.e the system is more likely to be backdrivable. At the same time a gear trains efficiency may be different for each side. For example in the case of worm gears, it will be zero for transmission of the torque from the load to the motor. Sometimes this property is good in robotics application, because it will help rejection of the disturbance torque, which may be a gravitational or frictional torque.
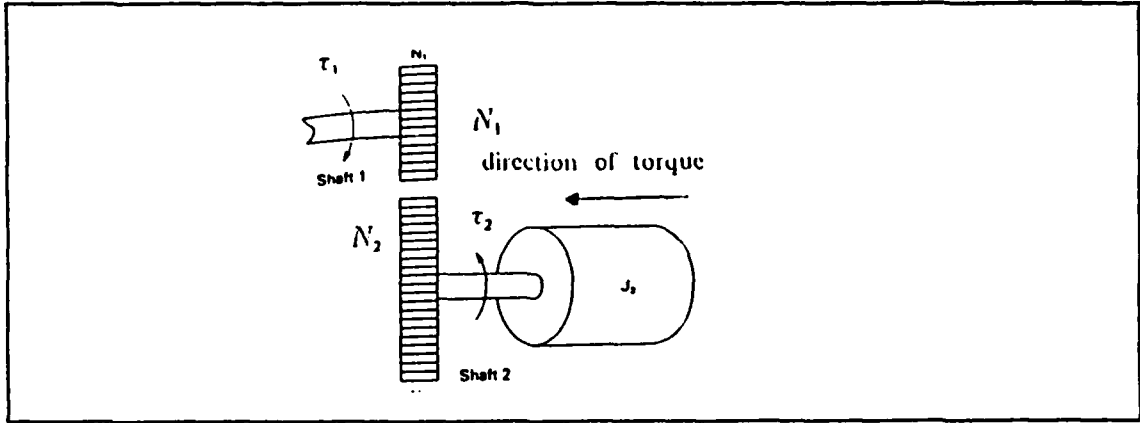
Figure 16.   Transition of the Disturbance Torque to the Motor.

At the same time, nonbackdrivablity will influence system stiffness, because the transfer function of the system will change.

The new equation of motion of the system will be as follows

$$\theta_o = \frac{1}{Ns(Js+c)} \left[\frac{K_T}{R_a} \{ -k_b\omega_m + k_a(\theta_i k_{pot} - \theta_o k_{pot} + \tau_d E) \} \right] \tag{2.44}$$

Keeping θ_i constant, the following transfer function of the system can be obtained.

$$\frac{\theta_o}{\tau_d} = \frac{(E)\dfrac{K_T}{R}}{NJs^2 + (cN + \dfrac{K_T}{R} k_b N)s + k_a \dfrac{K_T k_{pot}}{R}} \tag{2.45}$$

Steady state output of the system, assuming $k_a = 1$ will be

$$\frac{\theta_o}{\tau_d} = \frac{E}{k_{pot}} \tag{2.46}$$

The stiffness of the system will be

$$\frac{\tau_d}{\theta_o} = \frac{k_{pot}}{E} .$$

(2.47)

If positive feedback is used, the system stiffness will be positive infinite when E goes to zero. As E is increased, the stiffness of the system will decrease as shown in Figure 17 and Figure 18.

The effects mentioned above must be considered in our model in order to obtain high accuracy. Therefore as one can see from Figure 19, two new variables are added to the system. These are:

K = Nonbackdriveability constant

η = Efficiency of the gear train

Where, K = 0 (nonbackdriveable)

or   K = 1 (backdriveable)

for backdriveable systems. Again keeping θ_i constant, the new transfer function, compliance and stiffness of the system will be as follows

$$\frac{\theta_o}{\tau_d} = \frac{(E\frac{K_T}{R} + \frac{\eta K}{N})}{NJs^2 + (cN + \frac{K_T}{R}k_bN)s + k_a\frac{K_Tk_{pot}}{R}}$$

(2.48)

$$\frac{\theta_o}{\tau_d} = \frac{(E\frac{K_T}{R} + \frac{\eta K}{N})}{\frac{K_Tk_{pot}}{R}}$$

(2.49)

$$\frac{\tau_d}{\theta_o} = \frac{k_{pot}\frac{K_T}{R}}{E\frac{K_T}{R} + \frac{\eta K}{N}}$$

(2.50)

31

STIFFNESS (NONBACKDRIVABLE)
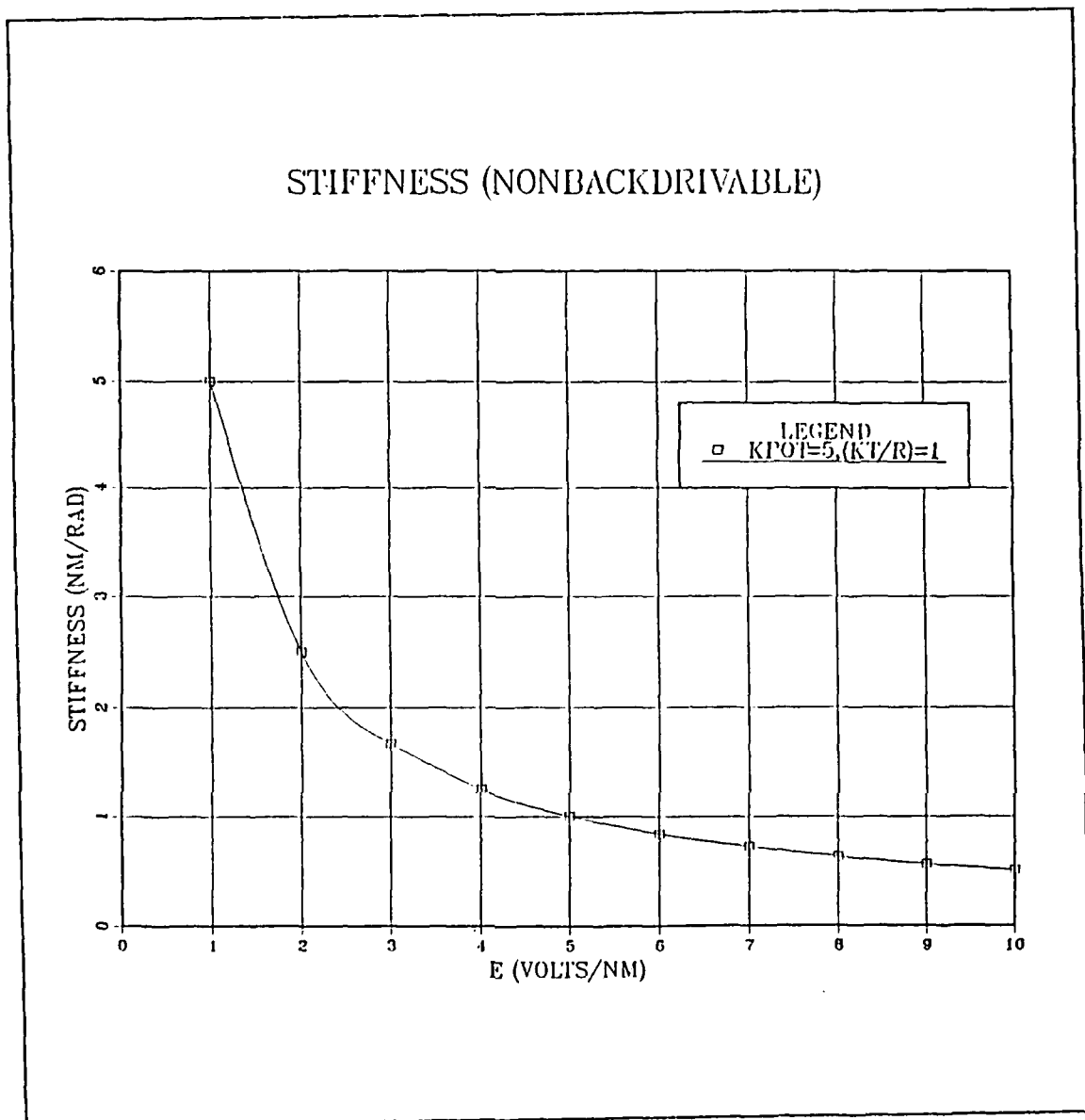
Figure 17. Stiffness Variation of a Servo System (nonbackdriveable).

The important conclusion drawn from the above discussion is that the system may have a finite stiffness by using disturbance feedback through E even though the original system was not backdriveable, corresponding to infinite stiffness.

COMPLIANCE (NONBACKDRIVABLE)
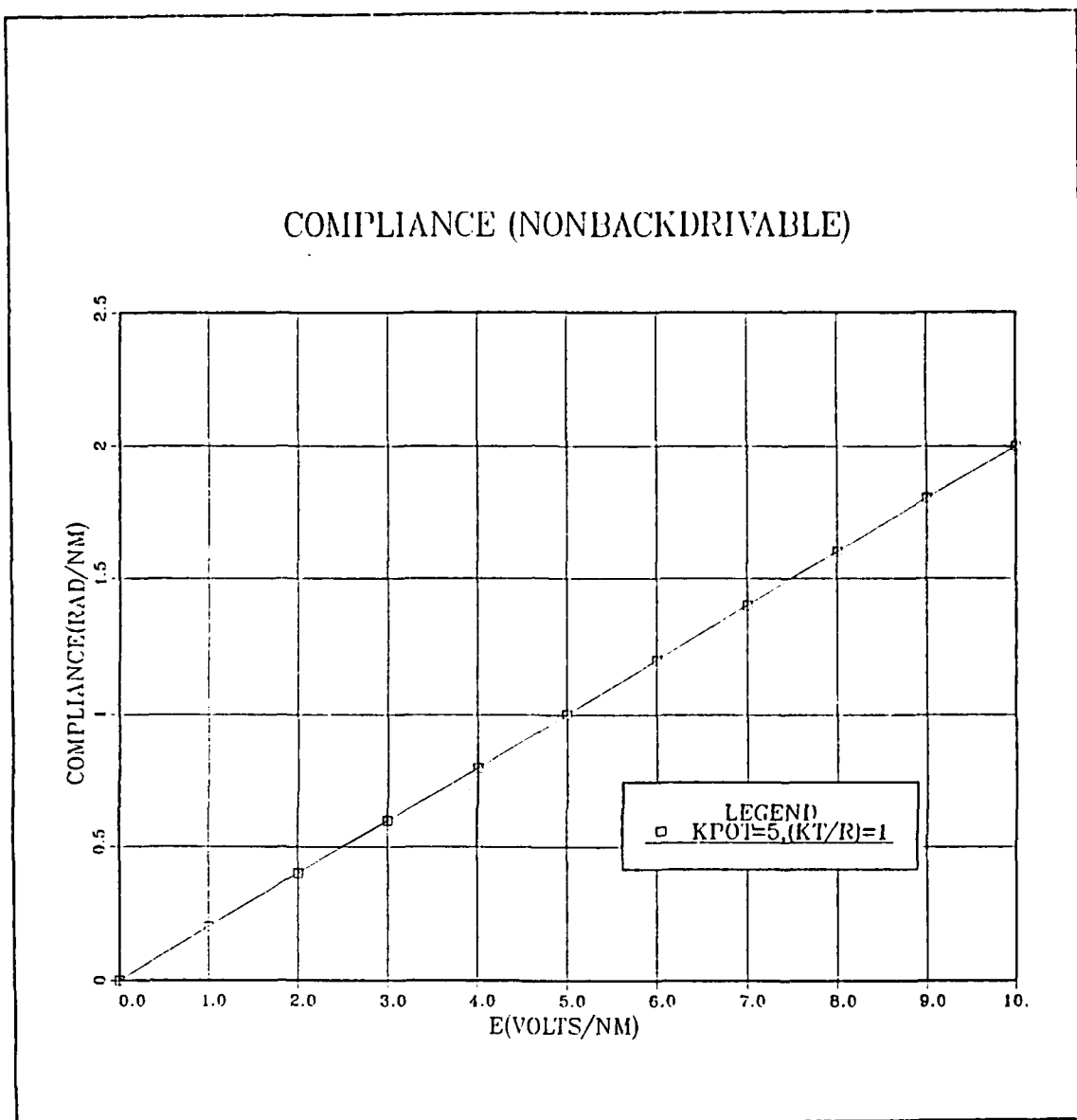
Figure 18.   Compliance Variation of a Servo System (nonbackdriveable).
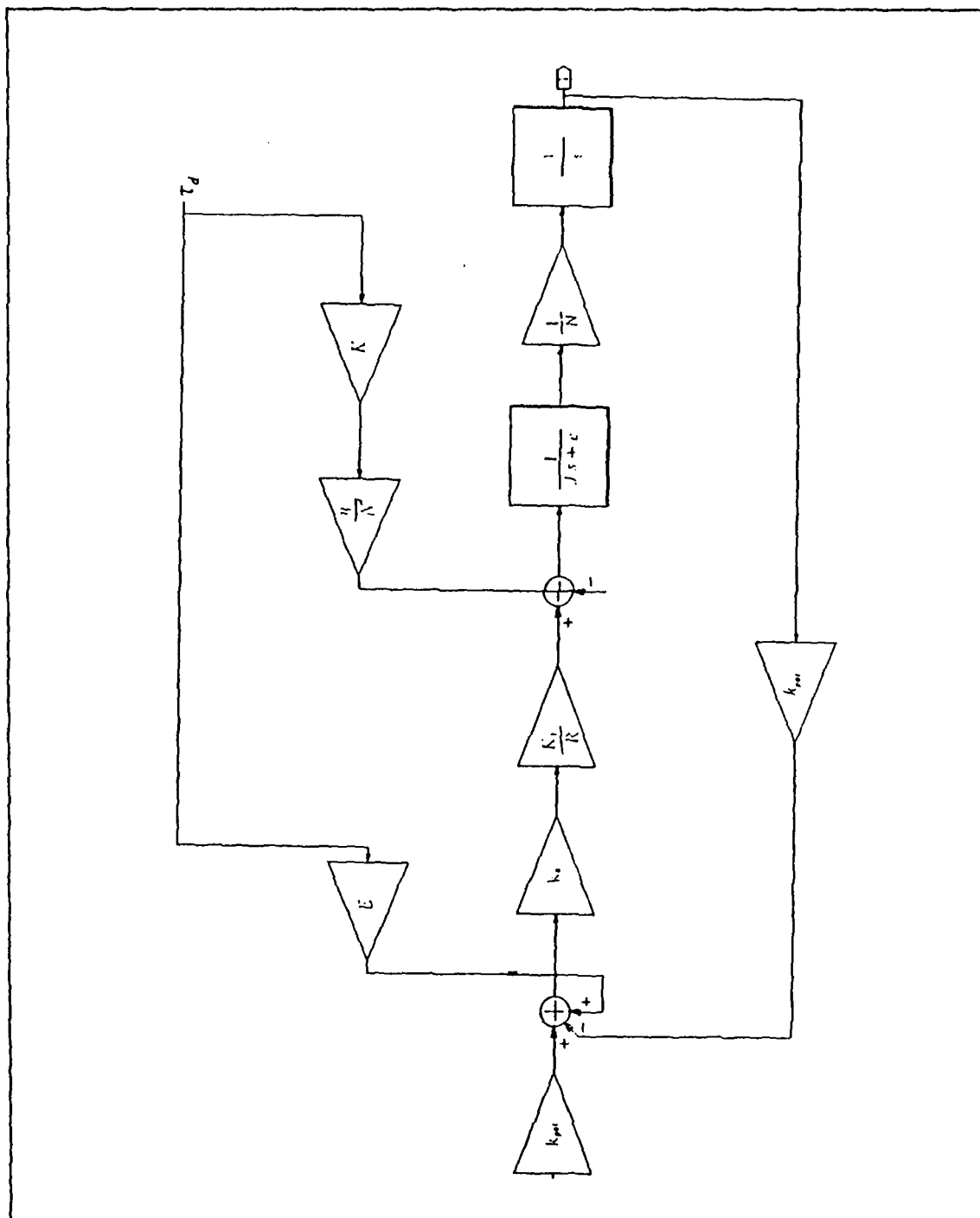
Figure 19. Position Control System Including Efficiency and Backdrivability.

III. SYSTEM PARAMETER IDENTIFICATION

Electric motors used with end effectors or robotic finger joints, are usually small motors, hence, it is difficult to observe the variation in the compliance and the stiffness of these kind of systems. It is also difficult to measure certain parameters experimentally, therefore, a larger servo system was used to observe and to prove compliance theory.

A feedback ES151 educational servo system, together with suitable test equipment was used to prove compliance and stiffness theory. This is a high quality electromechanical servomechanism, consisting of three basic units: actuator unit, educational servo unit and accessories and spare parts as shown in Figure 20.

The actuator unit is essentially a 24 v electric motor unit, a tachogenerator, gear box, output disc and a potentiometer.

The educational servo unit is the control unit of the system. It contains all the necessary power supplies for the system to operate. The main parts of this unit are command input, control circuits, preamplifier, servo amplifier, schematic of the actuator unit, current meter and on off switch as shown in Figure 21.

The ES151 educational system is built for standard position control. The block diagram of the general system as a standard position control system is shown in Figure 22. As can be seen from the block diagram after, applying a voltage to the motor, an angular velocity of the motor shaft is obtained. Dividing motor shaft's angular velocity by the gear ratio, the output shaft angular velocity is obtained. Integration of this angular velocity gives position of the output shaft. Voltage obtained by using another potentiometer attached to the output shaft, fed back to the system as a negative signal. The sum of two voltages gives an error voltage which drives the motor. Finally
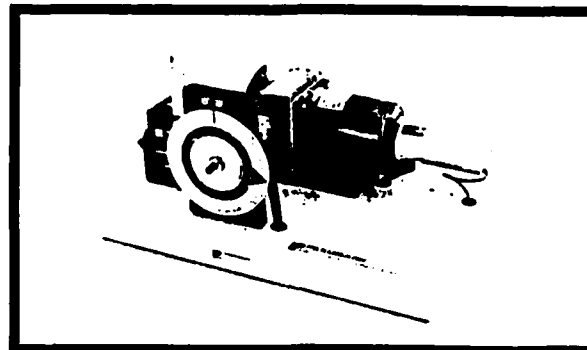
Actuator Unit
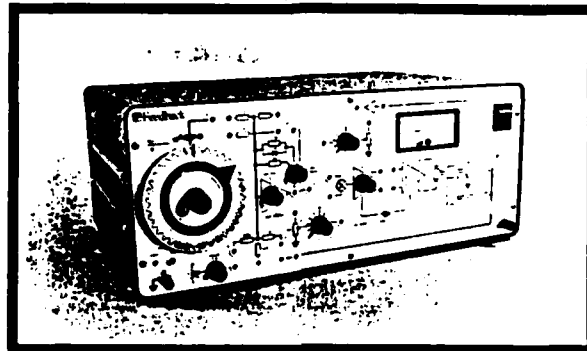
Educational Servo
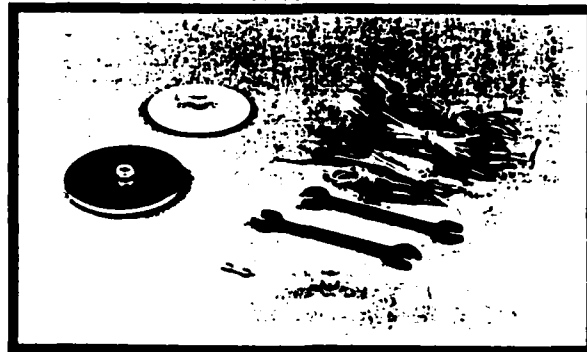
Accessones & Spares

Figure 20.   Feedback ES151 Educational Servo System.
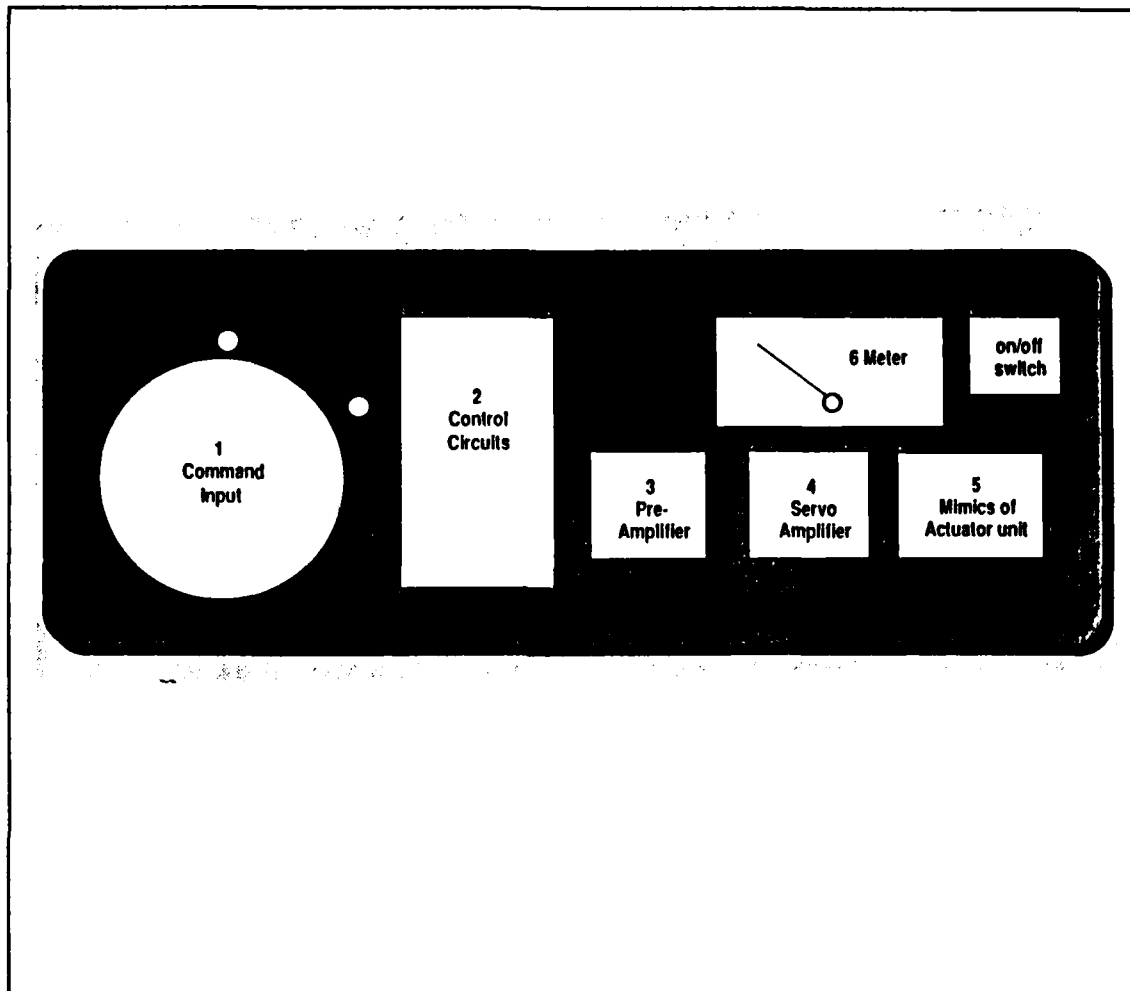
Figure 21. Educational Servo Unit.

the output shaft angular displacement will be the same as input displacement introduced to the system by using command input.

In the block diagram the following constants are used.

K_r = Motor constant (rad/sec/volt)

k_{pot} = Potentiometer constant (volt/rad)

k_b = Back emf constant (volt/rad/sec)

T_m = Mechanical time constant (sec)
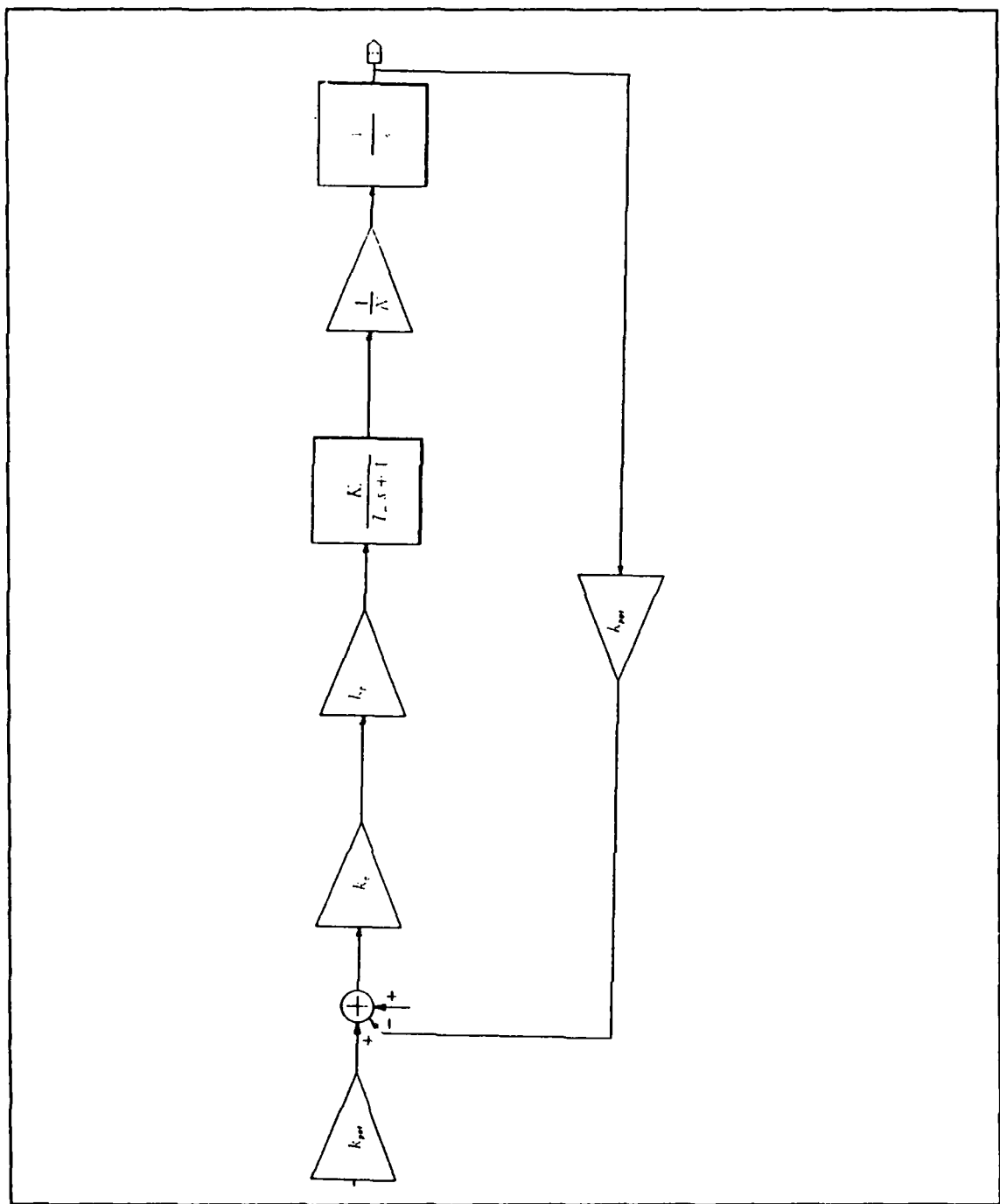
Figure 22. Block Diagram of Educational System As a Standard Position Control
system.

k_a = Control amplifier constant (forward path gain, servo amplifier gain)

k_p = Power amplifier constant

The main difference between this diagram and the standard position control system diagram, which was presented in chapter 2, is k_p. This constant gain is added to the system to increase the voltage going to the motor. It amplifies the potentiometer's output voltage and matching it to the DC motor. The procedure for finding these constants experimentally is a standard laboratory exercise (ME 3802) and presented in appendix A. Estimated values of these parameters are as follows

K_i = 270 rad sec/volt (when k_a = 0.7)

$k_v = k_b$ = 0.0022 volts/rpm

k_{pot} = 5.7   volts rad.

T_m = 0.25   sec. (open loop time constant)

and $0 < k_a < 1$.

As stated at the beginning of the chapter, the main reason for using this system is to experimentally prove the compliance and stiffness theory previously discussed. The block diagram for the ES151 system is somewhat different from that used in the development of the theory of variable compliance - see Figure 22 and Figure 23. For this reason, conversion of the identified parameters to those necessary to determine the stiffness are necessary. The following equations indicate the equivalence of the parameters. As can be seen from the figures, a new variable k_p is added to the both systems, in order to match educational systems block diagram with   position control systems block diagram.

$$\frac{\frac{K_T}{Rc}}{1 + \frac{J}{c}s} = \frac{K_s}{1 + T_m s} \tag{3.1}$$

Therefore,
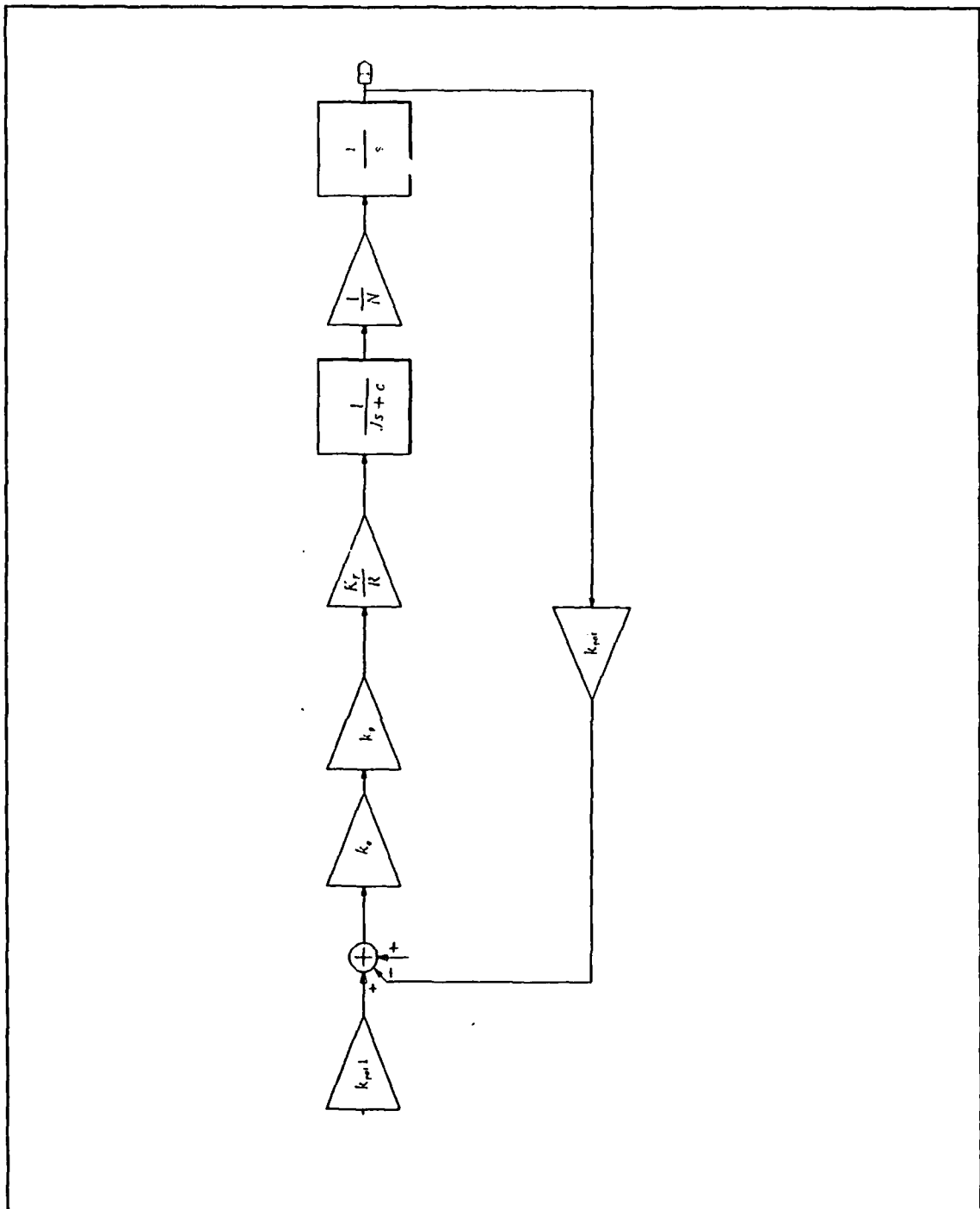
Figure 23. Block Diagram of Position Control System.

$$T_m = \frac{J}{c} \quad \& \quad K_s = \frac{K_T}{Rc}. \tag{3.2}$$

K_T = Motor torque constant (Nm/Amp)

R = Resistance (ohm)

J = Total inertia (Nm sec**2/rad)

c = Total damping (Nm sec/rad)

In equation (3.1) and (3.2), the value of T_m and K_s are known. Therefore, the value of c can be found after finding the value of J. The value of J may be found by performing a torsional pendulum experiment.

1. **Torsional pendulum experiment:**

This experiment requires a collet, a piece of wire with known modulus of rigidity and a stop watch. The armature of the motor is taken out and attached to the wire by way of the collet. Then the wire is attached to a fixed support where armature's free movement can be observed, as shown in Figure 24. A half twist is given to the armature and allowed to oscillate freely. The equation of motion of the system will be as follows

$$J\ddot{\theta} + K\theta = 0 \tag{3.3}$$

J = Moment of inertia of the armature.

K = Torsional stiffness of the wire.

The angular frequency of the system will be as follows

$$\omega = \sqrt{\frac{K}{J}} \tag{3.4}$$

ω = Angular frequency of the system.

41

Then, $J = \dfrac{K}{\omega^2}$.

To find the angular frequency of the system, time was recorded for ten oscillation of the armature. Dividing the time by number of oscillation gave the period of the motion in sec cycle. Then, it was converted into angular frequency in rad/sec. The stiffness of the wire was calculated by using following formulas.

$$\frac{T}{\theta} = \frac{GI}{l} \tag{3.5}$$

Where $I = \dfrac{G\pi d^4}{32l}$.

G = Modulus of rigidity.

l = Length of the wire.

d = Diameter of the wire.

T = Torque.

The measured dimensions and properties of the wire were:

d = 2.54E-4 m l = 0.61595 m

G = 40 Gpa.

The following results were obtained:

$\omega = 1.239 rad/sec$ & $K = \dfrac{T}{\theta} = 2.65E - 5 Nm/rad.$

So, $J = 1.726E - 5 \dfrac{Nm \, sec^2}{rad}$

Since, J is now known, the value of c can be calculated by using following equation.

$$c = \frac{J}{T_m} = \frac{1.726E - 5}{0.25} = 6.9E - 5 \frac{Nm \, sec}{rad.} \tag{3.5}$$

After finding the value of c, the only unknown will be $(\dfrac{K_T}{R})$. This value may be found by performing a speed-torque experiment.
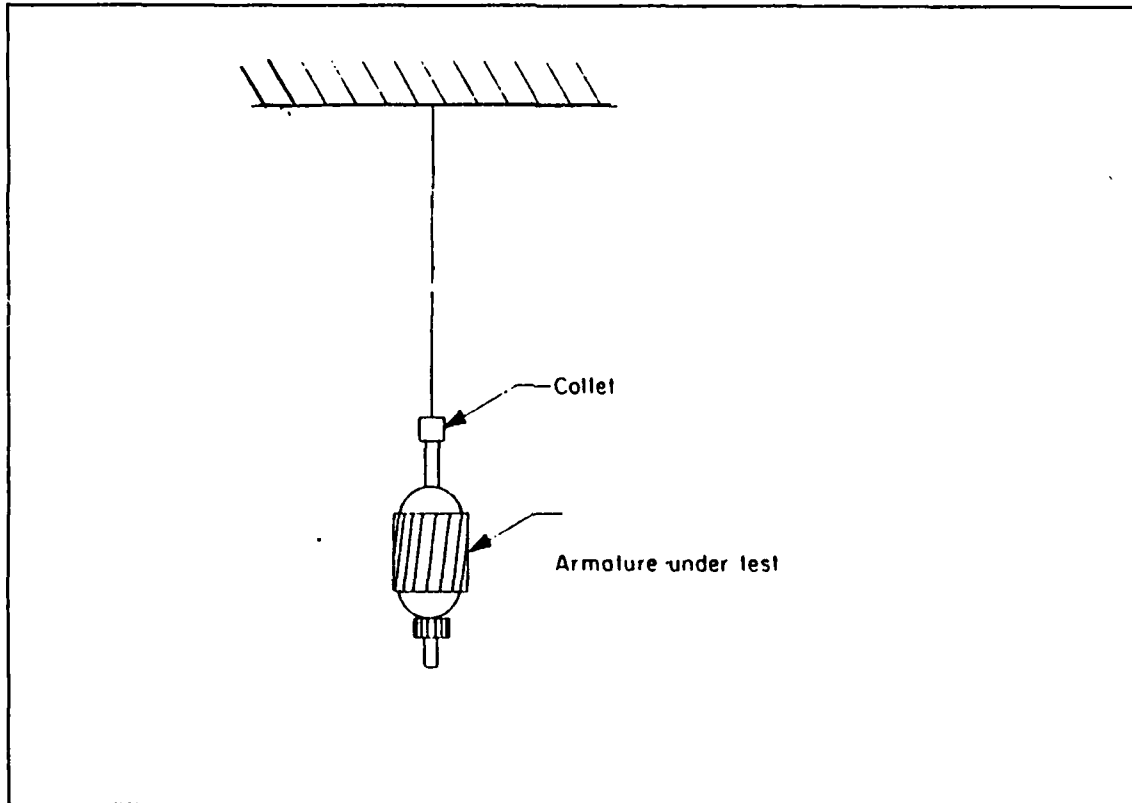
Figure 24.   Torsional Pendulum.

2.   Speed-Torque Experiment:

When a constant voltage is applied to the motor terminals, the motor shaft will accelerate and attain a final steady state velocity. This may be explained mathematically by using open loop block diagram of the position control system in Figure 25.

The equation of motion of the system will be as follows

$$\omega_m = \frac{1}{Js + c} \left[\frac{T_d}{N} + \frac{K_T}{R} (k_a k_p V_l - k_b \omega_m) \right]$$ (3.6)

Steady state response of the system into a step input as disturbance with constant V_l will be
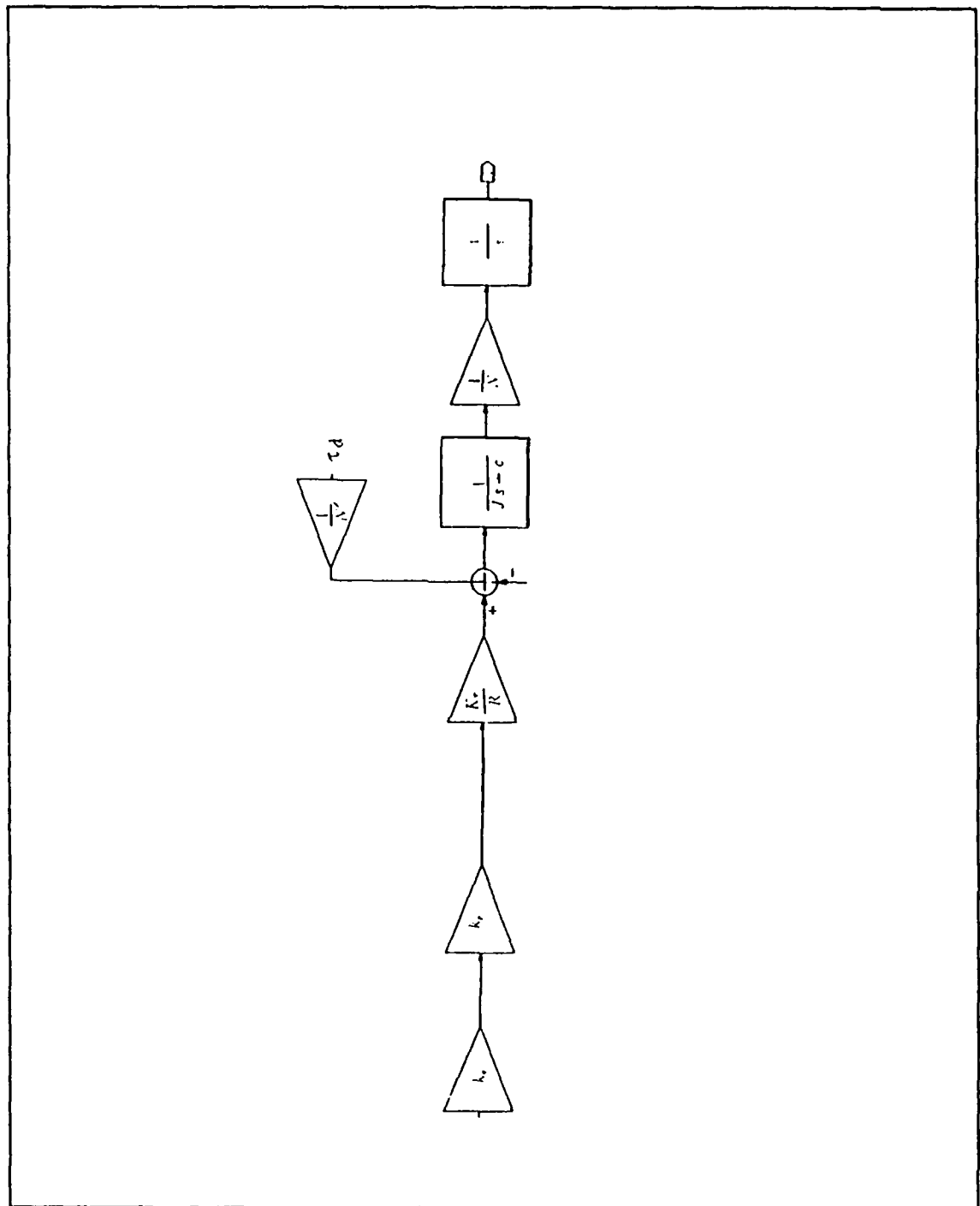
Figure 25.   Open Loop Speed Control System.

44

$$\omega_m = \left[\frac{-T_d}{N(c + \frac{K_T k_b}{R})}\right] + \left[V_i \frac{\frac{K_T k_p k_a}{R}}{c + K_T \frac{k_b}{R}}\right] \tag{3.7}$$

Assuming $\frac{K_T k_b}{R} \gg c$

$$\omega_m = \left[\frac{-T_d}{(N \frac{K_T k_b}{R})}\right] + \left[V_i \frac{k_p k_a}{k_b}\right] \tag{3.8}$$

In equation (3.8) the value of $T_d < 0$ and $V_i =$ a constant. This equation is an equation of a straight line, which may be written as

$$Y = -mX + C \tag{3.9}$$

Here, m is the slope of the curve and is equal to $(\frac{1}{N k_T \frac{k_b}{R}})$.

C equals to $(V_i \frac{k_p k_a}{k_b})$. The only variable in equation (3.8) is τ_d. Since the value of $\tau_d < 0$, this curve will have a negative slope. When a constant V_i applied to the terminals of the motor without a braking or disturbance torque, ω_m without load will be obtained and is known as the no-load speed. This point will be X = 0 & Y = $V_i \frac{k_p k_a}{k_b}$. When the braking or disturbance torque applies enough torque to stop the motor, (-mX) will equal to C. This point will be Y=0 & X=τ_d on the curve and is known as the stall torque of the motor. This curve is shown in Figure 26. Since two points are known, the line can be drawn. To get necessary data, the following procedure may be carried out.

1. Establish a constant voltage, V_i.
2. Calculate the value of k_p & k_a.
3. From no-load speed calculate k_b.

45

4. From slope calculate $\dfrac{K_T}{R}$

However, the braking torque can not be applied directly to the output shaft in the educational system, because of the gear box has a worm gear in it. As discussed in chapter 2, this means that system is nonbackdriveable and the motor can not be stopped by applying the braking torque directly to the output shaft. That's why, the braking torque is applied to the motor shaft, so the value of N becomes 1 and the speed torque test is performed on the motor shaft, rather than on the output shaft.

After establishing a constant angular velocity, V_i was measured and found to be 0.43 volts.

Before applying the voltage to the dc motor there are two amplifiers. As stated above these are controller amplifier and power amplifier as shown in Figure 27. To find k_a, V_c and V_i voltages are measured. The ratio of these two voltages, namely $\dfrac{V_c}{V_i}$ gives k_a. After measuring V_m, the ratio of $\dfrac{V_m}{V_c}$ will give k_p.

From the ratio of $(\dfrac{V_m}{\omega_{NL}})$, the value of k_b may be calculated. Where, V_m is the input voltage to the motor and ω_{NL} is angular velocity of the motor shaft under no-load conditions.

Braking torque is applied to the motor shaft by attaching a torque lever arm to the motor shaft. A scale was put under this arm to measure the braking torque applied to the motor shaft. When the angular velocity of the motor shaft was zero, the scale showed 40 grams. The braking torque was found to be

$$\tau_d = WL \tag{3.10}$$

Where, $W = (40/1000)\text{kg} * (9.81 \dfrac{m}{\sec^2}) = 0.3924$ N (lifted weight) and $L = 0.224$ m.(length of the arm). After multiplying W by L, the value of τ_d was found. Then, the value of τ_d and ω_{NL} were plotted on the speed torque diagram. The results of the experiment may be summarized as follows

Measured data:

$V_i = 0.43$ volts

$V_c = 0.206$ volts

$V_m = 8.45$ volts

Derived data:

$k_a = (0.206/0.43) = 0.48$
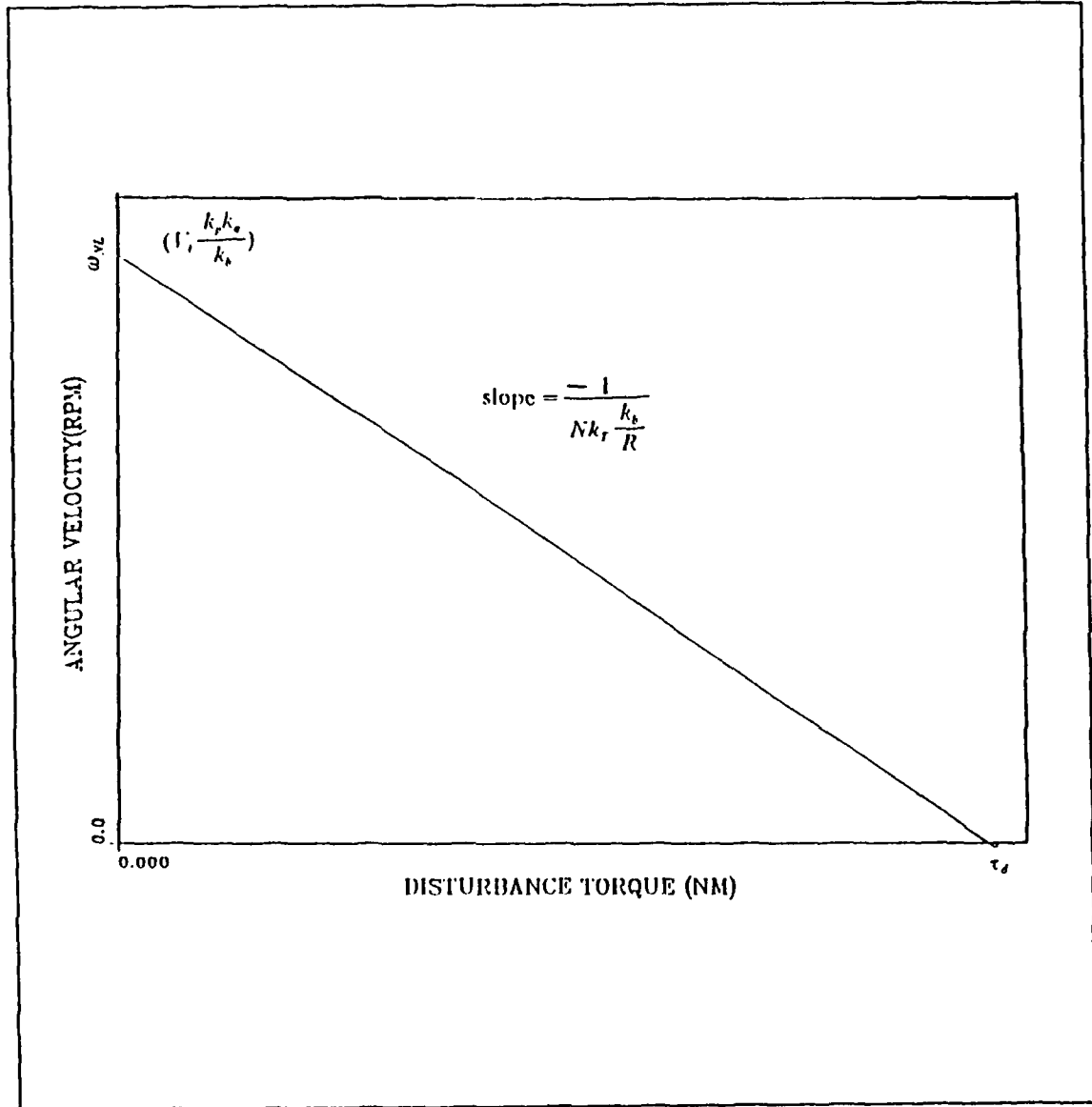
Figure 26.   Speed-Torque Curve.

$$k_r = (8.45/0.206) = 41$$

$$k_b = (8.45/5041) \text{volts/rpm} = 1.67\text{E-}3(\text{volts/rpm})$$

Hence finally

$$\frac{K_r}{R} = \frac{1}{mk_b} = 0.01 \, Nm/volts$$

The experimental speed/torque curve for the motor is shown in Figure 28.
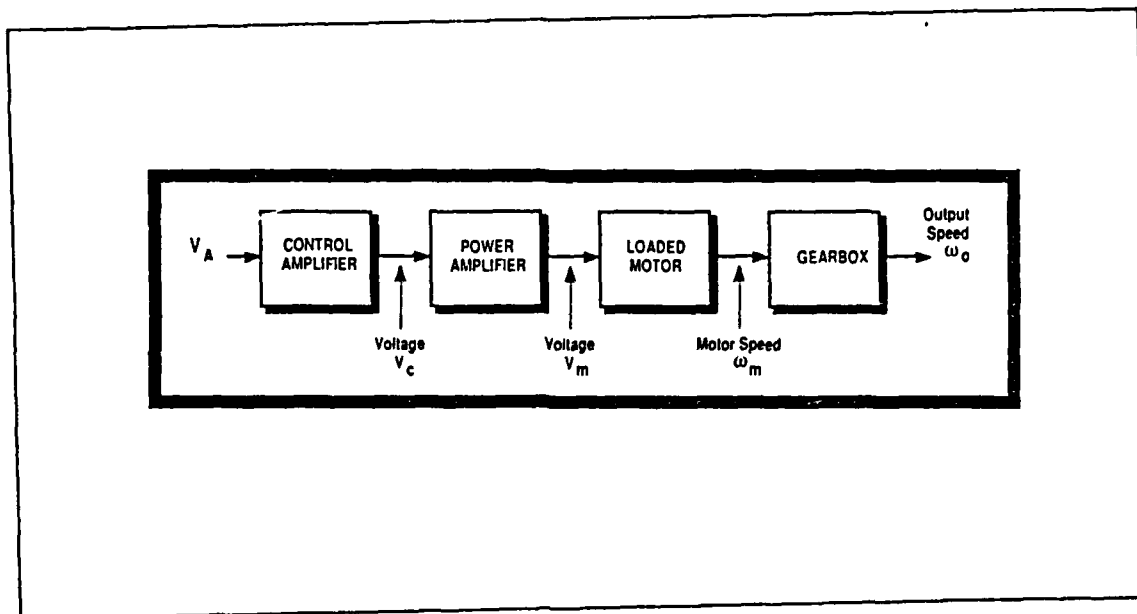
Figure 27. Power and Control Amplifier Block Diagram

Now that all parameters in the block diagram in Figure 23 have been identified, the system may be simulated in order to observe its steady state and transient response.

48
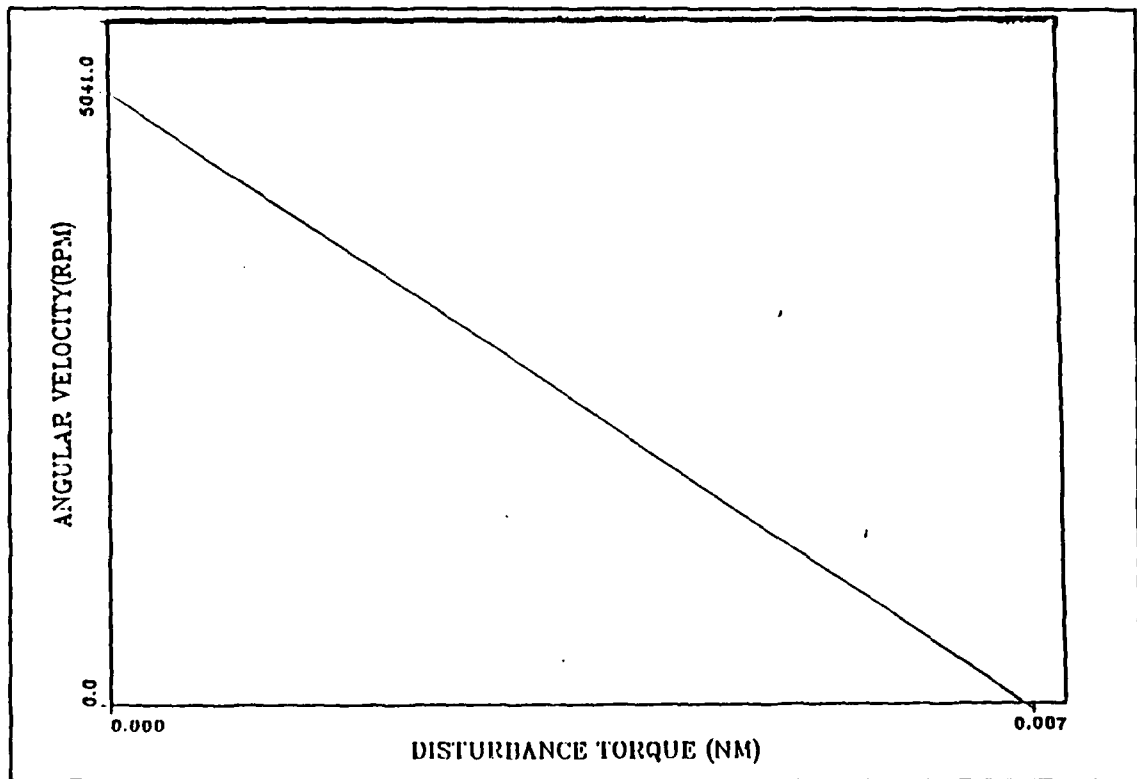
Figure 28.   Experimental Speed-Torque Curve.

IV. COMPUTER SIMULATIONS

Before performing experiments on the model, variation of the stiffness and compliance were observed by simulating the system with the *MATRIX$_x$* package program. Also, the system response to different kinds of inputs and the resulting transient response were observed.

As stated in Chapter III, the ES151 educational system has a worm gear in the gearbox, therefore the natural stiffness of the system was infinite. This means that, rotating the output shaft by using a disturbance torque, without feedback from the disturbance torque, was impossible. But this does not mean that motor shaft also has infinite stiffness. The following equations may give a better view of this situation.

$$K_o = \frac{\tau}{\theta_o} = \infty, \tag{4.1}$$

since, $\theta_o = 0$

However,

$$K_m = \frac{\tau}{\theta_m} \neq \infty \tag{4.2}$$

and therefore it is K_m which will be simulated.

K_o = system output stiffness.

K_m = motor shaft stiffness.

θ_m = motor shaft angular displacement.

θ_o = output shaft angular displacement.

Since, the disturbance torque is applied directly to the motor shaft, the gear ratio, the efficiency and backderiveablity constant will all be unity. The system block diagram

with gear ratio equals to one, including the parameters found in Chapter III, without feedback from the disturbance torque is shown in Figure 29.

As can be seen from the block diagram, a step disturbance was applie directly to the motor shaft, and θ_i is assumed to be constant.

The system step response is shown in Figure 30 ($\xi < 1$), Figure 31 ($\xi > 1$), and is seen to be that of a second order system.

Using the following formulas system characteristics may be found in terms of :

P.O. = Percent overshoot

T_p = Peak time

ξ = Damping ratio

T_s = Settling time.

$$T_p = \frac{\pi}{\omega_n \sqrt{1 - \xi^2}}$$

(4.3)

$$P.O. = 100e^{\frac{-\xi\pi}{\sqrt{1-\xi^2}}},$$

(4.4)

$$T_s = \frac{4}{\xi \omega_n}.$$

(4.5)

The transfer function of the system including the disturbance torque, k_p and keeping θ_i constant can be written as follows

$$\frac{\theta_o}{\tau_d} = - \frac{1}{NJs^2 + (cN + \frac{K_T}{R} k_b N)s + k_a k_p \frac{K_T k_{pot}}{R}}$$

(4.6)

51
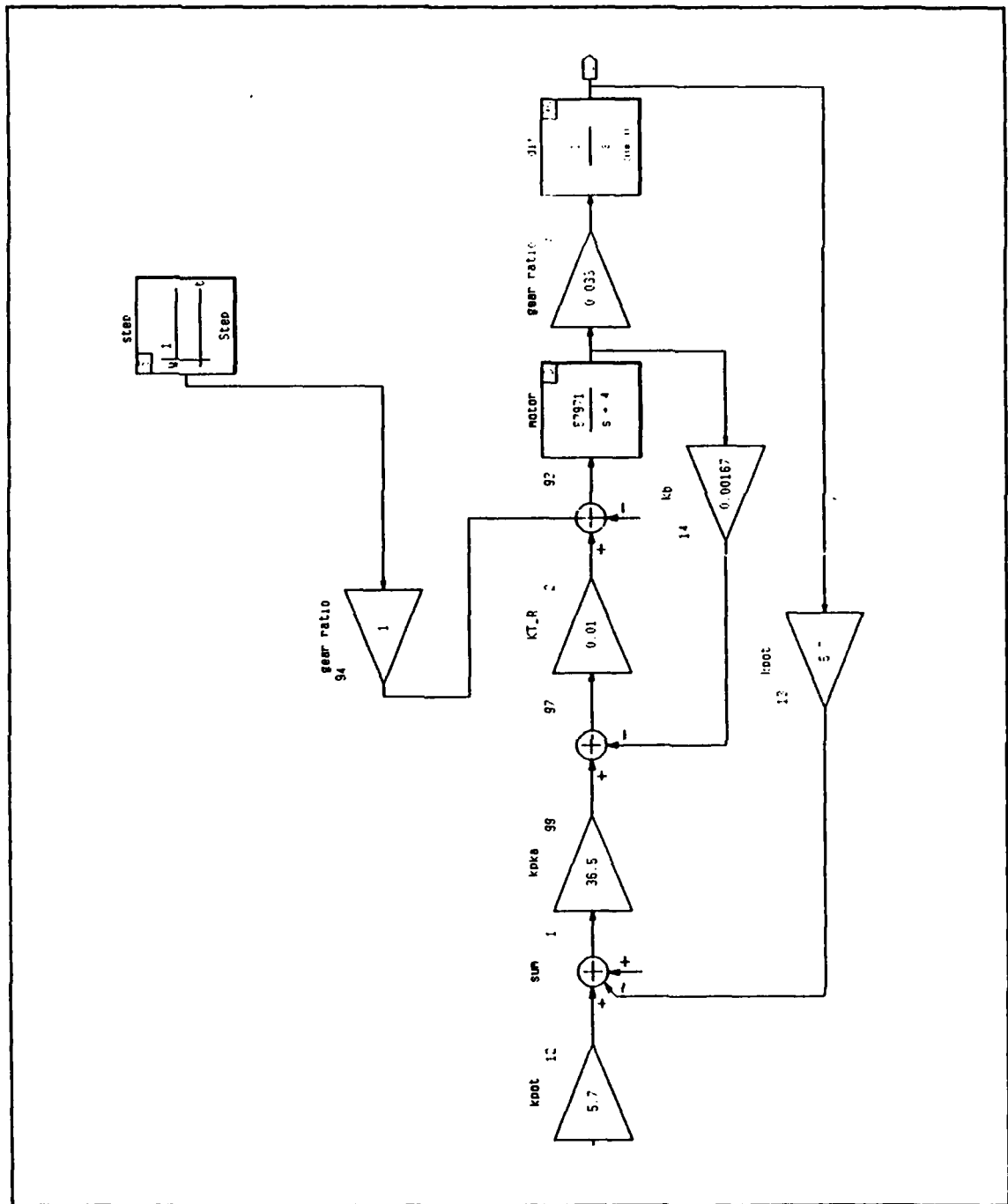
Figure 29. The Block Diagram of the Model With Unity Gear Ratio and Without Feedback From the Disturbance Torque.
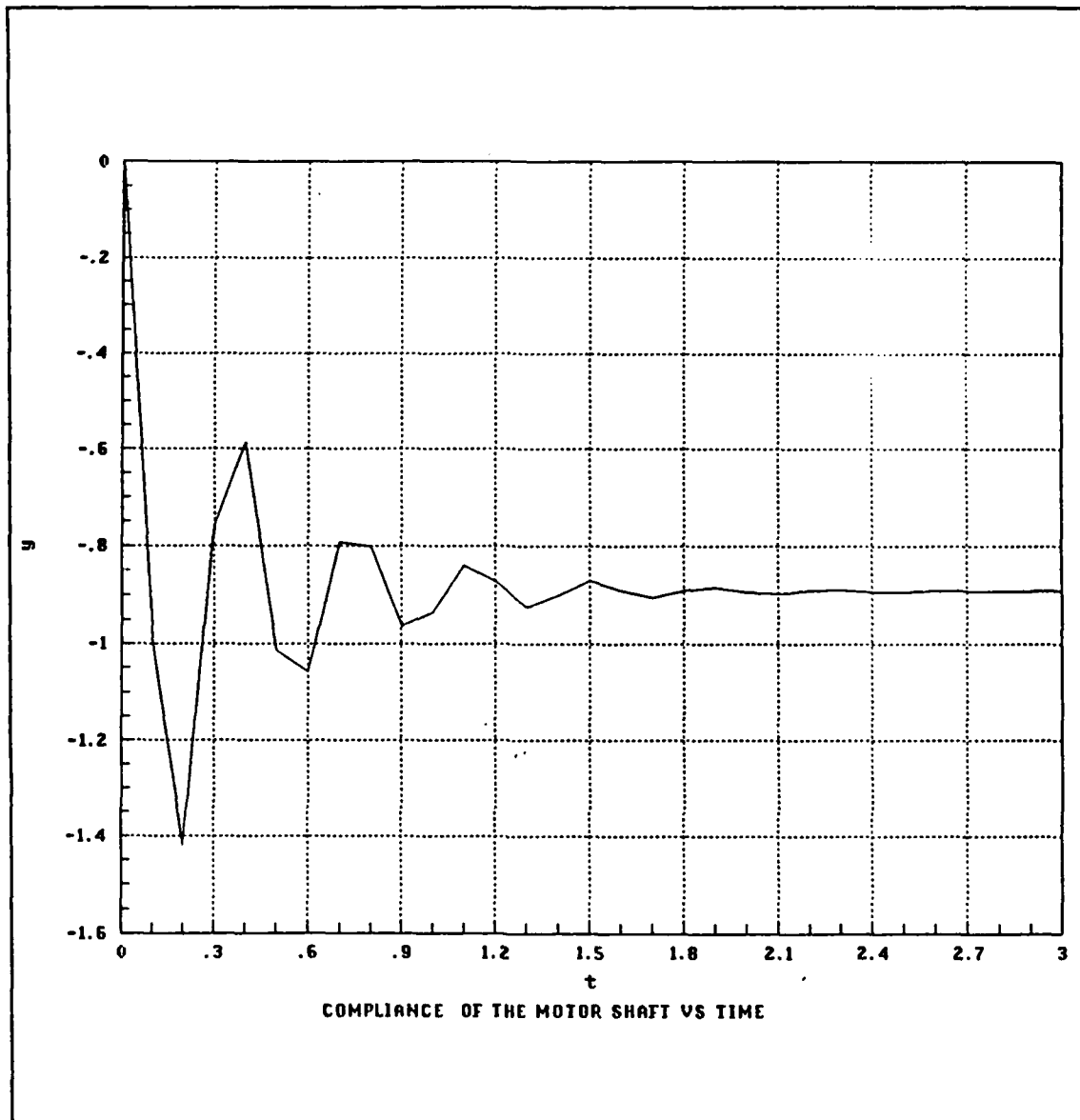
Figure 30. Step Response of the Motor Shaft, $\zeta < 1$.

Again using $\omega_m = Ns\theta_o$, the steady state response of the system to a disturbance torque is:

$$\frac{\theta_o}{\tau_d} = -\frac{R}{k_a k_p k_{pot} K_T} \tag{4.7}$$

53
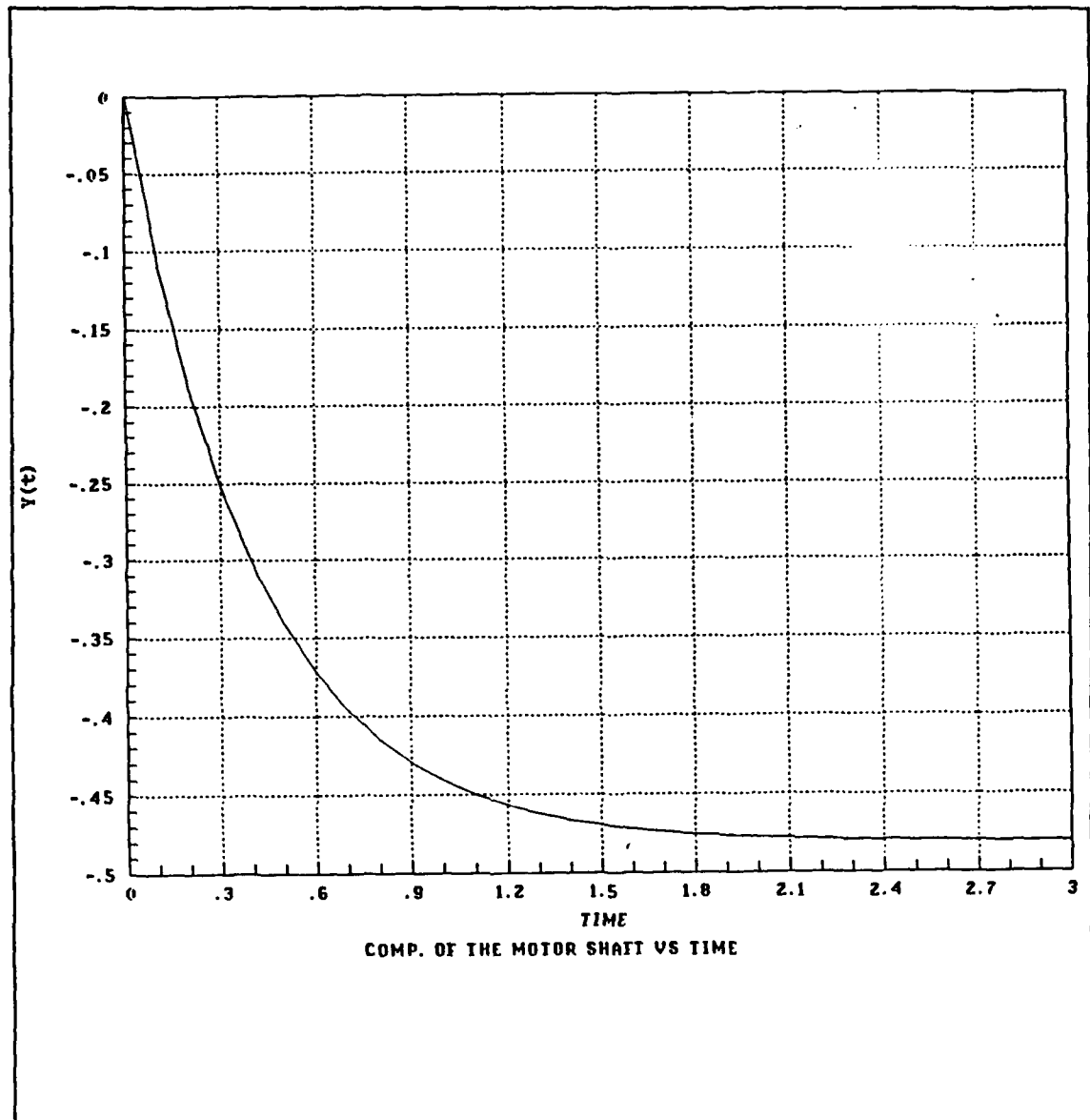
Figure 31. Step Response of the Motor Shaft, $\zeta > 1$.

So, the stiffness of the system will be

$$\frac{\tau_d}{\theta_o} = - \frac{k_a k_p k_{pot} K_T}{R} \tag{4.8}$$

54

Equation (4.6) may be approximated into the form of a regular second order transfer function. i.e.

$$\frac{\omega_n^2}{s^2 + 2\xi\omega_n s + \omega_n^2} . \tag{4.9}$$

To be able to get an ideal transient response, the damping ratio of the system must be adjusted. Having a P.O. close to 0 will provide the ideal transient response. For this reason, ξ or ω_n (natural frequency of the system) must be changed. The only variable in the system which can be effective in optimizing these values is k_a. As can be seen in equation (4.6), this value also effects the stiffness. To be able to obtain the optimum gain of k_a for ideal transient response and observe it is effect on the stiffness, the system was simulated with different values of k_a. It was observed that when $0.87 < k_a < 0.91$, the system had the ideal transient response as shown in Figure 31. The system response is presented in the form of compliance and as can be seen from the figure the steady state response of the system was as predicted in equation (4.7). But, it must be noticed that simulation gives us the compliance as measured at the output shaft, not the motor shaft, therefore, the result must be multiplied by the gear ratio which is 30 in this case. The inverse of this value gives the stiffness of the motor shaft.

$$\frac{\theta_m}{\tau_d} = \frac{-NR}{k_a k_p k_{pot} K_T} \tag{4.10}$$

where, $\theta_m = \theta_o N$.

Before designing and putting together the necessary experimental system, the effect of the gain E on the system transient response must be determined, therefore, the torque feedback as presented in the theory section was added to the system. After adding this feedback, the system stiffness may be changed from infinity to a finite value. Since, the

system is nonbackdiriveable, K is equal to zero. The complete system, with E = 1 and K = 0 is as shown in Figure 32.

The system was simulated by varying the gain E. It was observed that adding the torque feedback and changing the values of the gain E did not effect the transient response of the system. It was also observed that the variation of stiffness and the compliance was as predicted earlier in the theory section. To be able to observe the effect of backdriveablity, the system was simulated with K = 1 and efficiency equals to 0.95. These did not effect the transient response of the system either.

As a result, by changing the value of k_a system transient response can be adjusted and ideal value found to be 0.89. Adding the gain E, K , η to the system did not effect the transient response. The steady state response of the system also agreed with that predicted. It is concluded therefore that the system transient response and stiffness are independent, as may be shown from the complete transfer function ($\theta_i = constant$) for the system in Figure 32.

$$\frac{\theta_o}{\tau_d} = \frac{(E)\dfrac{K_T}{R}}{NJs^2 + (cN + \dfrac{K_T}{R}k_bN)s + k_a\dfrac{K_Tk_{pot}}{R}} \qquad (4.11)$$
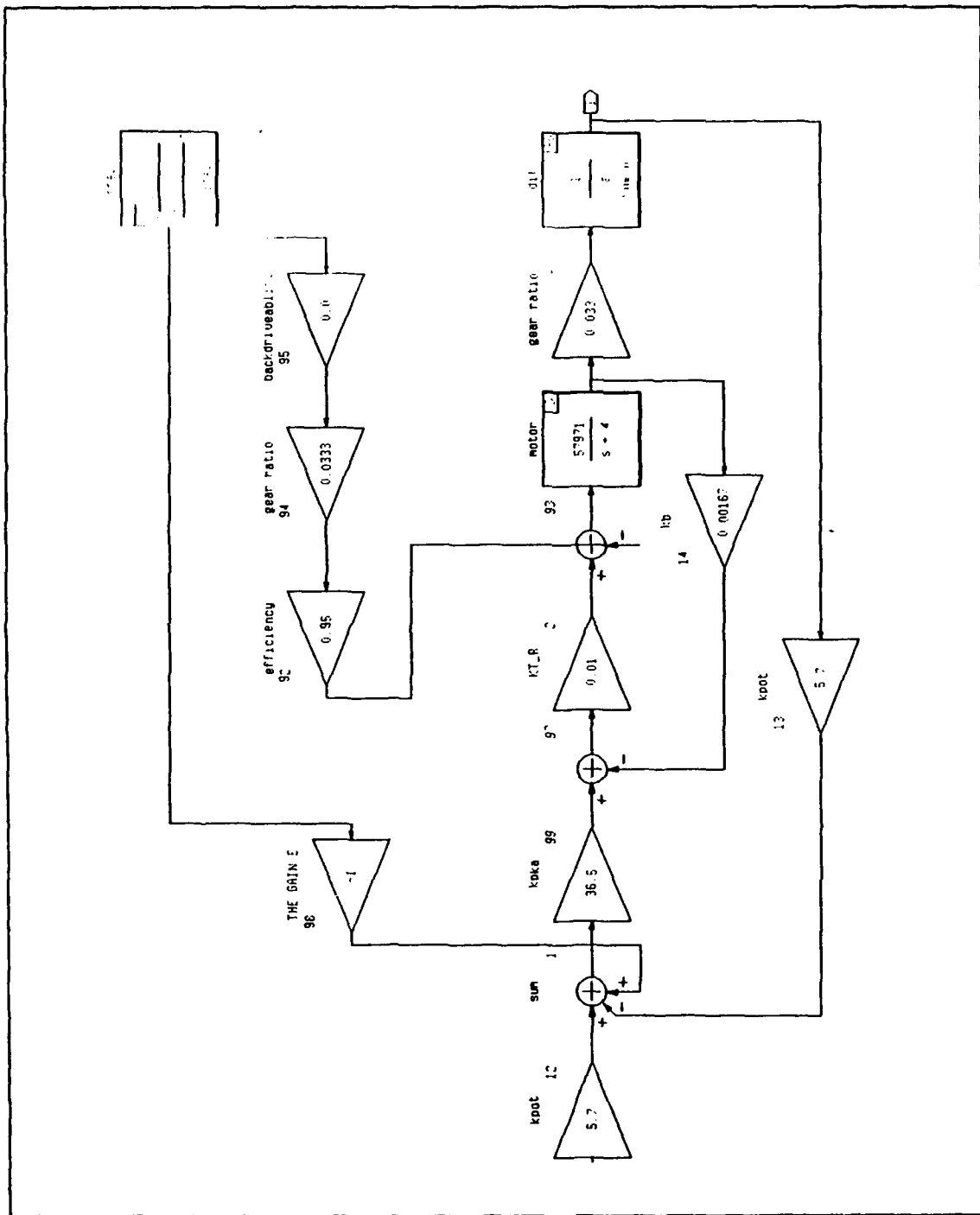
Figure 32.   Experimental Position Control System With E = 1 & K = 0.

V. EXPERIMENTAL STIFFNESS CONTROL

A. NATURAL STIFFNESS OF THE SYSTEM

As presented in the preceding chapters, every position control system has its own natural stiffness. One can feel the stiffness of the system when the output shaft is rotated. When we tried to rotate the output shaft of the educational system, it was observed that neither the output shaft nor the motor shaft rotated. Therefore, it was observed that the stiffness of the educational system was infinite. But when we tried to rotate the motor shaft, we felt the stiffness of the shaft. The stiffness felt at the motor shaft was very small, Therefore, it was not possible to measure it by attaching a lever arm to the shaft directly. The stiffness was not even enough to lift the weight of the lever arm. On the other hand it was enough to stretch a thin regular rubber band. Therefore, the stiffness of a DC motor shaft may be found by using a low force rubber band as a spring.

B. STIFFNESS TEST

For this experiment, a regular rubber band, a protractor, a ruler and two different weight units were used. The rubber band was attached to a fixed support where different weights can be applied. Then 0.25 lb.(0.1134 kg) unit applied to the band. Extended length of the band was measured and it was observed to be 4.8 in. (0.12192 m). When 0.50 lb. (0.2268 kg)was applied, the amount of stretch was 6.8 in. (0.17272 m). The stiffness curve (weight vs amount of stretch) was plotted by using these two measurement. The best fitting curve's slope gave the stiffness of the rubber band. The stiffness curve of the band is shown in Figure 33. Since, the stiffness of the rubber band is known, the amount of force applied by using this band may be found from the stiffness curve of the band or by using the following formula.

$$F = KX \tag{5.1}$$

Where, K = The stiffness of the band (the slope of the stiffness curve) and

X = Amount of stretch of the band.

If the applied force is known, torque may be found by multiplying the force by the moment arm.

$$\tau = FL \tag{5.2}$$

Where, L = Moment arm.

The protractor with a small screw on it was mounted to the motor shaft. The rubber band attached to the screw and stretched ensuring there was 90 degrees of angle between the rubber band and the moment arm as shown in Figure 34. Then, the amount of stretch in the rubber band length and the rotation of the shaft was measured. The following results were obtained:

X = 5 in. (0.127 m), rubber band extension.

L = 1.75 in (0.0445 m), moment arm.

θ_m = 80 degrees (1.4 radian), measured rotation of the motor shaft.

F = 1.226 N (from the curve using 5 in. extension), applied force. Then,

$$\tau = 1.226N \times 0.0445m = 0.055Nm. \tag{5.3}$$

So, the stiffness of the system was

$$\frac{\tau}{\theta_m} = \frac{0.055\ Nm}{1.4\ rad} = 0.039\ \frac{Nm}{rad.} \tag{5.4}$$

59
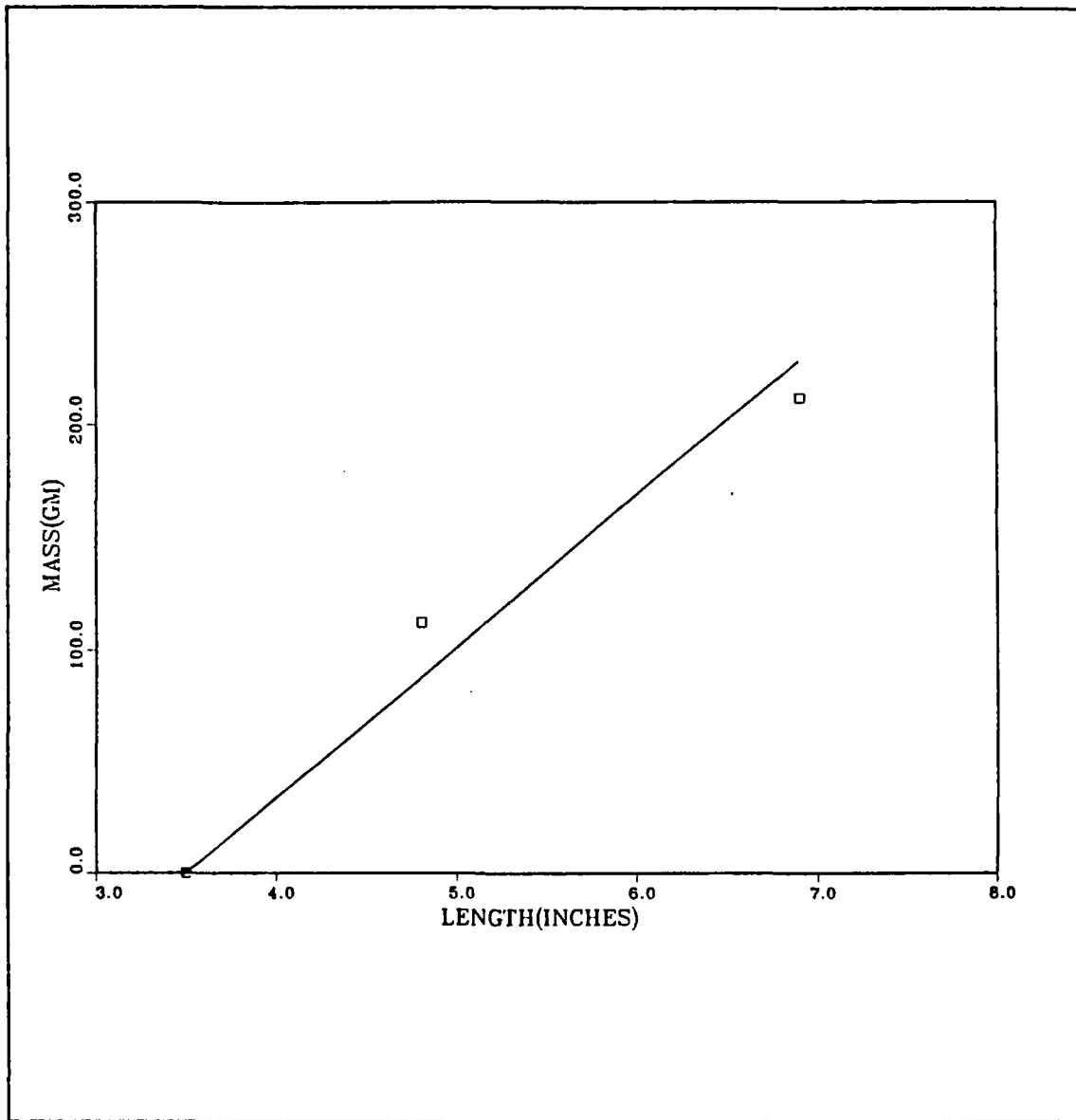
Figure 33.   The Stiffness Curve of the Rubber Band.

After the stiffness of the motor shaft was found, theoretical value of stiffness was calculated using the following equations.

The stiffness of the system, keeping θ_t constant, with $N'' = 1$ and using equation (4.6), may be written as

Figure 34. Application of the Rubber Band to the Motor Shaft.

$$\frac{\tau_d}{\theta_o} = -\frac{k_a k_p k_{pot} K_T}{R} \qquad (5.5)$$

Where, $\theta_o = \frac{\theta_m}{N}$. Then the stiffness of the motor shaft will be

$$\frac{\tau_d}{\theta_m} = -\frac{k_a k_p k_{pot} K_T}{RN} \qquad (5.6)$$

θ_m = Angular displacement of the motor shaft.

The measured values were

$k_a = 0.48$

61

$$\frac{K_T}{R} = 0.01 \ (\text{Nm / volt})$$

$$k_p = 41$$

$$N = 30$$

$$k_{pot} = 5.7 \ \frac{volts}{rad}$$

So, the stiffness will be

$$\frac{\tau_d}{\theta_m} = \frac{0.48 \times 41 \times 0.01 \times 5.7}{30} = 0.037 \ \frac{Nm}{rad} \tag{5.7}$$

When equation (5.7) and (5.4) were compared, it was observed that the percentage error was 5.4 %. So, it was concluded that the theoretical value of the natural stiffness of the motor shaft matched with the one found by performing the rubber band test.
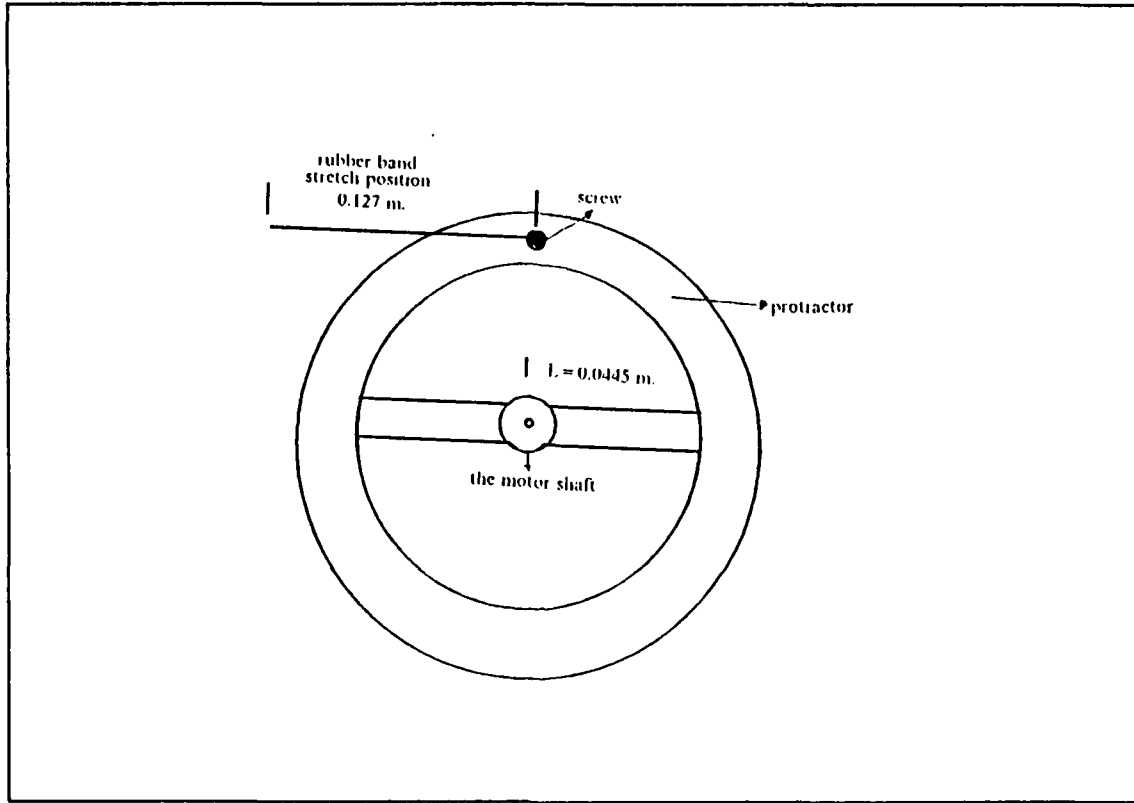
After finding the stiffness of the motor shaft, the variation of the stiffness of the system with the feedback gain E, may be observed and compared with the theory. The stiffness variation experiment may be performed to observe the variation of the stiffness.

C. STIFFNESS VARIATION EXPERIMENT

The disturbance feedback system was designed by using an aluminum lever arm, two strain gages, an amplifier, a protractor, a voltmeter and weight units.

Two strain gages were mounted on the site which is the closest point on the beam, to the output shaft. so as to be able to measure maximum strain. Also one strain gage was mounted top side and the other was mounted on the other side of the beam to be able to get maximum voltage as shown in Figure 35.

The beam was mounted on the output shaft as shown in Figure 35. The voltage obtained from two strain gages was fed back to system through an amplifier. The voltmeter was connected to the system to be able to measure and observe the value of the gain E. The amplifier provided us the ability to vary the gain E. The protractor was mounted on the motor shaft as in the rubber band test. The value of the gain E was
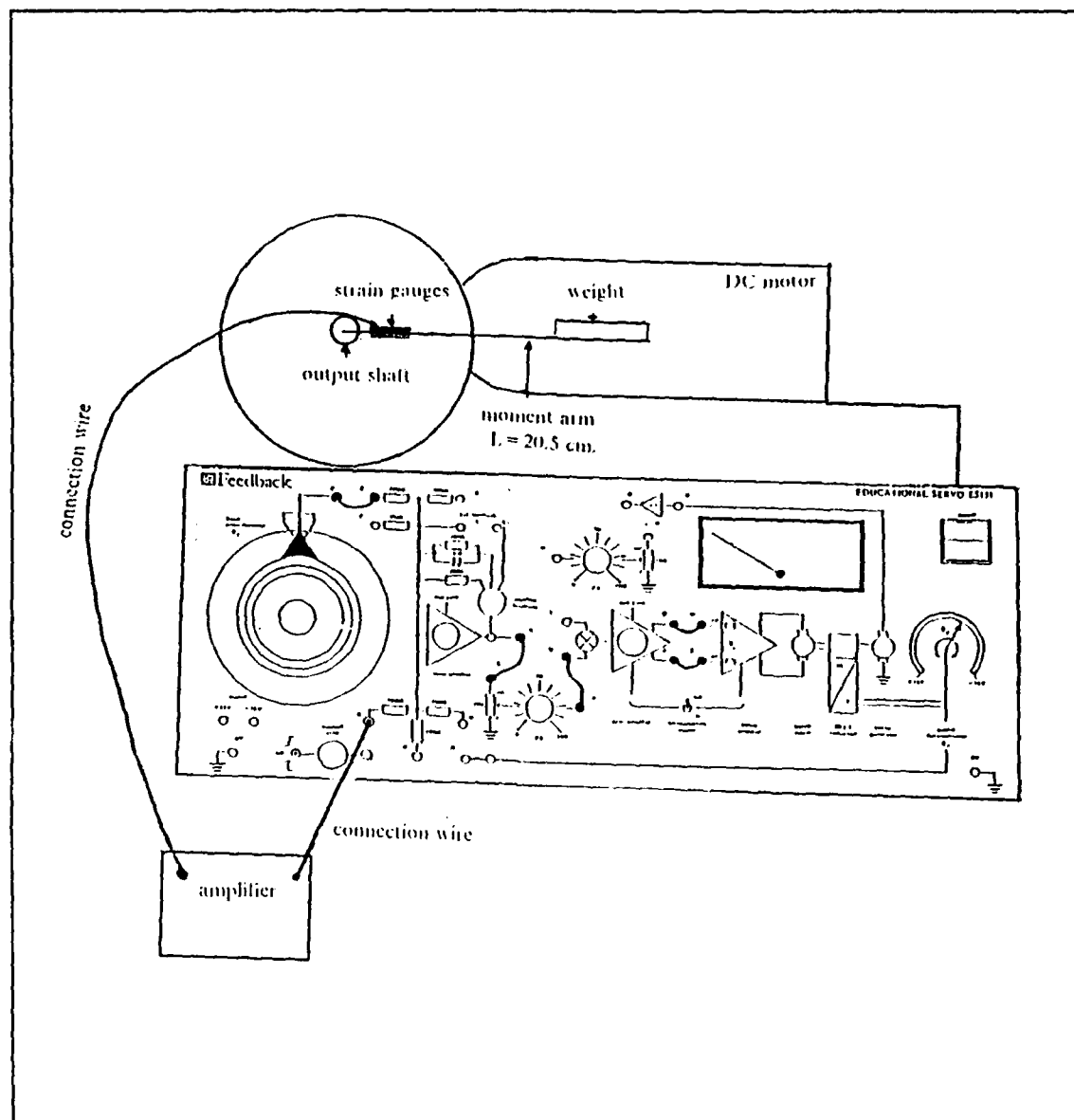
Figure 35. The Stiffness Variation Test.

changed by using the amplifier. After setting up the amplifier for certain values of the gain E, the beam was loaded with the weights as shown in Figure 35. Again the multiplication of the weight by the moment arm as presented in equation (5.3) gave the ap-

63

plied disturbance torque. The disturbance torque was calculated for two different weights. One set of data may be obtained by using the following method.

The gain E was adjusted to be 2 (volts Nm). The beam was loaded first with 0.25 lb.(0.1134 kg), then with 0.50 lb. (0.2268 kg) respectively. For each load the rotation of the motor shaft recorded. As can be noticed , the rotation was recorded for the motor shaft, not for the output shaft, because, it was easier to measure the rotation at this point. Then the applied disturbance torque was plotted against the rotation of the motor shaft for the two measurements as shown in Figure 36. The slope of the straight line gave us the stiffness of the system at the motor shaft. After obtaining necessary measurements, the stiffness of the motor shaft is converted to the stiffness of the system by using following formulas.

$$\frac{\tau_d}{\theta_m} = \frac{\tau_d}{\theta_o N} \tag{5.8}$$

The procedure may be summarized as follows.

Table 1.   EXPERIMENTAL DATA.

Load Torque, τ_d	Motor Shaft Rotation, θ_m	Strain gauge voltage.
0.228 Nm	3.157 rad.	0.456 volt.
0.456 Nm	6.6667 rad.	0.912 volt.

As can be seen above

$$E = \frac{0.456 volt}{0.228 Nm} = 2 \frac{volts}{Nm} \tag{5.9}$$
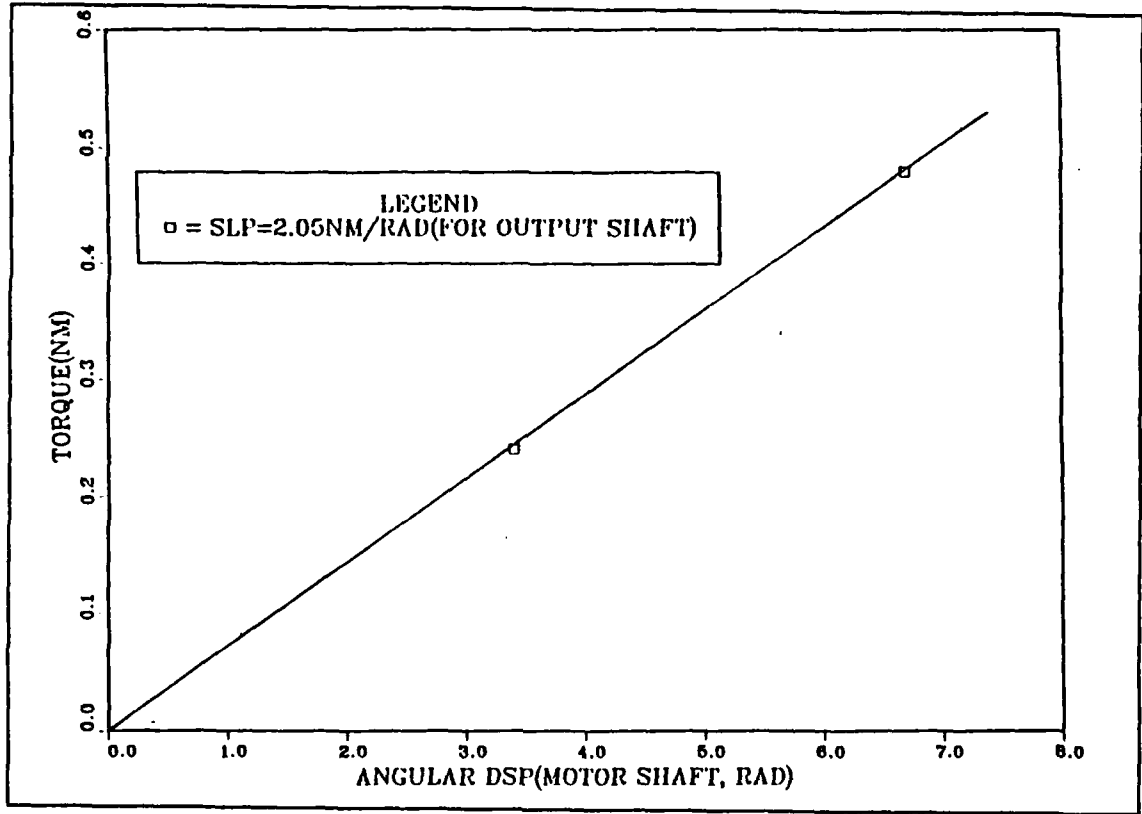
Figure 36.   The Stiffness Curve.

and from the plot the slope was 6.6366 E-2 (Nm / rad). The stiffness of the motor shaft was

$$\frac{\tau_d}{\theta_o} = 6.6366E - 2 \times 30 = 2.05 \frac{Nm}{rad} \qquad (5.10)$$

The above procedure was repeated for several values of E, and the corresponding stiffness determined. The results are summarized in table 2.

Table 2. EXPERIMENTAL RESULTS.

E(volt/Nm)	Stiffness (Nm/rad)
0.045	6.15
0.12	5.625
1.37	2.99
2	2.05
3	1.19

VI. ADAPTATION OF STIFFNESS CONTROL TO FINGER SYSTEM.

We have proven experimentally that we can vary the stiffness of a position control system by means of the torque feedback. We now apply this concept to our original goal of attempting to vary the stiffness of a single finger joint of a robotic hand . The problem is exactly the same as the one previously described, except that the motor characteristics are different and the motor used in the joint is smaller. Therefore, we may control the finger joint by using the same methodology used in the preceding chapters. The motor used in this research and its characteristics are shown in Figure 37. Some of the parameters may be obtain from the catalogue [Ref. 1]. These are :

K_T = 3.2 mNm A (0.453 oz-in/A)

R = 26 ohm

J = 0.03 E-7 kgm^2

T_m = 7 msec.

η = 0.6

N = 362

10 volts may be considered as a typical voltage that can be applied to a motor in a finger joint. If the potentiometer has 270 degrees of scale, then

$$k_{pot} = \frac{10 \ volts}{270 \ degrees} = 0.037 \frac{volts}{degrees} = 2.11 \frac{volts}{rad} \tag{6.1}$$

The value of k_b may be found from the following equation:

$$T_m = \frac{J}{c + \frac{K_T k_b}{R}} \tag{6.2}$$

67

scale 1:1
dimensions in mm
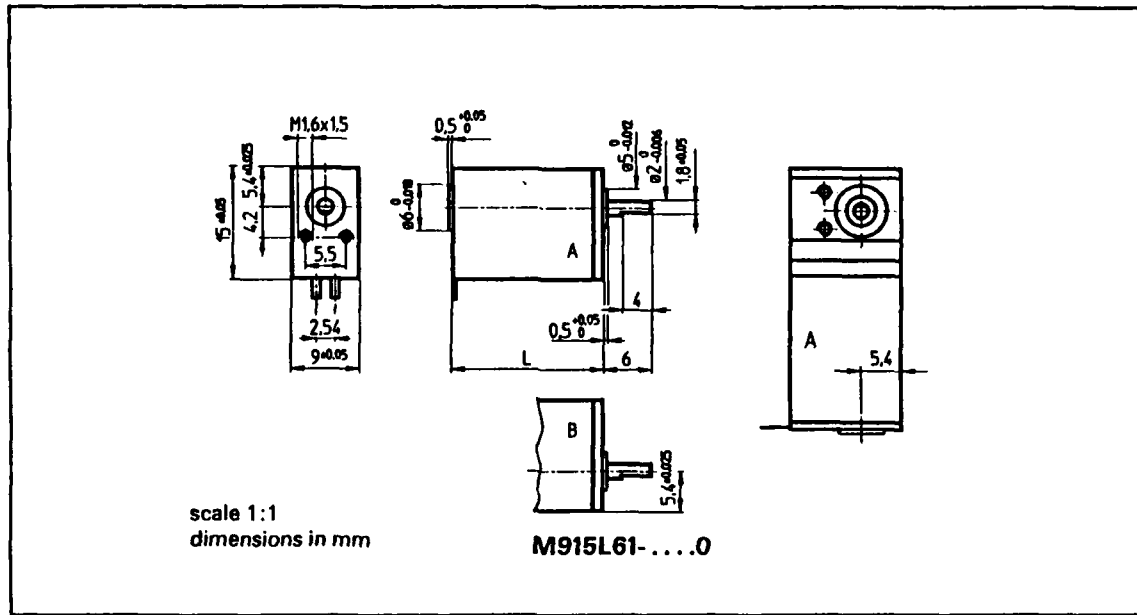
M915L61-....0

Figure 37.   M915L61 Electric Motor.

We can derive the following equation from equation (3.6), (3.7), (3.8).

$$T_m = \frac{RJ}{k_b K_T}$$

(6.3a)

Then,

$$k_b = \frac{RJ}{T_m K_T} .$$

(6.3b)

All values in equation (6.3b) can be obtained from the catalogue. So, $k_b = 3.48E - 3 \frac{volts\ sec}{rad}$.

Since, spur gears were used in the system, the system will be backdriveable. Therefore, K = 1.

After finding the necessary parameters, we can simulate the system. The block diagram of the system is shown in Figure 38. The only difference of this system from the

68

educational servo system is k_p. We don't need this gain in the finger joint system, because enough voltage can be supplied to the motor directly, but k_a can be used in the finger system to obtain desired close loop time constant. To be able to obtain an ideal transient response without overshoot the forward path gain must be $0 < k_a < 106$. The natural stiffness of the system, where $k_a = 1$ will be

$$\frac{\tau_d}{\theta_o} = \frac{\dfrac{K_T}{R} k_{pot}}{\dfrac{\eta}{N}} = \frac{1.23E - 4 \times 2.11}{0.0016572} = \frac{1}{6.385} \frac{rad}{Nm} = 0.157 \frac{Nm}{rad} \qquad (6.4)$$

In equation (6.4) the value of the natural stiffness of the system is also given as the inverse of the compliance, because again our simulation plot was the system compliance vs time. As can be seen from Figure 39, the system has no overshoot. Therefore, the system has ideal response and it is suitable for our goal. The system was also simulated for different values of the gain E and it was observed that the gain E doesn't effect the transient response of the system as expected. The stiffness variation of the system is presented in Figure 40.

To be able to adapt the position control system presented above to the finger system, the M915L61 electric motor was installed inside a brass case before the finger joint as shown in Figure 41 and an aluminum beam was used as a torque measurement system.

One of the most important parameter which will decide the dimensions of the beam for the finger tip was the length and the width of the strain gages. The total length was therefore determined to 1.5 cm (0.59 in). and the width was 0.3 cm (0.118 in). Two strain gauges for each side, a total four strain gauges were mounted on the beam to get maximum voltage. The width of the beam was decided to be 0.95 cm (0.375 in). The maxi-
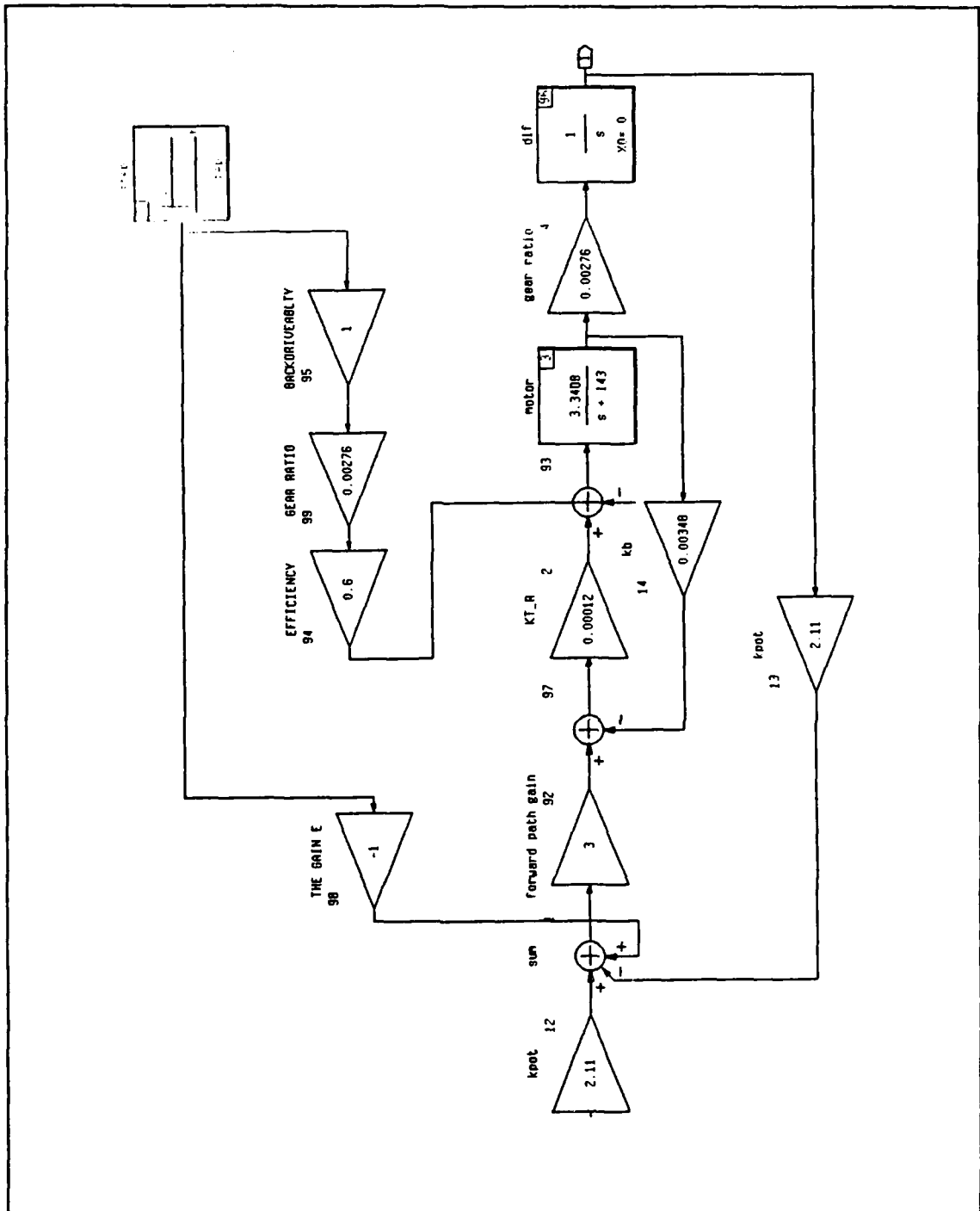
Figure 38. The Finger Joint System Block Diagram.
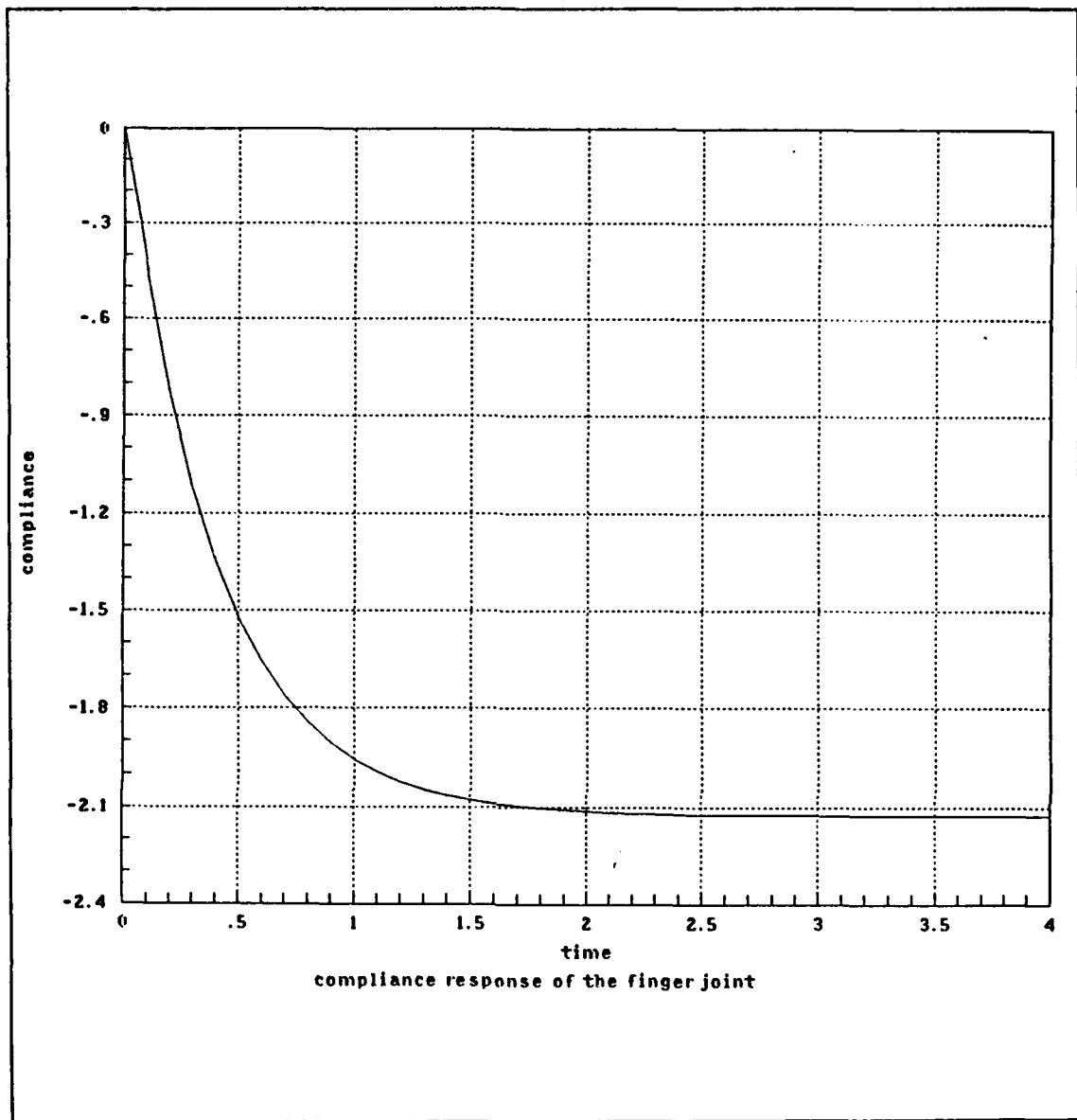
Figure 39. The Finger Joint Simulation, $k_a = 3$, $E = 0$ (without torque feedback)

mum force can be applied to the beam was considered to be 10 lbf or 44.48 N. Therefore, using the following formula, the deflection of the beam may be obtained.

$$y_{max} = \frac{F\ l^3}{3\ E\ I} \qquad (6.5)$$

71

Figure 40.   Variation of the Stiffness in the Finger Joint System.

Where,

y_{max} = Maximum deflection of the beam

F = Applied force

l = Working distance of the beam, 2.54 cm. (1 in)

72
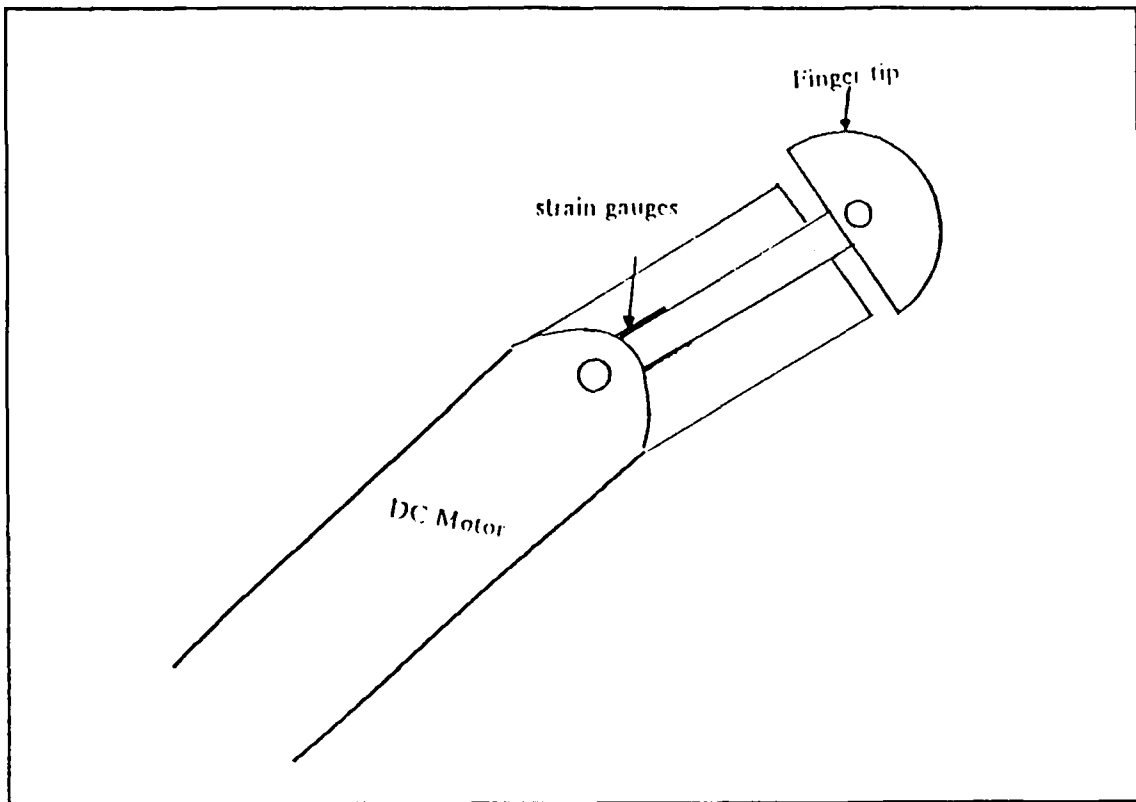
Figure 41. The Finger Joint System.

E = Modulas of elasticity, for aluminum, 71 Gpa.

I = Moment of inertia, 3.167 E-4 cm^4.

b = Width of the beam, 0.95 cm (0.375 in)
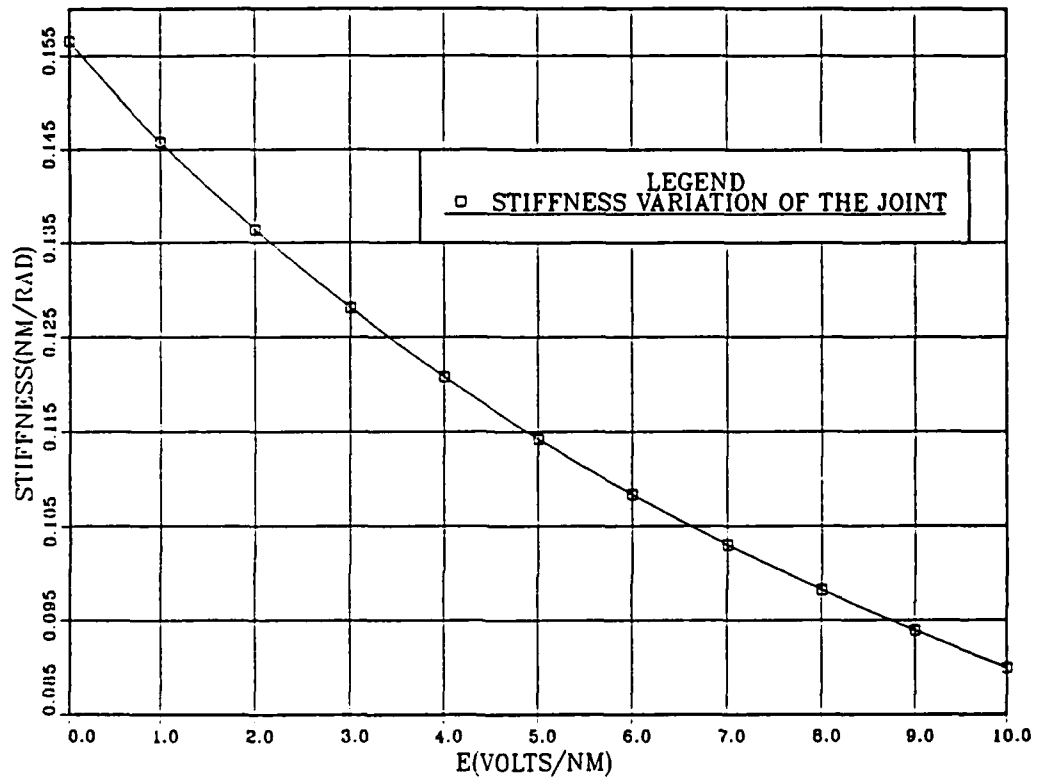
h = Thickness of the beam, 0.159 cm. (0.0625 in)

A plot of deflection of the beam for different forces is presented in Figure 42.

As can be seen from the Figure 41, the finger tip is only attached to the beam and not to the finger case, therefore it is free to move. When the disturbance torque is applied to the finger via finger tip, the beam to which the tip is attached will be deflected. So, by feeding back the voltage obtained from the strain gauges to the system, the stiffness of the system may be changed as presented in preceding chapters.

FORCE VS DEFLECTION

Figure 42.   Deflection of the Beam.

VII. DISCUSSION

A. MODELING OF THE SYSTEM:

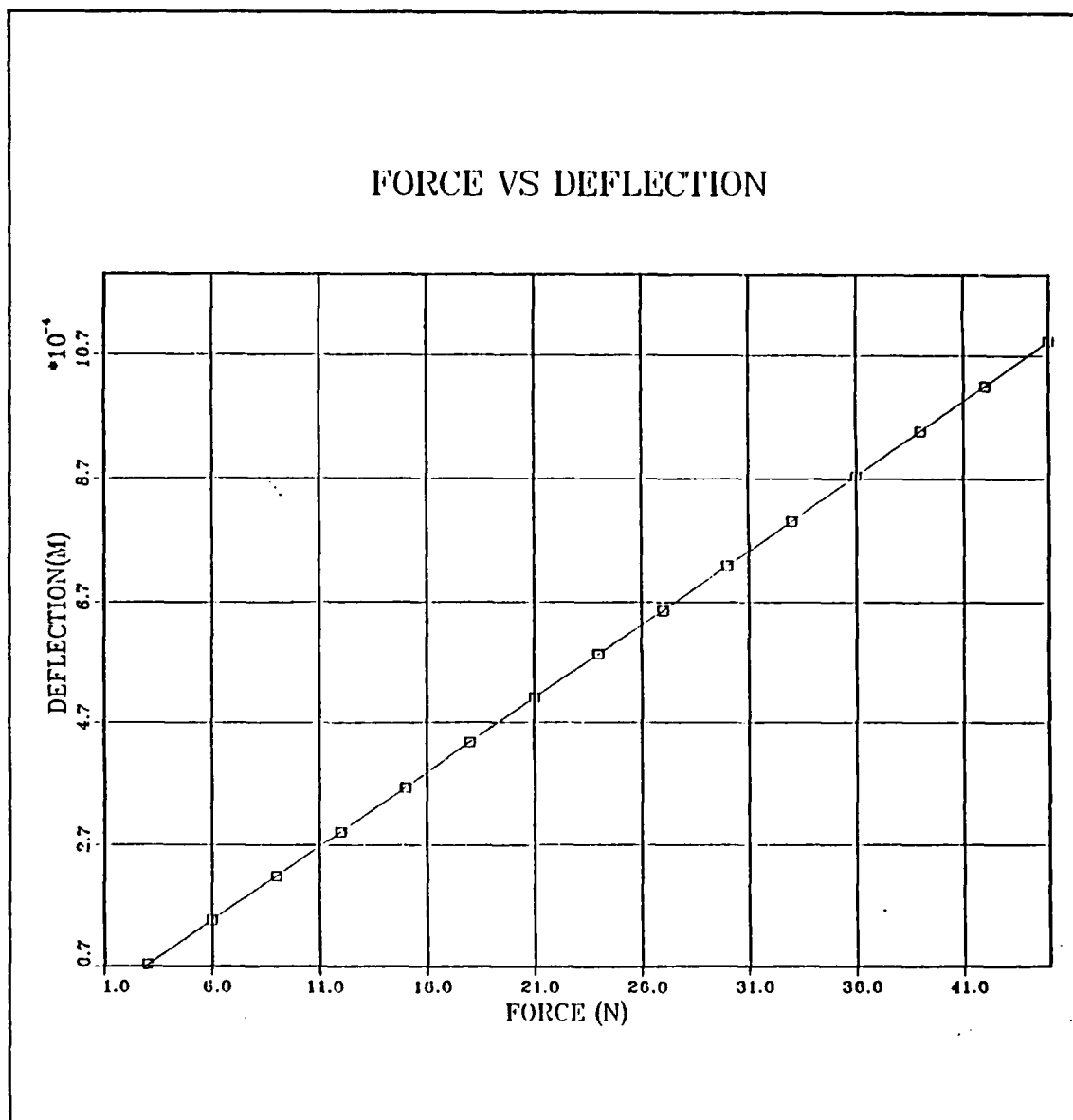The main goal of this research was to be able to control the amount of torque applied to an object by a robotic finger which was actuated by a small electric motor through a gearbox. The torque applied on an object by the finger can be changed by varying the stiffness of the servomechanism installed into the finger. The stiffness variation ability can be provided to the system by feeding back the disturbance torque measured from the object to the system through a variable gain E.

Since we are mainly interested in controlling the torque, the efficiency and the backdriveabilty of the gearbox used in the system must be taken into account when modeling the system. As the efficiency increases the backdriveablity will be higher, i.e the system will be more likely to be backdriveable. It is also important to notice that the efficiency of the gear train does not effect the actual transfer ratio of the gears in terms of displacement, velocity or acceleration, but greatly effects any torque related property.

Different types of gearboxes can be used in a servomechanism. Gearboxes with high gear ratios can be used to increase the torque applied by the output shaft. Gearboxes with high gear ratios will help disturbance rejection. The effects discussed above must be added to the system block diagram to obtain an accurate model of the system in order to control the torque applied on the object.

B. VARIABLE STIFFNESS CONTROL:

After adding torque feedback to system, the stiffness of the system will be a function of the gain E and the system will have its natural stiffness when the gain E is equal to zero. In the nonbackdriveable case, the natural stiffness of the system will be infinite, but this does not mean that the motor shaft stiffness will be infinite also. As the gain E

increases, the stiffness of the system will decrease as shown in Figure 43. As the gain E increases, the stiffness decreases, the amount of rotation of the output shaft for the same amount of the disturbance torque measured, will be directly proportional to the gain E. Namely, to be able to obtain a higher rotation for the same amount of the disturbance torque, the gain E must be increased.

The variation of the stiffness in a servomechanism was also proved experimentally on a larger model. As can be seen in Figure 43, the variation of the stiffness of the system measured experimentally has the same characteristics as predicted theoretically. For different values of E, the stiffness of the system measured experimentally was lower than the ones predicted theoretically. The main reason of this may be the nonlinearity that exist in DC motors. Since we are mainly interested in the stiffness variation, the experimental data proves that our prediction is correct, and that a variable stiffness servo system can be constructed.

As presented before, the stiffness of the educational system was infinite, namely it was not possible to rotate the output shaft or the motor shaft by applying a disturbance torque to it due to the nonbackdriveablity of the gearbox. After adding the torque feedback, it was possible to achieve different stiffness by varying the value of the gain E. Therefore, it is still possible to vary the stiffness of the system even when it is nonbackdriveable.

Another parameter which effects the magnitude of the natural stiffness in a servo system is k_a (forward path gain). As k_a increases the natural stiffness of the system will increase. We didn't consider using k_a for changing the stiffness of the system because for certain values of k_a, the system may become unstable. Since, k_a also effects the transient response of the system, after finding the values of k_a which will give the desired transient response without overshoot, by keeping the magnitude of k_a in defined limits, the time constant of the system can be changed to a certain value. It was also observed that
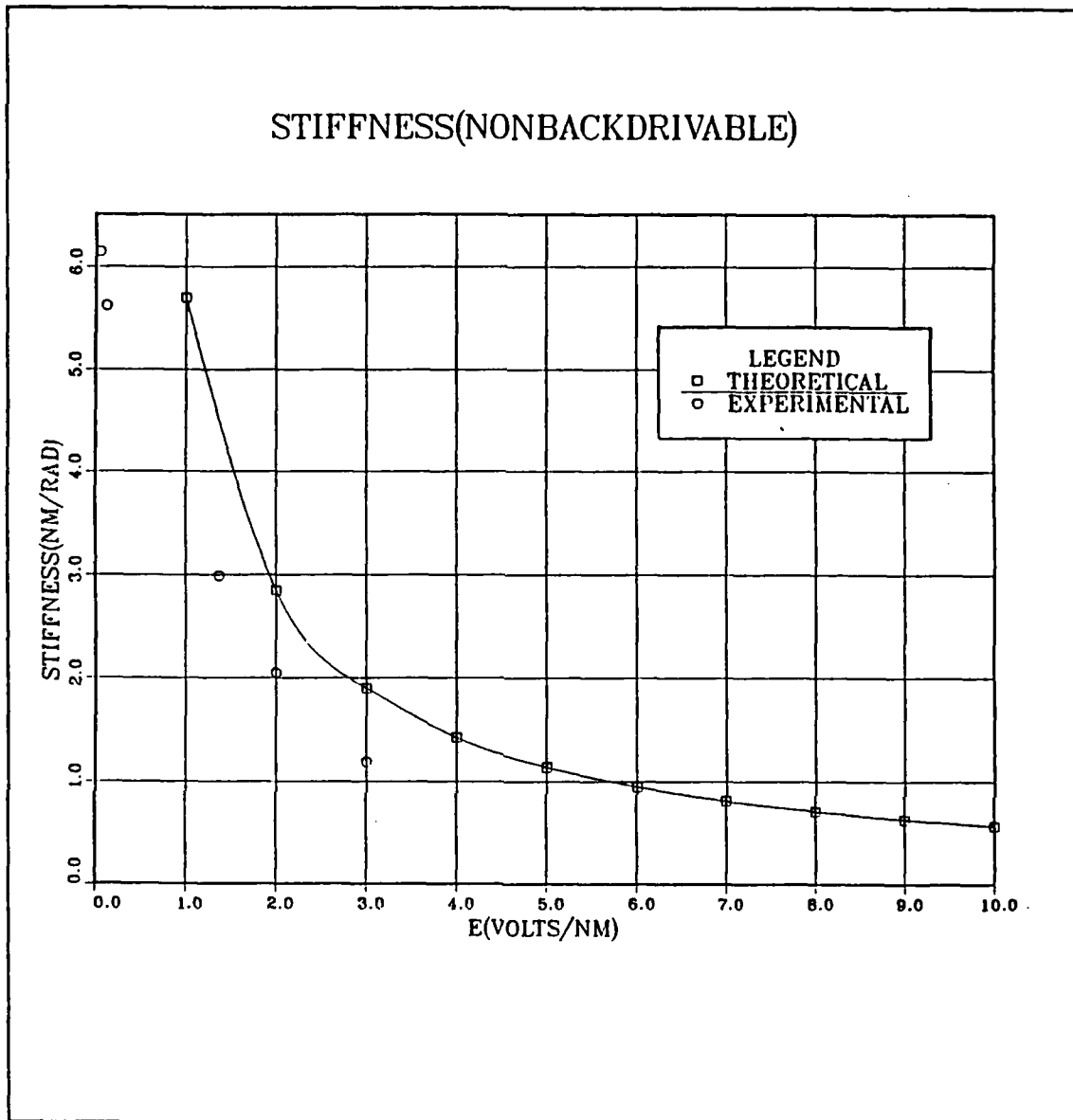
STIFFNESS(NONBACKDRIVABLE)

Figure 43.   Comparison of Theoretical and Experimental Stiffness Variation

adding the torque feedback to the system will not effect the transient response of the

system.

77

C. APPLICATION TO ROBOTIC FINGER SYSTEM:

Adaptation of the theory of variable stiffness to the finger joint was another important part of the research. Since the finger joint is not a large end effector, the design of the torque measurement system must have certain size constraints. However, the problem was exactly the same as the one described in the large model analysis. Therefore, by using the same block diagram and obtaining certain parameters from the catalog and from related equations, the variable stiffness system can be adapted to a robotic finger joint.

One of the main differences between the model used for experiments and the finger system was the dimensions of the beam. The beam, on which the strain gauges were mounted required careful design. Since a small beam was used in the design, to be able to get higher voltage, four small strain gauges were used. The size of the strain gauges was one of the main parameters which has an important effect on the design of the beam.

VIII. CONCLUSIONS

1. The torque applied by an end effector to an object can be controlled by changing the stiffness of the servomechanism.

2. Certain parameters must be added to the system block diagram to obtain an accurate model of the system in order to control the torque applied on the object.

3. After adding the torque feedback to the system, the stiffness of the system will be a function of the feedback gain, while adding the torque feedback does not effect the system transient response.

4. Even if the gearbox is nonbackdriveable, variable stiffness control of the servomechanism is possible.

5. The variable stiffness concept may be easily applied to the design of a robotic finger tip.

APPENDIX A.   ME3802 LABORATORY EXPERIMENT 2 DC SERVO
SYSTEM-SPEED CONTROL

A. OBJECTIVES

The purpose of this experiment is to:

1. Become familiar with the components of an electro-mechanical speed control system

2. Use basic measurement equipment to perform experiments

3. Measure the transfer functions of the components of the speed control system

4. Perform a close loop speed control test of the system

B. EQUIPMENT :

For this experiment,you will need the following equipment

1.Feedback educational servo system type ES151

2.Dual trace oscilloscope

3.Digital voltmeter

4.Chart recorder

5.A stop watch

6.Miscellaneous leads, wires and connectors

Examine and familiarize yourself with the equipment, and determine how to operate and connect the various pieces together.

C. METHOD

1. Compare the close loop feedback control system shown in Figure 44 and Figure 45 with the schematic shown on the front panel of the servo system, Figure 46. Figure 44 shows the complete schematic, while Figure 45 shows only those parts that will be used in the experiment 2. Be sure to identify the correspondence between all elements in both systems. Note the availability of certain system signals at the bottom of the front panel.

2. The first part of the experiment deals with the identification of the various parameters shown in Figure 45. Connect the system as shown in Figure 47, making sure the INTERNAL COMPENSATION switch is IN. Switch on, set input potentiometer θ_1 to zero and use the SERVO AMPLIFIER and OPERATIONAL AMPLIFIER SET
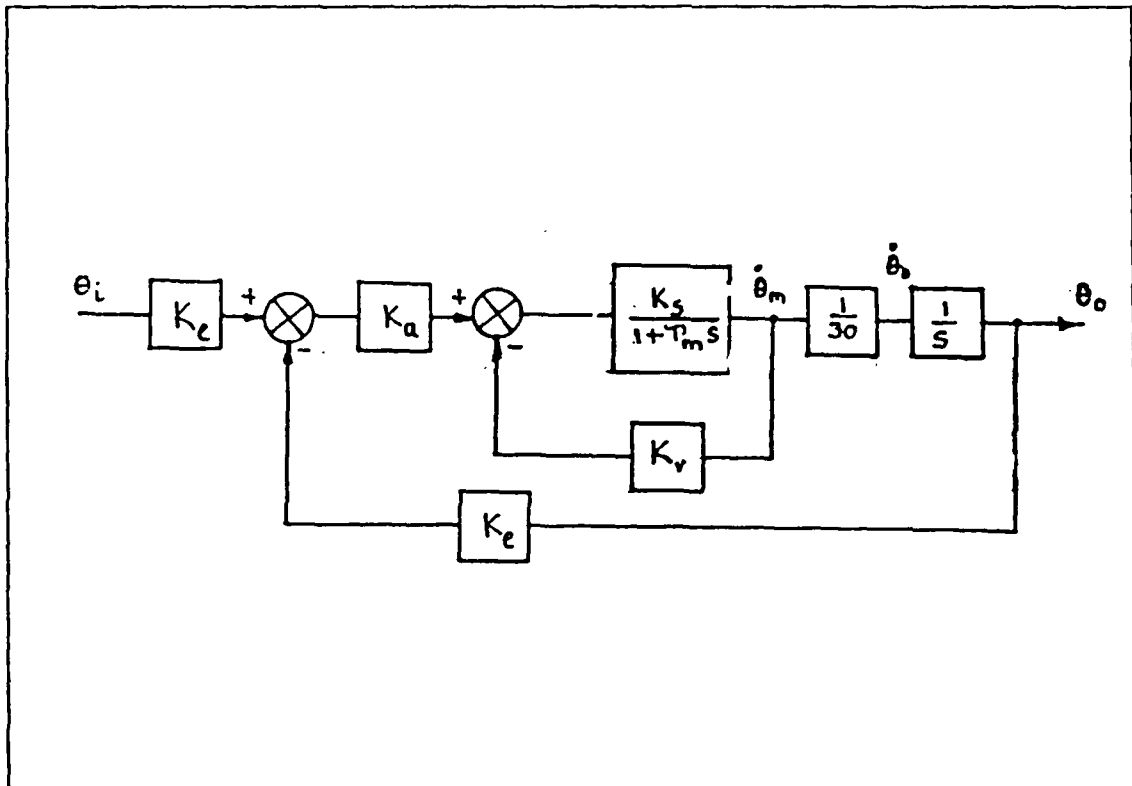
Figure 44.   Position Control System   Block Diagram

ZERO controls to achieve no motor rotation with minimum motor current shown on the panel meter. Ensure that the FEEDBACK SELECTOR switch is fully anti-clockwise.

   3. Tachometer Constant k_t

   In this test, the output voltage from the tachometer is recorded for various speeds. The slope of the line of voltage plotted against speed then gives the tachometer constant in volts/RPM. Connect the system as shown in Figure 47, and set P1 to 1 and P2 to 1. With the digital volt meter connected as shown, turn the input potentiometer to obtain constant speed of rotation of the motor. Using a stop watch, record the time for a given number of revelations (say 25). Note that the tachometer is mounted on the motor shaft, before the 30:1 gearbox driving the output potentiometer. Take this in to account when calculating the speed of the tachometer shaft. Change the setting of input potentiometer and repeat the test to obtain a total of five readings. Plot voltage against speed, draw the best straight line you can and calculate the slope. The expected result should be about 0.00245 volts/RPM.
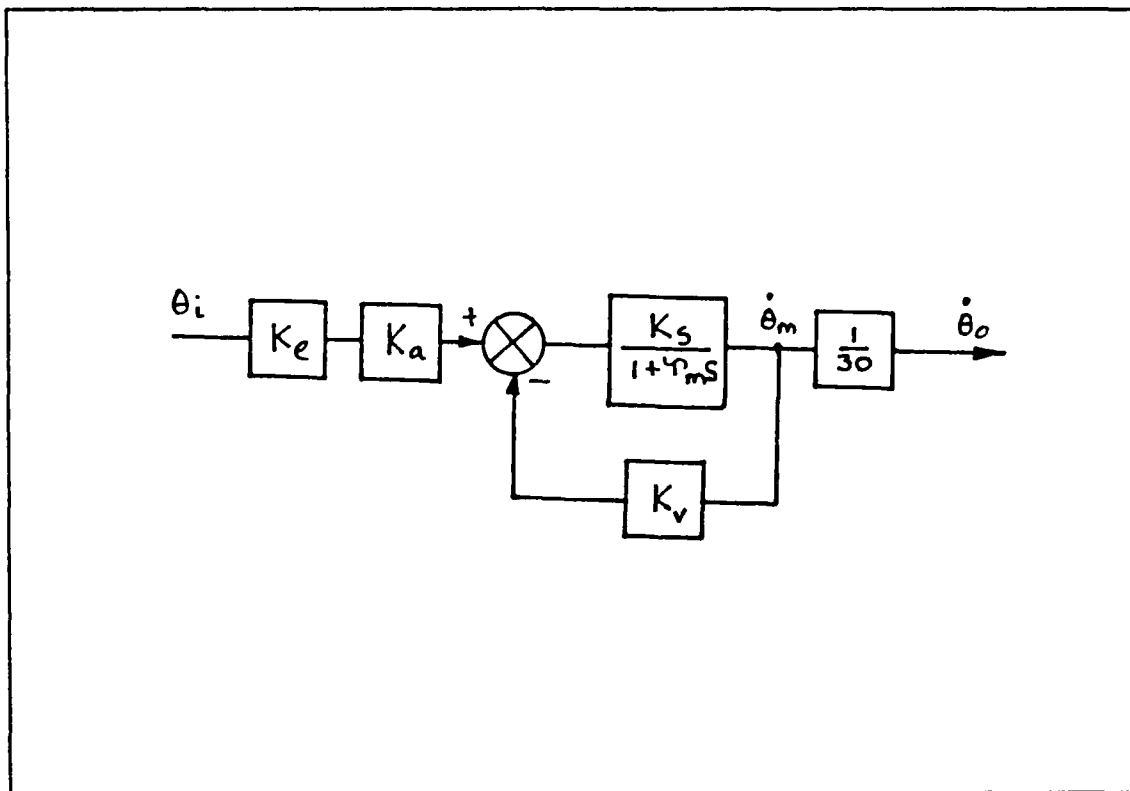
Figure 45. **Open Loop Speed Control Block Diagram**

4. Potentiometer Constant k_{pot}

Connect the apparatus as shown in Figure 48, noting that the system is open loop. In this test we will determine the potentiometer constant i.e. the relationship between the angular rotation of the potentiometer and the resulting voltage generated. Note that both input and output potentiometers are identical. Set the input potentiometer to point to zero degrees and record the error voltage. Rotate the input potentiometer from zero to 120 degrees in 20 degree steps. For each step record the voltage and subtract the voltage corresponding to zero degree position. Plot voltage against angular position and from the slope of the best straight line that fits the data determine k_{pot}. The expected result should be in the region of 5.7 volt/radian.

5. Motor & Servo Gain K,

This parameter is defined as the ratio of the output speed of the motor divided by the input voltage to the servo amplifier. Connect the system as shown in Figure 49, with P2 set to 0.7, and use the input potentiometer to establish a constant speed of the motor

82

shaft. Use the digital voltmeter to measure the input voltage to the servo amplifier and record this value. Determine the motor speed by connecting the digital voltmeter to the VELOCITY socket, record the voltage and use the previously calculated value of tachometer constant k_v to calculate the speed of the motor. Adjust the input potentiometer to give a different speed and repeat the test for five data points. Plot motor speed against input voltage and from the best straight line through the data points determine K_r. The expected value is about 270 radians / sec per volt.

6. Motor Time Constant T_m

In this test, the system is connected as an open loop speed control system, as shown in, Figure 50 subject to a step input. The step input is obtained from a function generator which should be set to provide a square wave output with a frequency of about 0.1 Hz, corresponding to a step input every 5 seconds. Set P2 to 0.2. To avoid using excessive record paper, use the oscilloscope to observe the output speed and to qualitatively verify the response. The output should look similar to that shown in Figure 51. The purpose of the experiment is to determine the time constant of the exponential increase in motor speed in response to the step change in demanded speed. Once a trace similar to that shown in Figure 51 is observed, obtain a copy on the chart recorder by switching it on, adjusting the sensitivity, and recording a few input responses. Make a note of the time base for the chart recorder. The time constant is calculated by determining the time taken for the system to achieve 63% of the demanded output, as shown in Figure 52. Measure the time constant from at least 3 response curve and calculate the average value. The expected time constant is $T_m = 0.25 seconds$.

7. Connect the system as a close loop feedback control system as shown in Figure 53. Set P1 to 1. All parameters shown in Figure 44 on page 81 are now known except for the gain k_a. For the servo system this gain is actually the product of the operational amplifier gain and the value of the potentiometer P2. Note that P2, being a potentiometer, is actually an attenuator and hence its gain components must be less than unity. When socket B is connected to socket E, the gain of the operational amplifier is 1, while connecting B to F reduces the gain to 0.1. Set P2 to 1 and perform a close loop step response as described in the previous section for the open loop. Observe the results on the oscilloscope, and make a sample chart recording output to determine the time constant the closed loop system. By analyzing the close loop transfer function together with the experimental values obtained. calculate a theoretical time constant for the close loop step response, and compare it with the measured values.
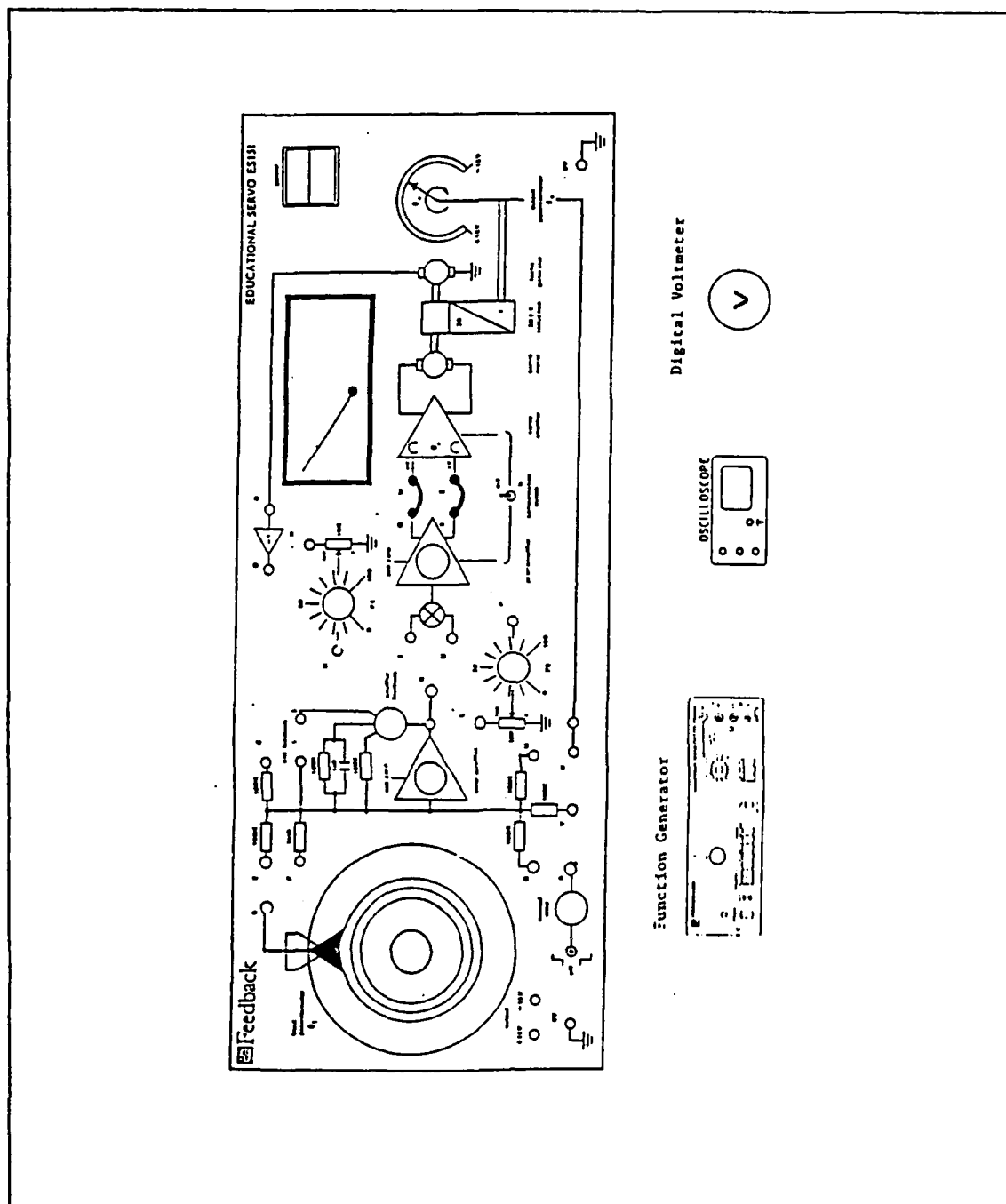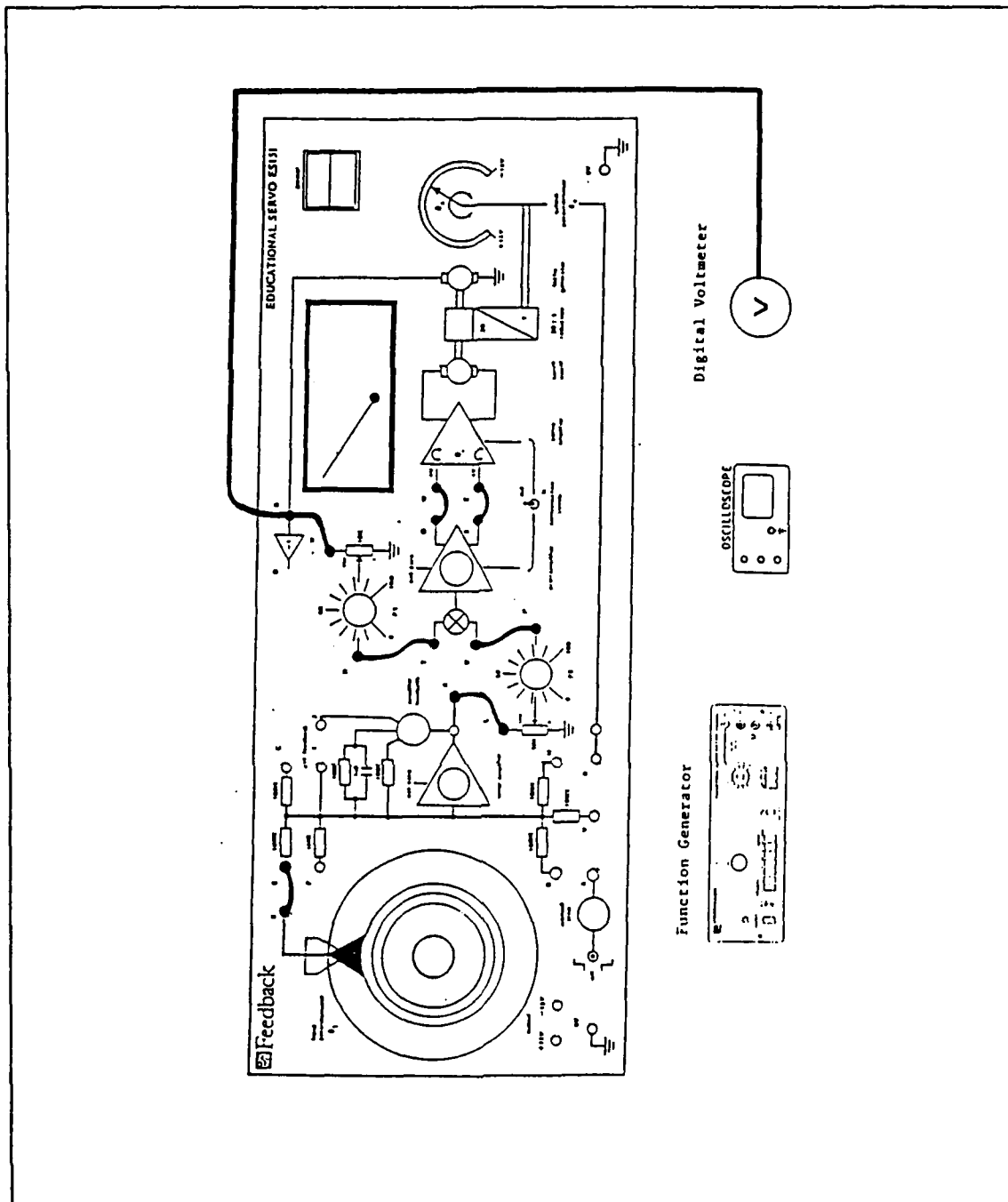
Figure 46. Equipment Configuration
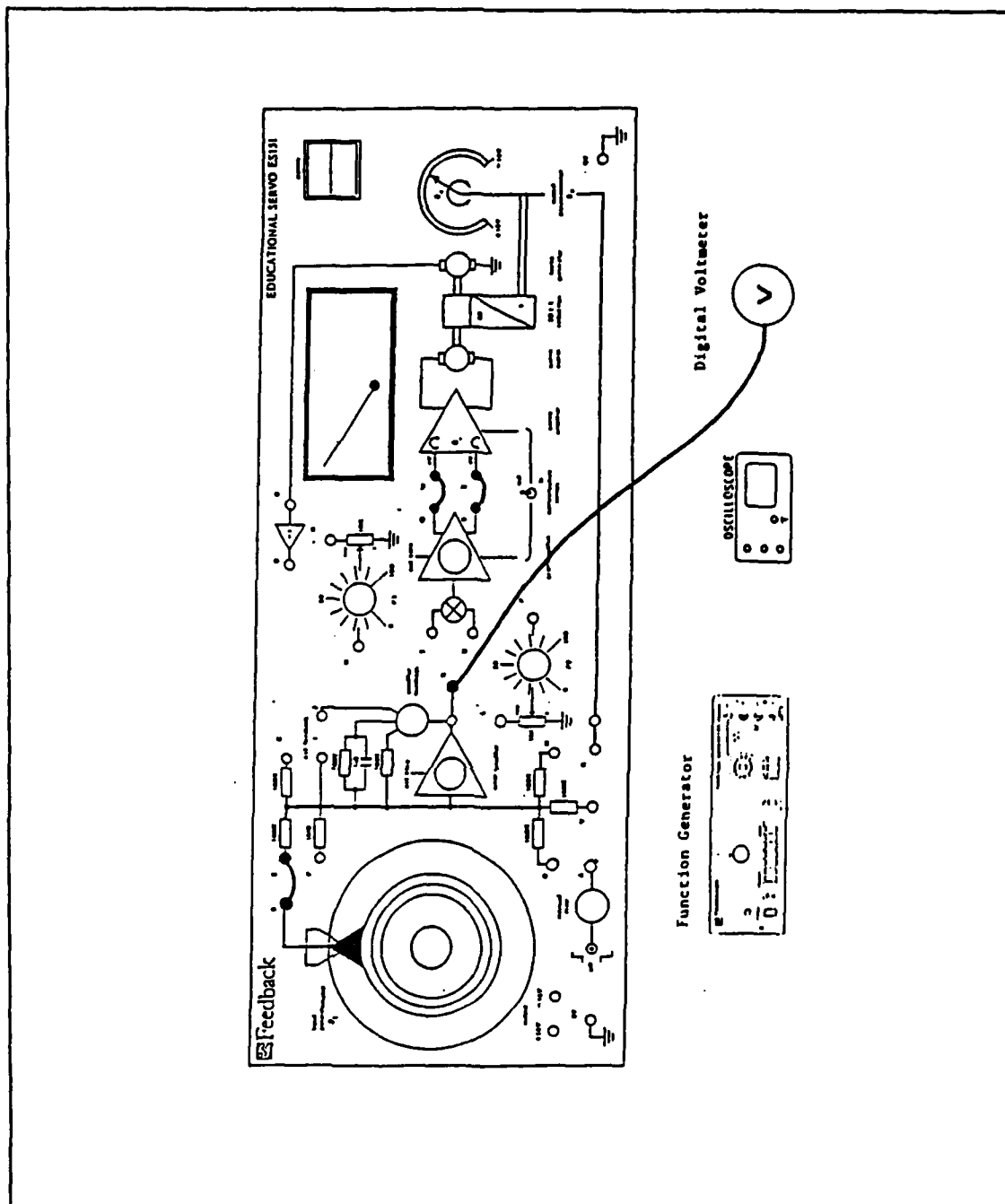
Figure 47.   Equipment Configuration
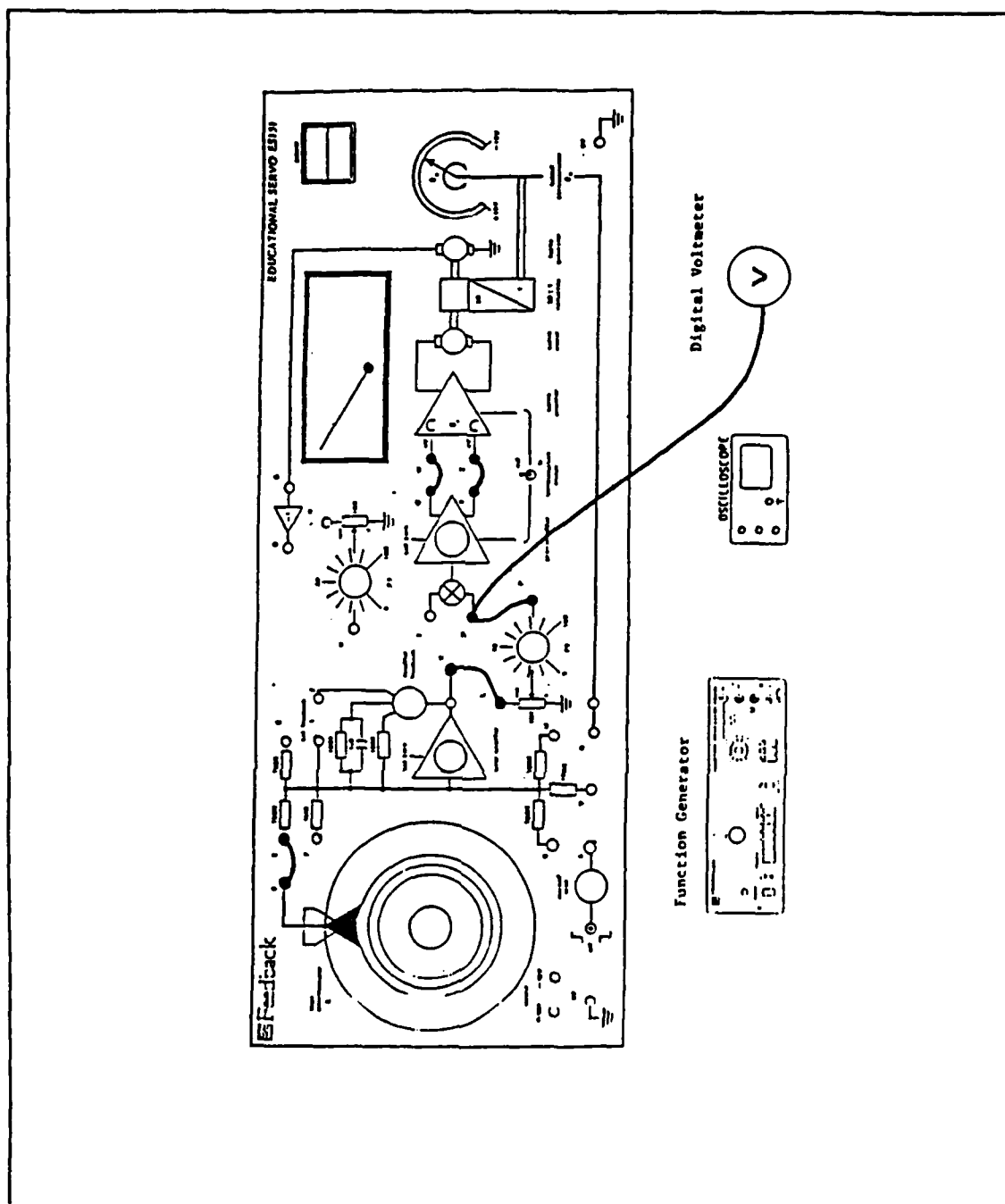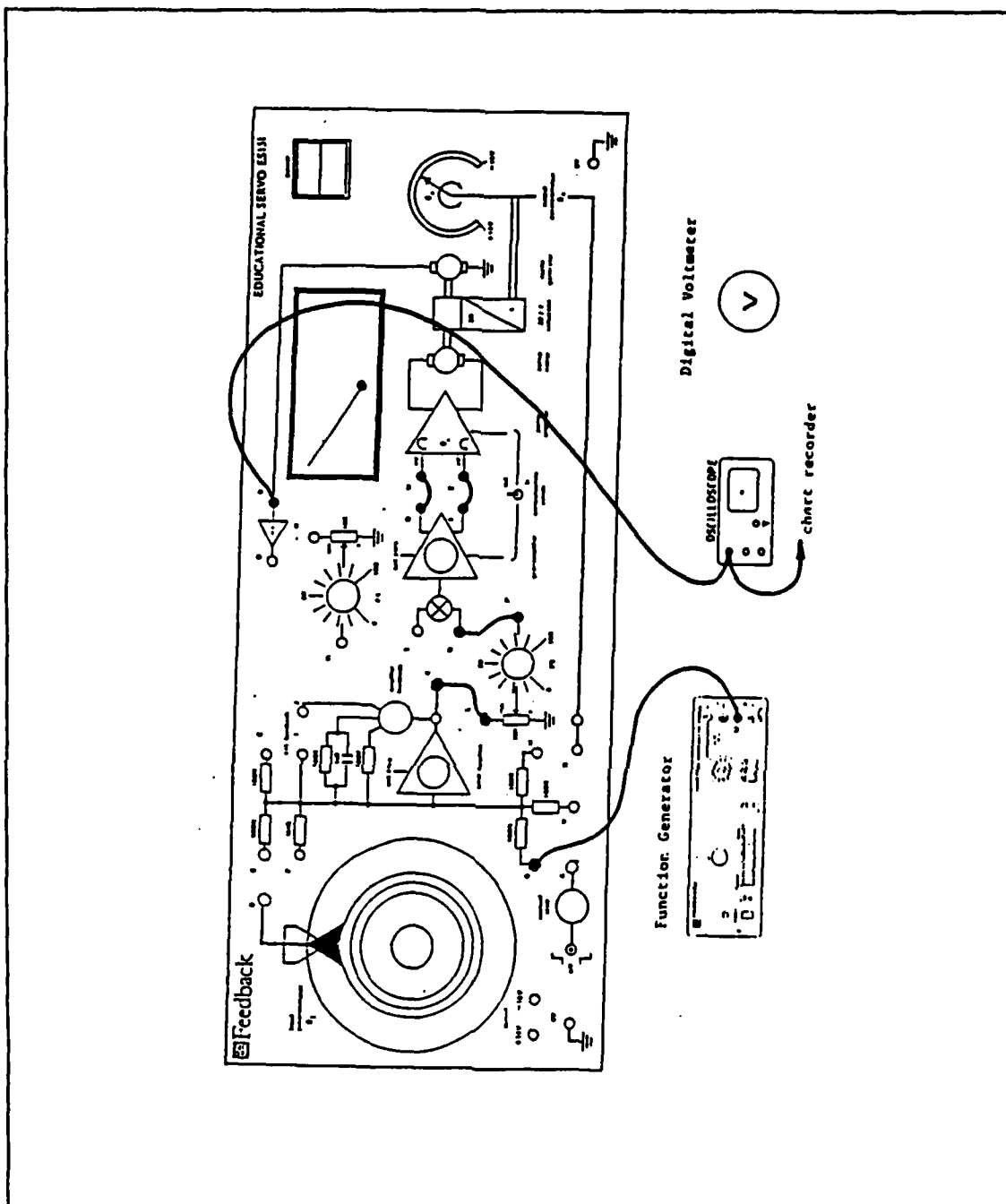
Figure 48.   Equipment Configuration

Figure 49. Equipment Configuration

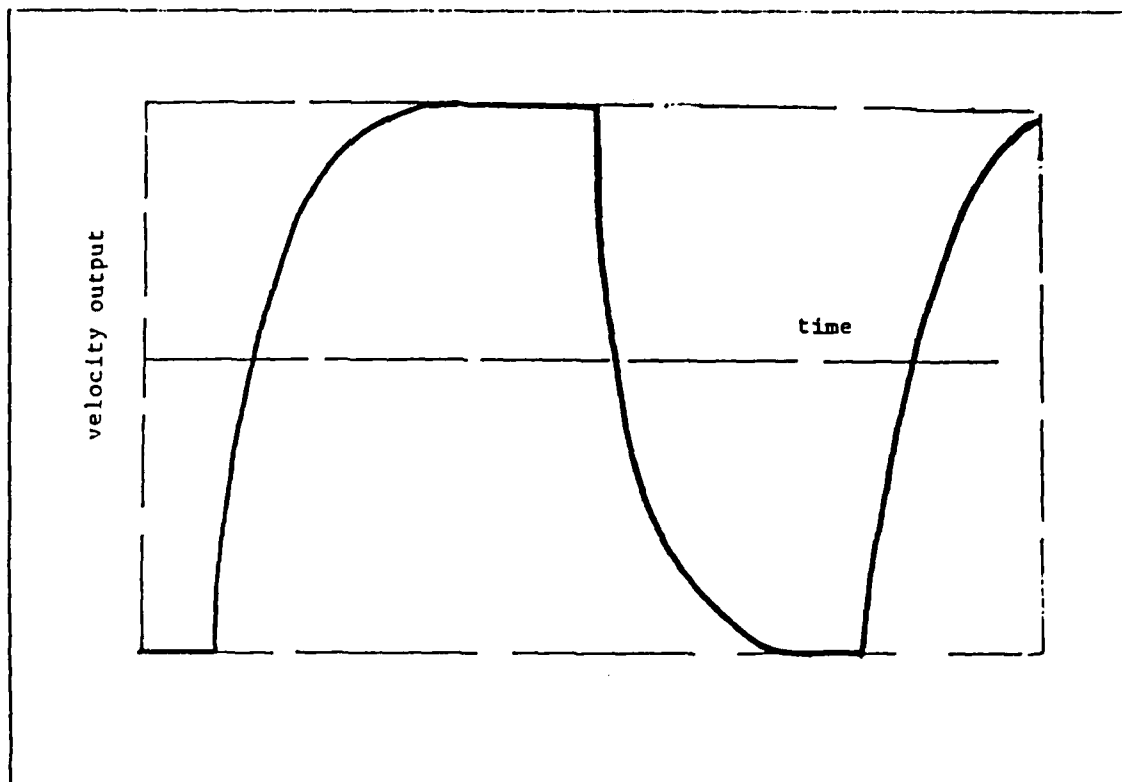Figure 50.   Equipment Configuration

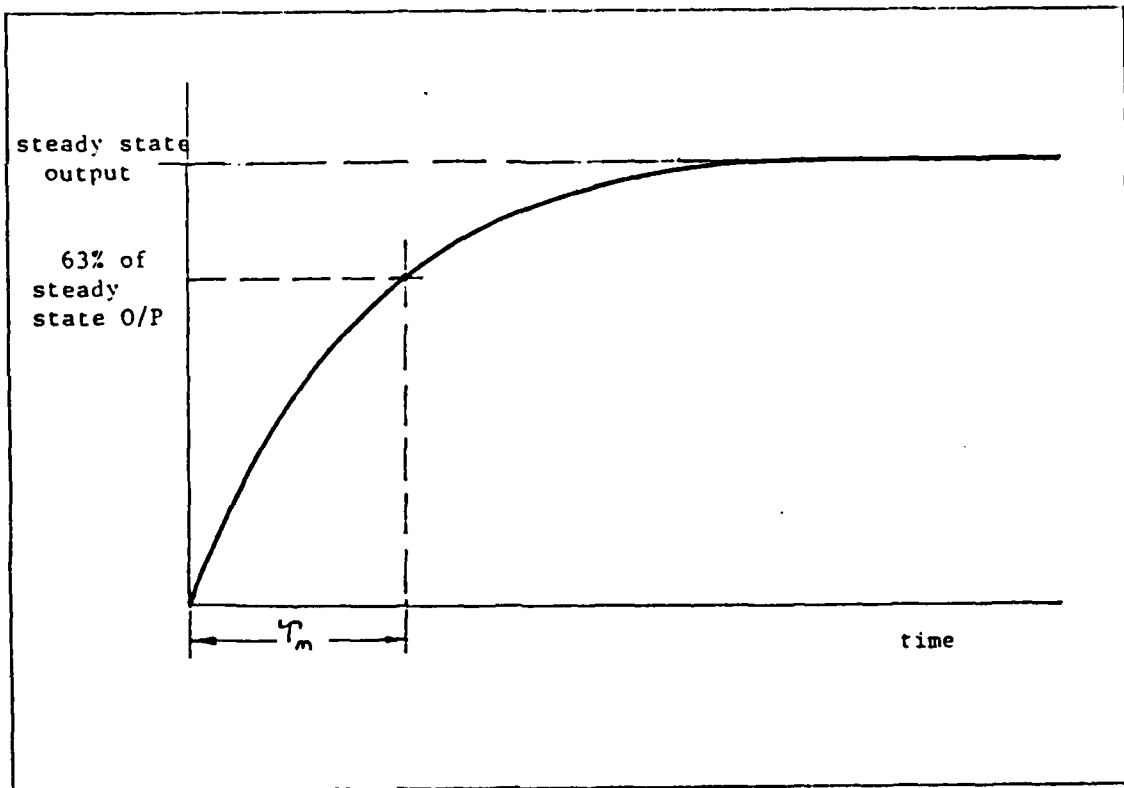Figure 51.   Output Speed

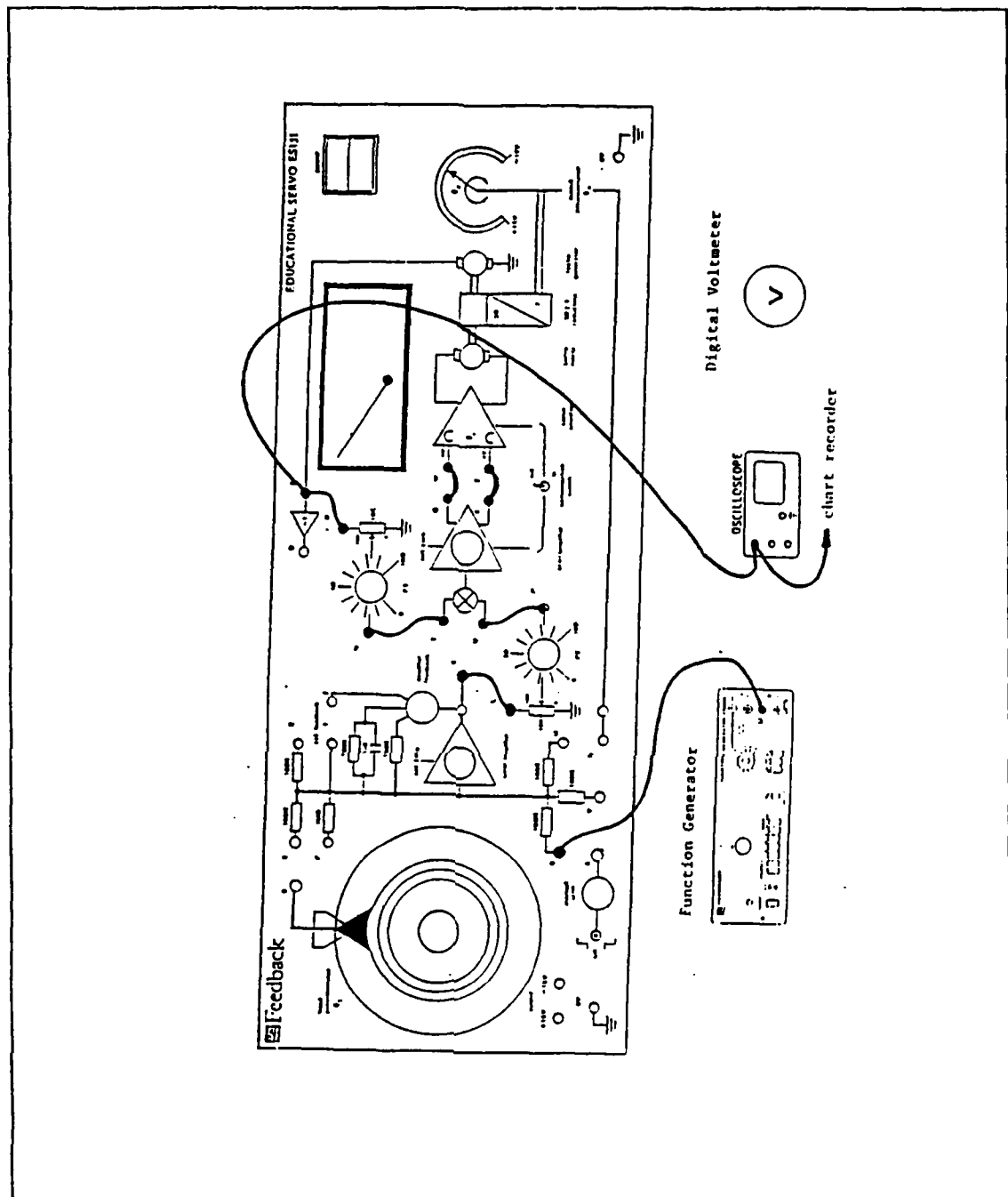**Figure 52.** Time Constant Calculation

Figure 53. Equipment Configuration

LIST OF REFERENCES

1. ESCAP motion systems catalogue

BIBLIOGRAPHY

Richard P. Paul,

Robotic Manipulators, The Massachusetts Institute of Technology press, 1982.

R. D. Klafter, T. A. Chmielewski, Michael Negin.

Robotic Engineering an Integrated Approach, Prentice-Hall, Englewood cliffs, New jersey, 1989

John Bradley,

Introduction to Analogue Control ES151, Fl. Ltd, Crowborough England.

DC Motors, Speed controls, Servo systems, Electro-Craft Corp, 1975.

Richard C. Dorf

Fifth Edition, Modern Control System, Addison-Wesley Publishing Company, 1989.

INITIAL DISTRIBUTION LIST

		No. Copies
1.	Defense Technical Information Center Cameron Station Alexandria, VA 22304-6145	2
2.	Library, Code 52 Naval Postgraduate School Monterey, CA 93943-5002	2
3.	Kara Kuvvetleri K.ligi Personel Sube Bsk.ligi Bakanliklar, Ankara / TURKEY	1
4.	Kara Harp Okulu K.ligi Kutuphanesi Bakanliklar, Ankara / TURKEY	1
5.	Orta Dogu Teknik Universitesi Okul Kutuphanesi Balgat, Ankara / TURKEY	1
6.	Professor Morris R. Driels, Code ME/Dr Department of Mechanical Engineering Naval Postgraduate School Monterey, CA 93943-5002	5
7.	Departman Chairman, Code ME Department of Mechanical Engineering Naval Postgraduate School Monterey, CA 93943-5002	1
8.	Milli Kutuphane Md.lugu Bahcelievler Ankara / TURKEY	1
9.	Yavuz Turkgenci K.K. Atli Spor Egt. Mrk. Bahcelievler Ankara / TURKEY	1